Rafael Gomes da Costa

Insights into the spreading of ataxin-2 through extracellular vesicles

Master's degree in Biomedical Sciences

This work was done under the supervision of:

Clévio Nóbrega, PhD

Carlos A. Matos, PhD

UNIVERSIDADE DO ALGARVE

Faculdade de Medicina e Ciências Biomédicas

2021

Insights into the spreading of ataxin-2 through extracellular vesicles

Authorship statement

I hereby declare to be the author of this work, which is original and unpublished. Authors and papers consulted are duly cited in the text and are listed in the included references.

(Rafael Gomes da Costa)

Para a minha avó Zezinha

Agradecimentos

Depois de um ano muito atípico, repleto de máscaras e álcool gel, eis que finda uma etapa importante da minha vida académica. Foram tempos particularmente duros, vividos num contexto de medo e preocupação constantes, mas que me deram a oportunidade de refletir sobre as matérias que realmente importam e sem as quais nada do que eu sou, ou do que eu fiz, seria possível. Nesta etapa final, desejo demonstrar a minha gratidão aos professores, amigos e família, que sempre acreditaram em mim e me deram a força que eu precisava para a realização deste trabalho. Por isso, e muito mais, esta tese é para todos vós.

Ao Professor Doutor Clévio Nóbrega, agradeço por mais um ano decorrido na presença de uma das melhores pessoas que eu jamais poderia ter conhecido. Obrigado pelos ensinamentos, por demonstrares o que é a paixão pela ciência e pelo desconhecido, sem nunca teres medo de falhar. A força com que te agarras às tuas ambições faz de ti um modelo que me leva a querer ser mais e melhor, que me leva a ter força para lutar pelos meus objetivos e crescer um pouco a cada dia que passa. Contudo, nem só da academia e do trabalho vive o Homem, e tu bem sabes disso. Obrigado pela contagiante paixão que tens de viver, de aproveitar cada segundo como se fosse o último, vivendo na felicidade junto das pessoas que te rodeiam. Obrigado por todo o apoio que me deste, enquanto orientador e amigo. Apesar das incertezas que o futuro reserva, estou convicto de que a nossa amizade prevalecerá por muitos anos e, quanto a isso, só posso esperar, ansiosamente, pelo que estará por vir. Com toda a minha sinceridade, obrigado!

Ao Doutor Carlos Matos, agradeço o apoio incondicional prestado sempre que eu necessitava, mesmo que essa necessidade surgisse a cada cinco minutos. Contudo, devo-te um pedido de desculpas por te ter arrastado para veres o sistema de eletroforese “avariado” que me fez perder a amostra preciosa…afinal, os elétrodos estavam montados ao contrário…típico, não é? Obrigado pela tua amizade, pelos milhares de ensinamentos que tentas transmitir-me, mesmo sabendo que, muito provavelmente, eu irei esquecer-me de todos eles. Obrigado pelo companheirismo, pela tua enorme bondade, pela enorme inteligência que não pára de surpreender. Obrigado por me teres dado uma nova identidade que eu adoptei com carinho. Um não-obrigado por ganhares constantemente no “Catan”, que te leva a fazer a “dança da vitória”. Obrigado por aceitares a difícil tarefa de me orientar nesta tese de mestrado, mesmo que isso tenha implicado fazer correções até ao último minuto. Obrigado por me contagiares com a tua boa disposição e por me fazeres querer ser melhor. Mas, o mais importante de tudo…obrigado por teres ido buscar gasolina quando fiquei apeado! Essa é uma dívida que jamais serei capaz de pagar. Agora a sério, obrigado por seres assim, obrigado por tudo!

Aos meus colegas de bancada, André, Rebekah, Ricky, Inês e Adriana, as nossas aventuras no laboratório têm outro sabor ao som dos anos 90, não é verdade? Obrigado a todos pela vossa amizade e pelo verdadeiro companheirismo que demonstram. Obrigado pela vossa vontade de trabalhar em equipa, sempre predispostos a ajudar o próximo! Obrigado, André, por me ajudares a filtrar os meios de cultura à seringa, quando as minhas mãos já fraquejavam. Obrigado, Ricky, por teres ajudado a isolar exossomas quando eu estava a fazer 30 experiências em simultâneo, mesmo que tenhas colapsado dois tubos na ultracentrifuga! Prometo que não digo ao chefe ;) Obrigado, Inês, pela paciência invejável que tens em ensinar a fazer um trabalho tão monótono como as imunohistoquímicas e pelas horas despendidas na microscopia. Obrigado, Adriana, por me teres ajudado com as imunos para que eu não saísse do laboratório à meia-noite. Obrigado, Rebekah, pelas minipreps que fizeste por mim e pela tua boa disposição, sempre presente. A todos vós, um enorme bem-haja! Espero que continuemos a ser uma equipa durante muito tempo!

Aos vizinhos de bancada, Sofia, Leo e Mónica, obrigado por estarem sempre dispostos a discutir a ciência que nos une, ou neste caso que nos separa, literalmente, através de três prateleiras de reagentes e material descartável. Obrigado por estarem sempre abertos a uma

boa gargalhada e por contribuírem para o excelente ambiente amigável que abunda no nosso laboratório.

Não posso deixar de agradecer à Vanda, a minha amiga de longa data e colega de licenciatura. Depois destes anos todos, sinto um enorme orgulho em, finalmente, partilharmos o mesmo espaço de trabalho. Obrigado pela tua amizade!

Agradeço, também, com um enorme carinho, à Professora Doutora Isabel Palmeirim e à Renata Sandres, por me terem prestado um apoio imensurável numa fase tão frágil da minha vida. Obrigado a ambas pela ajuda e pela enorme bondade que demonstraram!

Deixo, também, um agradecimento especial à Belén Garcia, por me ter ajudado com as análises de microscopia eletrónica e de força atómica, no Centro de Instrumentación Científica, em Granada, Espanha. Obrigado ao Jorge Pontes pela ajuda na utilização do Zetasizer para a caracterização das vesículas extracelulares. Agradeço, também, ao serviço de proteómica do IPATIMUP pelas análises de espectrometria de massa. Sem estas pessoas, a realização desta tese não teria sido possível.

Aos meus amigos de longa data, Ling, Sara, Maria, Diana, Maggy e Cherie, obrigado pela vossa amizade ao longo de todos estes anos e obrigado por sempre acreditarem em mim e por me incentivarem sempre a seguir os meus sonhos.

Os agradecimentos mais especiais são dedicados à minha família, que sempre fez tudo o que podia para que me fosse permitido chegar até aqui. Aos meus pais, Serafim e Clementina, agradeço-vos por todo o sacrifício que têm feito nos últimos anos para me possibilitarem de ter esta oportunidade tão bela que é estudar. Obrigado por se preocuparem comigo constantemente, por me perguntarem todos os dias se ando a comer e a dormir bem, por me amarem incondicionalmente e fazerem os possíveis para que eu seja verdadeiramente feliz. Como não conheço nenhuma palavra melhor para descrever aquilo que sinto, apenas vos digo “obrigado”! À minha irmã Sandra, agradeço-lhe a cumplicidade que temos vindo a partilhar desde o início. Obrigado por me teres quase rachado a cabeça quando eramos pequenos, por me pregares partidas constantemente porque “era divertido”, por me fazeres chorar e tentares acalmar-me quando ouvias os passos furiosos da mãe em aproximação…velhos tempos! Agora que estamos crescidos, vejo-te como um exemplo e tenho um orgulho enorme ao ver-te alcançar os teus objetivos com o teu próprio mérito. A próxima tese será a tua, e eu tenho a certeza que ficará fantástica, como tudo aquilo que tu fazes. És o meu orgulho!

O meu último e mais importante agradecimento vai para a minha avó Zezinha. Agradeço-lhe a oportunidade de ter partilhado parte da minha vida consigo, por me ter amado e acarinhado. Agradeço-lhe por todas as vezes que disse que tinha orgulho em mim, por todas as vezes que acreditou que eu seria alguém. Lamento que não consiga estar cá neste momento tão importante para nós, por isso, esta tese, dedico-a a

Table of contents

List of figures

List of tables

List of abbreviations

4E-BP1	eIF4E-binding protein 1
A2BP1	ataxin-2-binding protein 1
AD	Alzheimer's disease
AFM	atomic force microscopy
ALS	amyotrophic lateral sclerosis
APP	amyloid-beta precursor protein
ARF6	ADP-ribosylation factor 6
ARRDC1	arrestin domain-containing protein 1
Aβ	β-amyloid
BSA	bovine serum albumin
CAG	cytosine-adenine-guanine codon
Cdk5	cyclin-dependent kinase 5
CHMP6	charged multivesicular body protein 6
CIN85	Cbl-interacting protein of 85 kDa
CM	conditioned medium
CNS	central nervous system
CSF	cerebrospinal fluid
DAPI	4′,6-diamidino-2-phenylindole
DARPP-32	dopamine- and cAMP-regulated neuronal phosphoprotein
DDX6	DEAD box protein 6
DLB	dementia with Lewy bodies
DLS	dynamic light scattering
DMEM HG	Dulbecco's Modified Eagle's Medium High Glucose with L-Glutamine
DRPLA	dentatorubral-pallidoluysian atrophy
eGFP	enhanced green fluorescent protein
EGFR	epidermal growth factor receptor
eIF4E	eukaryotic initiation factor 4E
ELISA	enzyme-linked immunosorbent assay
Eps15	epidermal growth factor receptor substrate 15
ER	endoplasmic reticulum
ERK	extracellular signal-regulated kinase
ESCRT	endosomal sorting complexes required for transport
EVs	extracellular vesicles
FBS	fetal bovine serum

FSC-H	forward scatter height
FUS	fused in sarcoma
GCIs	glial cytoplasmic inclusions
GluN1	subunit 1 NMDA receptors
GPCRs	G protein-coupled receptors
HD	Huntington’s disease
HEPES	4-(2-hydroxyethyl)-1-piperazineethanesulfonic acid
HRS	hepatocyte growth factor regulated tyrosine kinase substrate
ILVs	intraluminal vesicles
InsP3R1	inositol 1,4,5-trisphosphate receptor type 1
IP3	inositol 1,4,5-trisphosphate
ISEV	international society for extracellular vesicles
LC3-II	light chain 3 isoform II
Lsm	like sm
LsmAD	Lsm-associated domain
MBNL1	muscleblind-like protein 1
mGluR1	metabotropic glutamate receptor subtype 1
MHC-II	major histocompatibility complex class II
miRNAs	microRNAs
MJD	Machado-Joseph disease
MLCK	myosin light chain kinase
MRI	magnetic resonance imaging
mRNAs	messenger RNAs
MS	multiples sclerosis
MSA	multiple system atrophy
mTOR	mammalian target of rapamycin
mTORC1	mTOR complex 1
MTSS1	metastasis suppressor protein 1
MVBs	multivesicular bodies
MVs	microvesicles
N2a	neuro2A cell line
NAT	natural antisense transcript
NEDD4	neural precursor cell expressed developmentally down-regulated protein 4
NMDA	N-methyl-D-aspartate
nSMase	neutral sphingomyelinase
NTA	nanoparticle tracking analysis
p62/SQSTM1	sequestosome-1

PABP	poly(A)-binding protein
PAM2	poly(A)-binding protein (PABP) interacting motif
PBS	phosphate buffered saline
PCR	polymerase chain reaction
PD	Parkinson’s disease
PEI	polyethylenimine
PFA	paraformaldehyde
PI3Ks	phosphoinositide 3-kinases
PI3P	phosphatidylinositol 3-phosphate
PINK1	PTEN-induced kinase 1
PolyQ	polyglutamine
PPC	polypropylene copolymer
PrP	prion protein
PS	phosphatidylserine
PVDF	polyvinylidene difluoride
Rac1	Ras-related C3 botulinum toxin substrate 1
RBFOX1	RNA-binding protein fox-1 homolog 1
RBM9	RNA-binding motif protein 9
RBP	RNA-binding protein
RBPMS	RNA-binding protein with multiple splicing
RGS8	regulator of G protein signaling 8
RIPA	radioimmunoprecipitation assay
RNAi	RNA interference
RT-PCR	reverse transcription polymerase chain reaction
S6K	ribosomal S6 kinase
SBM1	SH3 domain binding motif 1
SBM2	SH3 domain binding motif 2
SBMA	spinal and bulbar muscular atrophy
SCA	spinocerebellar ataxia
SCA2	spinocerebellar ataxia type 2
SCA3	spinocerebellar ataxia type 3
SDS	sodium dodecyl sulfate
SEC	size exclusion chromatography
SEM	scanning electron microscopy
SFK	Src family of non-receptor tyrosine kinases
SGs	stress granules
SH3	Src homology 3

siRNAs	small interfering RNAs
SNAP23	synaptosome-associated protein 23
SNARE	soluble N-ethylmaleimide-sensitive fusion factor attachment protein receptor
SOD1	Cu/Zn superoxide dismutase
STAM1	signal transducing adaptor molecule 1
STAU1	staufen-1
TBS-T	tris-buffered saline-Tween-20
TDP-43	TAR DNA-binding protein 43
TEM	transmission electron microscopy
TSG101	tumor susceptibility gene 101
UBAP1	ubiquitin-associated protein 1
UPS	ubiquitin-proteasome system
UTR	untranslated regions
VAMP	vesicle-associated membrane protein
VPS28	vacuolar protein sorting-associated protein 28 homolog
VPS36	vacuolar protein-sorting-associated protein 36
VPS4	vacuolar protein sorting-associated protein 4
VTA1	vacuolar protein sorting-associated protein VTA1 homolog
α-syn	α-synuclein

Abstract

Spinocerebellar ataxia type 2 (SCA2) is a neurodegenerative polyglutamine disease caused by an aberrant expansion of the trinucleotide CAG in the coding region of the *ATXN2* gene. As a result, ataxin-2, the protein product resulting from this gene, harbors an abnormally expanded polyglutamine tract, which renders it more prone to aggregation and consequent formation of inclusion bodies within the brain of SCA2 patients. Moreover, a toxic gain-of-function of ataxin-2, accompanied by the reported toxicity of an *ATXN2* antisense RNA, are thought to induce cellular alterations with subsequent neuronal death. Although only some neuroanatomical regions are primarily affected in SCA2, the neurodegeneration process seems to progress towards other brain regions, in latter stages of the disease. Nevertheless, the mechanisms responsible for this apparent disease spreading phenomenon have never been addressed.

In the last decade, recurrent evidence has shown that extracellular vesicles (EVs) can mediate neuron-neuron transfer of aggregate-prone proteins associated with many neurodegenerative diseases. In some cases, it was also reported that this mechanism can induce toxicity in healthy recipient cells, suggesting an explanation for disease spreading.

This study aimed to investigate the possibility of ataxin-2, in its protein and/or mRNA forms, being intercellularly transferred, similarly to what has been reported for proteins involved in neurodegenerative diseases. We show that eGFP-tagged ataxin-2 can be detected in non-transfected neuroblastoma cells when these are cultured in conditioned medium derived from eGFP-ataxin-2-transfected cells. Moreover, we show that ataxin-2 mRNA was found within two different types of extracellular vesicles, which were able to induce the formation of ataxin-2 aggregate-like structures within recipient cells, both *in vitro* and *in vivo*.

Overall, this study suggests for the first time that EV-mediated transport of ataxin-2 mRNA can induce the formation of ataxin-2 aggregates in healthy recipient cells, possibly representing a novel mechanism involved in SCA2 pathogenesis.

Keywords: spinocerebellar ataxia type 2 (SCA2), ataxin-2, extracellular vesicles, exosomes, microvesicles, disease spreading.

Resumo

A ataxia espinocerebelosa tipo 2 (SCA2, do inglês *spinoceberellar ataxia type 2*) é uma doença neurodegenerativa que pertence ao grupo das doenças de poliglutaminas. A SCA2 é causada por uma expansão aberrante de uma região repetida de codões CAG presente na região codificante do gene *ATXN2*. Esta mutação resulta na síntese de uma proteína denominada ataxina-2, que contém uma sequência repetitiva de glutaminas anormalmente expandida, na sua região N-terminal. Os monómeros de ataxina-2 mutante tendem a agregar, levando à formação de oligómeros e, eventualmente, de agregados proteicos de natureza amilóide. De facto, uma das características da SCA2, à semelhança de outras doenças de poliglutaminas, é a presença de agregados proteicos constituídos por diversas proteínas no tecido nervoso dos doentes, denominados de corpos de inclusão. Contudo, existe uma grande incerteza no que concerne à possibilidade de estes agregados serem a causa direta da toxicidade observada na SCA2, uma vez que alguns estudos sugerem a ausência de correlação entre a presença de agregados e neurodegeneração. De facto, à semelhança do que acontece no contexto de outras doenças neurodegenerativas, alguns autores sugerem a possibilidade de pequenas espécies proteicas, como os oligómeros de ataxina-2, constituírem a verdadeira causa de toxicidade, enquanto a agregação macromolecular destas espécies poderá constituir um mecanismo celular de proteção, que pode contrariar a morte neuronal. Por outro lado, a ataxina-2 mutante poderá interagir de forma aberrante com certas proteínas ou perder a sua capacidade intrínseca de se associar com outras, resultando num quadro geral de disfunção da ataxina-2. Consequentemente, a falta de ataxina-2 funcional poderá levar a mecanismos de patogénese que incluem disfunção da autofagia, efeitos deletérios resultantes do processamento aberrante de pré-mRNA, toxicidade mediada por RNA, aumento de stress oxidativo, alterações na sinalização celular e perturbações na homeostasia de cálcio.

Tanto a presença de agregados de ataxina-2 como o processo de neurodegeneração são especialmente marcados em regiões particulares do encéfalo, nomeadamente no cerebelo e ponte dos doentes de SCA2. Contudo, a neurodegeneração aparenta estender-se a outras regiões neuroanatómicas, concomitantemente à progressão da doença. Apesar da aparente seletividade regional onde a morte neuronal ocorre, os mecanismos responsáveis pela sua propagação até diferentes áreas anatómicas interconectadas permanecem pouco compreendidos na SCA2, bem como no contexto de outras doenças neurodegenerativas.

Durante a última década, diversos estudos têm vindo a demonstrar a participação de vesículas extracelulares na propagação de proteínas com conformações aberrantes, associadas a diversos processos neurodegenerativos. Em alguns casos, verificou-se que este tipo de mecanismo de transporte intercelular constituía uma verdadeira causa de propagação

de toxicidade para células saudáveis, sustentando a hipótese da existência de um mecanismo de disseminação de doença. As vesículas extracelulares são estruturas delimitadas por uma bicamada lipídica, que são secretadas, virtualmente, por todos os tipos celulares. Existem diversos tipos de vesículas extracelulares que diferem fisicamente, molecularmente e funcionalmente entre si. Contudo, existe um conjunto de sobreposições de caraterísticas entre os diferentes grupos de vesículas extracelulares que dificultam a sua correta caracterização e classificação. Apesar das diferenças, na sua generalidade, as vesículas extracelulares são capazes de transportar um conjunto de cargas variadas entre células, nomeadamente proteínas, lípidos e diversos tipos de RNAs, que podem, potencialmente, influenciar o comportamento da célula que as internaliza, seja num contexto fisiológico ou patológico.

O facto de as vesículas extracelulares serem recorrentemente implicadas na propagação de proteínas com conformação aberrante em diversas doenças neurodegenerativas levou-nos a questionar se este potencial mecanismo de disseminação de doença poderia existir na SCA2 e, assim, explicar, pelo menos em parte, a progressiva neurodegeneração que é observável nos doentes. Deste modo, o objetivo principal deste trabalho consistiu em determinar se a ataxin-2 ou o seu transcrito de mRNA são transportados intercelularmente e se este processo contribui para a propagação de um fenótipo de doença.

Na primeira parte deste estudo, observámos que a incubação de células de neuroblastoma de murganho (N2a) com meio condicionado obtido a partir de células que expressam ataxina-2 humana conduz à deteção da proteína humana naquelas células. Adicionalmente, verificámos que o mRNA da forma humana da ataxina-2 mutante se encontra presente em dois tipos diferentes de vesículas extracelulares (exossomas e microvesículas) obtidas a partir de células N2a que expressam a proteína humana. Observámos, ainda, que ambos os tipos de vesículas extracelulares isolados foram capazes de induzir, em células N2a, a formação de estruturas intracelulares semelhantes a agregados de ataxina-2, que aumentaram em número e volume de forma progressiva.

Na segunda parte deste trabalho, averiguámos a possibilidade de as vesículas extracelulares serem capazes de propagar a forma humana da ataxina-2 mutante por diferentes regiões do encéfalo de murganhos. Para isso, isolámos exossomas e microvesículas de células N2a que expressavam a ataxina-2 mutante e injetámos, separadamente, as vesículas extracelulares no ventrículo lateral direito dos animais, através de cirurgia estereotáxica. Vinte e quatro horas depois, verificámos a presença de foci contendo ataxina-2 em diversas regiões anatómicas do encéfalo, em diferentes graus de abundância. Por exemplo, as células de Purkinje do cerebelo, que se sabem estarem especialmente afetadas na SCA2, apresentavam uma maior quantidade de foci,

comparativamente ao caudoputamen. Por outro lado, as células das camadas granular e molecular do cerebelo não mostravam qualquer presença destas estruturas. Estas discrepâncias observadas poderão ser explicadas pela especificidade de internalização das vesículas extracelulares, que poderá variar de acordo com o tipo celular que as internaliza.

Em conclusão, este estudo sugere pela primeira vez que a ataxina-2 mutante é transportada intercelularmente, pelo menos na forma de mRNA, através de vesículas extracelulares que promovem a formação de agregados de ataxina-2 em células saudáveis. Este processo poderá contribuir para a patofisiologia da SCA2 e para a seletividade regional da neurodegeneração que se verifica na doença.

Palavras-chave: ataxia espinocerebelosa do tipo 2 (SCA2), ataxina-2, vesículas extracelulares, exossomas, microvesículas, propagação de doença.

CHAPTER 1 – INTRODUCTION

1. Polyglutamine diseases

Repeat expansion disorders comprise a class of genetic diseases that arise from abnormally expanded sequences dispersed throughout the human genome. Currently, there are over 40 different disorders known to be caused by repeat expansions, and the trinucleotide repeat diseases are the most frequent and were the first to be discovered. Nonetheless, repeat expansions come in different sizes (from single nucleotides to tetra-, penta-, hexa-, and even dodeca-nucleotide repeat expansions) and may occur both in coding and non-coding regions of distinct genes (Ellerby, 2019; Paulson, 2018). Polyglutamine (polyQ) diseases include a group of nine rare neurodegenerative disorders caused by an abnormal expansion of the trinucleotide CAG beyond a certain threshold, in their causative genes. This particular group of diseases contrasts with the majority of other repeat expansion disorders because the CAG expansion is in the coding region of the affected genes, originating an abnormally expanded polyQ tract in the codified protein. On the other hand, other repeat expansion diseases typically harbor the expansion in non-coding sequences, such as introns and 5'- or 3'-untranslated regions (UTR) (Nóbrega and Pereira de Almeida, 2018; Paulson, 2018). PolyQ disorders-associated genes and protein products are thought to be unrelated and do not share a significant degree of homology, apart from the CAG/polyQ tract (Ordway et al., 1997).

Currently, the nine polyQ diseases described are Huntington's disease (HD), dentatorubral-pallidoluysian atrophy (DRPLA), spinal and bulbar muscular atrophy (SBMA), and six different types of spinocerebellar ataxia (SCA): SCA 1, 2, 3, 6, 7, and 17 (table 1.1) . All these diseases are highly incapacitating and fatal. Moreover, to date, no successful therapy or treatment has been discovered to stop or delay their progression, emphasizing the utmost urgency in devoting efforts to this research field (La Spada and Taylor, 2010).

Although polyQ diseases display distinct symptomatology and regional patterns of neurodegeneration, they share a few common clinical, genetic, and neuropathological features. Clinically, they all present the phenomenon of anticipation, which is characterized by a greater severity and precocity of symptoms, in successive generations (Schols et al., 2004). Genetically, polyQ diseases exhibit generational instability in the CAG repeat extension, and future generations tend to inherit longer stretches of the CAG tract, which may explain the anticipation phenomenon described. Pathologically, they share a propensity for their associated protein products to aggregate and form intracellular inclusions in patients' neuronal tissue, which constitutes a neuropathological hallmark of polyQ diseases (Gatchel and Zoghbi, 2005; Williams and Paulson, 2008). Although polyQ diseases have identified monogenic causes, the molecular mechanisms leading to pathogenesis remain elusive. It is believed, however, that these mechanisms may be common amongst different polyQ disorders

(Nóbrega and Pereira de Almeida, 2018). Collectively, understanding the differences and similarities between these diseases may help unveil the underlying molecular mechanisms of pathogenesis and enable the development of novel therapeutic strategies.

Table 1.1 – General characteristics of polyglutamine diseases

POLYQ DISEASE	GENE	PROTEIN PRODUCT	NORMAL / PATHOGENIC REPEAT NUMBER	PRIMARY TARGETS OF NEUROPATHOLOGY
HD	*HTT*	Huntingtin	6-35 / 36-121	Caudate nucleus, putamen, globus pallidus (external segment
DRPLA	*ATN1*	Atrophin-1	3-35 / 48-88	Cerebellum (dentate nucleus), red nucleus, globus pallidus (externals segment), subthalamic nucleus
SBMA	*AR*	Androgen receptor	9-36 / 38-62	Motor neuron in anterior horn cells of the spinal cord and brainstem
SCA1	*TAXN1*	Ataxin-1	6-38 / 39-83	Cerebellum, red nucleus, inferior olive, pons, anterior horn cells and pyramidal tracts
SCA2	*ATXN2*	Ataxin-2	14-31 / 35-500	Cerebellar Purkinje cells, brainstem, spinal cord
SCA3	*MJD/ATXN3*	Ataxin-3	12-40 / 54-86	Cerebellar dentate neurons, basal ganglia, brainstem, spinal cord
SCA6	*CACNA1A*	Ca^{2+} channel	4-19 / 20-30	Cerebellar Purkinje cells, dentate nucleus, inferior olive
SCA7	*ATXN7*	Ataxin-7	4-35 / 37-200	Cerebellum, brainstem, macula, visual cortex
SCA17	*TBP*	TATA-binding protein	29-42 / 47-55	Cerebellum, cortex (diffuse atrophy), caudate and putamen

Adapted from Bettencourt et al., 2016 and Rego and de Almeida, 2005.

2. Spinocerebellar ataxia type 2

Amongst the nine polyQ disorders, SCAs comprise a subgroup of clinically, pathologically, and genetically heterogeneous neurodegenerative diseases. Nonetheless, all SCAs involve a loss of balance and motor coordination arising from the degeneration, and consequent dysfunction of the cerebellum and its afferent and efferent neuronal pathways, spinal cord, peripheral nerves, and brainstem (Velazquez-Perez et al., 2011).

Spinocerebellar ataxia type 2 (SCA2) is the second most prevalent SCA worldwide, only surpassed by Machado-Joseph disease, or spinocerebellar ataxia type 3 (MJD/SCA3), the most common subtype that reaches its higher prevalence in Portugal, in the islands of Azores (Lima et al., 1997; Schols et al., 2004). SCA2 was first documented in India by Wadia and Swami, in 1971, who examined 16 patients from nine families, and reported early and marked slow saccades (simultaneous movement of both eyes towards a fixed point)

associated with cerebellar degeneration (Wadia and Swami, 1971). It was only twenty-five years later that the underlying mutation was independently revealed by three distinct laboratories in the USA, Japan, and France (Imbert et al., 1996; Pulst et al., 1996; Sanpei et al., 1996).

Despite its rarity, extensive research efforts have been directed to understand SCA2, since it was discovered, and, today, it is one of the best-known polyQ diseases. However, the knowledge acquired so far has not been sufficient to develop any treatment that could halt or delay SCA2 progression.

2.1. Epidemiology

SCA2 has been described as the second most common subtype of SCA after SCA3, presenting a global frequency of 15% in comparison to other SCA subtypes (Schols et al., 2004). Particular populations present higher prevalence rates that can be explained by the influence of populational genetic phenomena occurring in certain geographic regions, such as the founder effect. For example, SCA2 has been observed to be the prevalent ataxia in some populations, such as in the Indian and Cuban populations (Saleem et al., 2000; Velazquez Perez et al., 2009). In Mexico, SCA2 was also determined to be the most common ataxia, representing 45.4% of all SCAs (Alonso et al., 2007). SCA2 families have also been found in Australia, Martinique, Tunisia, Germany, Italy, Poland, and Southern Brazil (Trott et al., 2006; Velazquez-Perez et al., 2011). Nevertheless, few epidemiological studies have been conducted on SCAs, hence it is believed that the data about the prevalence of these disorders does not reflect their real occurrence, which is, thus, underestimated worldwide. The strong genetic bias caused by the founder effect, along with the few epidemiological studies focused on isolated geographic regions, hamper the estimation of an accurate worldwide prevalence of particular subtypes of SCA such as SCA2 (Schols et al., 2004).

SCA2 reaches its highest prevalence in Cuba, more precisely in the Holguín province, in the north-eastern region, where 40.18 in 100,000 inhabitants are affected (Velazquez Perez et al., 2009). It is believed that the marked SCA2 prevalence in Cuba is due to Hispanic founders who immigrated to the eastern region during the XVII century. This hypothesis is supported by the fact that SCA2 Cuban families have a long documented story of Hispanic origin and almost all share the same chromosomal haplotype in the vicinity of the locus where the SCA2 mutation occurs (Hernández et al., 1995). However, these Cuban families have dispersed throughout the island, and this does not explain the higher prevalence rates of SCA2 in the Holguín province. Cultural and environmental events can have deep influence on genetic variability and can restrict mutations to particular populations. Regarding this matter, it is

possible that the endogamous and closed cycle marriages of Holguín people living in the XVII century may have restricted SCA2 to the Holguín province (Velazquez Perez et al., 2009).

2.2. Clinical features

SCA2 is characterized by progressive degeneration of the cerebellum and its associated neuronal pathways (Dohlinger et al., 2008; Jacobi et al., 2011), which usually culminates in gait ataxia, the most noticeable clinical feature of SCA2, and common to all SCAs. However, clinical, electrophysiological, and imaging evidence suggest that neuronal dysfunction starts years before ataxia onset, manifested by subtle motor and unspecific non-motor traits, and preceding the clinical diagnosis by up to 15 years (Velazquez-Perez et al., 2017). Although gait ataxia is present in most SCA2 patients, variant phenotypes of motor incoordination residing outside of the cerebellar spectrum have been defined, including L-DOPA-responsive parkinsonism and motor features of amyotrophic lateral sclerosis (ALS) (Gwinn-Hardy et al., 2000; Infante et al., 2004; Nanetti et al., 2009; Van Damme et al., 2011). Patients with these variant phenotypes present idiopathic forms of parkinsonism or ALS, making SCA2 diagnosis frequently challenging for neurologists, especially when the family's history is not available (Antenora et al., 2017).

Other signs and symptoms of SCA2 also originating mainly from cerebellar degeneration include appendicular ataxia with instability of stance, motor difficulties of speech (dysarthria), and oculomotor deficits presented by nystagmus and ocular dysmetria (Buijsen et al., 2019; Scoles and Pulst, 2018). However, SCA2 symptomatology is characterized by additional non-cerebellar manifestations, arising from the neurodegeneration of the pons, the basal ganglia, and the cerebral cortex. For instance, slow or absent saccadic movements are a predominant ocular feature of SCA2 originating from the degeneration of neurons in the oculomotor brainstem. In addition, frequently, ataxia onset coincides with painful muscle cramping, presumably resulting from a hyper-excitability state of the motor neurons, caused by collateral sprouting processes in their distal portions, after subtle axonal damage (Kanai and Kuwabara, 2009; Velazquez-Perez et al., 2017). Other non-cerebellar symptoms include involuntary muscle contractions (dystonia), muscle twitching or jerking (myoclonus), neuropathy (typically presenting as numbness, tingling, muscle weakness, and pain in the affected area), muscle spasticity, and cognitive, emotional, and behavioral difficulties arising from injuries in the frontal lobe of the brain (Geschwind et al., 1997; Velazquez-Perez et al., 2017).

Generally, SCA2 typically manifests during adulthood at the average age of 35 years, in patients carrying 32 or more CAG repeats in the *ATXN2* gene (Velazquez Perez et al., 2009).

However, the age of onset may vary depending on the extension of the polyQ sequence. Usually, larger polyQ tracts are associated with the earlier emergence of symptoms. Although SCA2 is considered a late-onset disease, infantile cases have been described associated with exceptionally large CAG sequences, ranging from 230 to 500 repeats (Mao et al., 2002). Pediatric cases of SCA2 often exhibit symptoms during the first months or years of life. These symptoms are usually displayed as retinitis pigmentosa (which can lead to vision loss, especially night blindness due to progressive loss of rod photoreceptor cells), myoclonic epilepsy, tetraparesis (muscle weakness of the four limbs), developmental delay, dysphagia (swallowing difficulties), facial dysmorphism, and infantile spasms (Babovic-Vuksanovic et al., 1998; Di Fabio et al., 2012; Mao et al., 2002; Moretti et al., 2004; Paciorkowski et al., 2011; Rufa et al., 2002). Additionally, infantile SCA2 can manifest as a global and severe cognitive regression, comprising a progressive deterioration of expressive language, comprehension, memory, graphomotor skills and dysarthria.

2.3. Neuropathology

Macroscopic neuroanatomical studies in post-mortem brain samples from SCA2 patients revealed a significant atrophy of major structures in the central nervous system (CNS), including the cerebellum, brainstem, frontal lobe, and nearly all cranial nerves, resulting in a reduction of the overall size of the brain (figure 1.1). A reduction in white matter was also described in the cerebrum and cerebellum, along with depigmentation of the midbrain substantia nigra, which may be related with the parkinsonian features in SCA2 (Estrada et al., 1999; Gwinn-Hardy et al., 2000; Infante et al., 2004; Seidel et al., 2012).

The most affected neurons in SCA2 are the Purkinje cells of the cerebellum, and histopathological studies demonstrated a pronounced loss of the Purkinje cell layer, accompanied by a reduction in the dendritic arborizations and torpedo-like deformations of the axons, in the early stages of the disease. Moreover, the granular cells and their parallel fibers as well as the climbing fibers arising from the inferior olive are sparse in SCA2 patients, compromising the input that the remaining Purkinje cells receive from these pathways. On the other hand, the dentate nucleus, one of the three deep cerebellar nuclei to where Purkinje cells project their axons, is relatively spared (Estrada et al., 1999). Further microscopic investigations showed that neuronal loss was more widespread, though still occurring in a region-selective manner. The brainstem from SCA2 patients had a noticeable loss of inferior olive and pontine neurons, and degeneration of other pre-cerebellar brainstem nuclei was also reported. In the mesencephalon, a noteworthy reduction of the neurons from the substantia nigra was observed. Moreover, the cerebral cortex, basal forebrain, thalamus, and spinal cord

also showed signs of neurodegeneration (Estrada et al., 1999; Gierga et al., 2005; from Rub et al., 2007; Seidel et al., 2012).

Neuroanatomical features of SCA2 have also been studied in living patients using advanced brain imaging techniques. Magnetic resonance imaging (MRI) scans revealed severe cerebellar volume loss in both white and gray matter, with atrophy of the pons, medulla oblongata, spinal cord, parietal cortex, and thalamus (Baldarcara et al., 2015; Hernandez-Castillo et al., 2015). MRI scans also suggested that atrophy was not uniform but rather region-specific within the pontocerebellar system. Both post-mortem observations and imaging studies suggest that different subregions could be differentially vulnerable to the pathogenetic mechanisms of SCA2 (Jung et al., 2012). However, the reason for this apparent region selectivity in SCA2 is still unknown.

Brain imaging techniques were also successful in detecting atrophy and/or dysfunction in preclinical SCA2 carriers. For example, positron emission tomography analyses detected a decrease in glucose metabolism in the pontocerebellar system, in two out of three SCA2 preclinical carriers, suggesting that degeneration of this area was taking place before the emergence of the first symptoms (Inagaki et al., 2005). In another study, MRI scans were able to identify cerebellar, pons, and frontal cortex atrophy in 24 SCA2 asymptomatic carriers (Velazquez-Perez et al., 2014). Altogether, these advanced brain imaging techniques are of great relevance when it comes to early diagnosis, serving as key instruments to identify SCA2 prior to the appearance of the first symptoms.

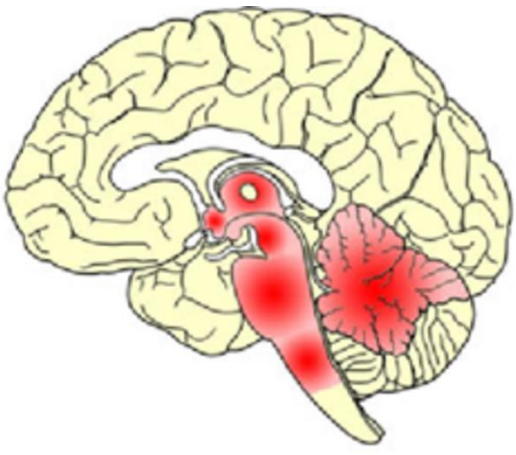

Figure 1.1 – Schematic representation of the most affected brain regions in SCA2. Anatomical regions of the brain displaying significant atrophy include the cerebellum, brainstem, and cranial nerves, which results in a reduction of the overall size of the brain. From Seidel et al., 2012.

2.4. SCA2 genetics

In 1996, the causative mutation of SCA2 was identified independently by three laboratories, in Japan, France, and USA, as an abnormal expansion of the CAG triplet repeats present in the first exon of the *ATXN2* gene (NCBI reference sequence: NG_011572.3) (Imbert et al., 1996; Pulst et al., 1996; Sanpei et al., 1996).

The *ATXN2* gene is located in the 12q23-24.1 chromosomal region, containing 25 exons and spanning 147,463 bp (figure 1.2) (Gispert et al., 1993). The CAG repeat tract encodes a polyQ sequence in the N-terminal region of the resulting protein ataxin-2. The canonical wild-type transcript length is 4,699 bp (Scoles and Pulst, 2018), but distinct isoforms have been described (Affaitati et al., 2001; Lastres-Becker et al., 2019; Nechiporuk et al., 1998). The *ATXN2* gene has two in-frame start codons at the 5'-end of the sequence, the second being located just four codons upstream of the CAG repeat region. The codon responsible for initiating translation is not consensual among the scientific community, because Western blot analyses typically produce a single band with a molecular weight consistent with the isoform that uses the most upstream ATG, while artificial luciferase-tagged *ATXN2* lacking the second ATG fails at expressing ataxin-2 (Scoles et al., 2012; Scoles and Pulst, 2018).

Normal *ATXN2* alleles carry 13-31 CAG repeats and more than 90% of the population harbors a 22 CAG tract (Andres et al., 2003). The high frequency of this allele may be explained by the great stability of the inherited repeats, which is thought to be conferred by the presence of one or two CAA interruptions in between the CAG units, following the $(CAG)_8$-CAA-$(CAG)_4$-CAA-$(CAG)_8$ pattern. Interestingly, slightly expanded alleles, comprising 28-33 CAG repeats and interrupted by CAA units, seem to predispose the carriers to elevated risk of developing ALS or Parkinson-plus syndrome (Furtado et al., 2002; Kim et al., 2007a; Ross et al., 2011). Because CAG and CAA are redundant codons, both coding for glutamine residues, the differences in the disease phenotypes may be determined by means of RNA toxicity rather than protein toxicity, in these cases (Charles et al., 2007; Yu et al., 2011).

On the other hand, SCA2-associated ATXN2 alleles usually present an uninterrupted, pure, CAG tract expanded beyond 32 CAG repeats, with full penetrance above 35 CAG units (Sequeiros et al., 2010). The absence of CAA interruptions in SCA2-associated alleles is thought to contribute to the lack of genetic stability, increasing their propensity to expand. The genetic instability echoes through the offspring, leading to larger expansions within each generation (Paulson, 2018). Usually, this results in earlier onset and increased severity of the disease, a phenomenon termed anticipation that enables the appearance of pediatric cases of SCA2 with very large CAG expansions, reportedly of up to 230-500 CAG units (Mao et al., 2002). Importantly, the variability in the age of onset is explained by the size of the CAG

expansion in only 60 to 80% of cases, suggesting that other mechanisms may be responsible for modulating the moment when the disease emerges, such as the existence of modifier genes, genetic polymorphisms, epigenetic factors, and unknown environmental determinants. For example, variations within the CAG repeat length of two distinct genes encoding other polyQ-containing proteins, *CACNA1A* and *RAI1*, were observed to be modifiers of SCA2 age of onset (Hayes et al., 2000; Pulst et al., 2005). In addition, a mitochondrial complex I gene variant and the GSTO2 rs2297235 "AG" single nucleotide polymorphism were both associated with the earlier onset of SCA2 (Almaguer-Mederos et al., 2017; Simon et al., 2007). Therefore, the study of allelic association in SCA2 may be of relevance to predict the age of onset of the disease with a higher degree of accuracy.

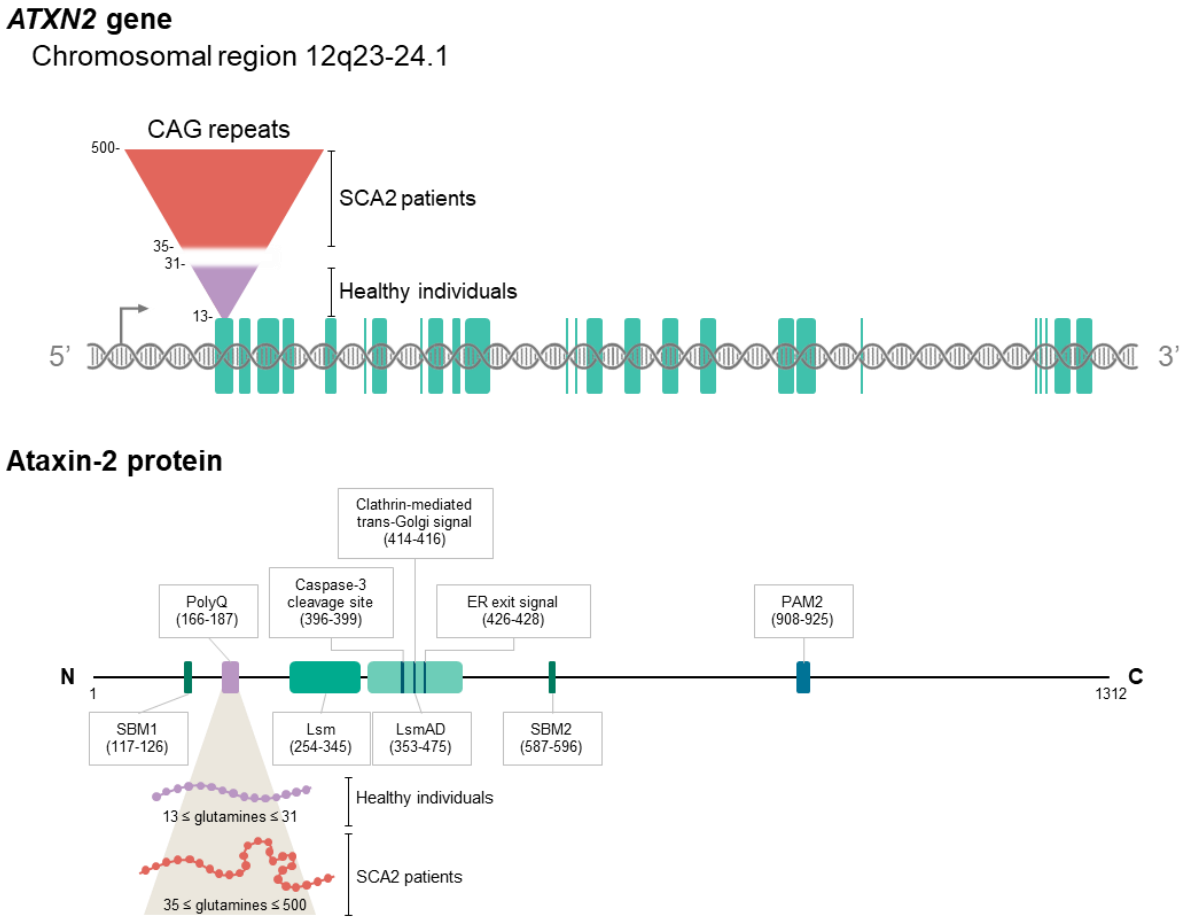

Figure 1.2 – Schematic representations of the ATXN2 gene and the ataxin-2 protein. The *ATXN2* gene comprises 25 exons (green) encoding ataxin-2. *ATXN2* contains a repetitive CAG region of variable length that may lead to development of SCA2 when this sequence is expanded beyond 31 CAG units, with full penetrance at 35 repeats. Ataxin-2 is comprised of 5 protein domains apart from the polyQ tract: SBM1, Lsm, LsmAD, SBM2 and PAM2. Expanded *ATXN2* alleles result in expanded polyQ tracts within ataxin-2, which may lead to alterations in intra- and intermolecular dynamics.

A strong positive correlation was observed between large normal alleles (23-31 CAG repeats) and SCA2 frequencies in most of the countries where epidemiological studies were conducted. It was found that Cuba, the country with the highest prevalence of SCA2, was also the one with the highest frequency of large normal alleles (Laffita-Mesa et al., 2014). Large normal alleles are genetically unstable, and this can lead to a continuous increase in the SCA2 prevalence as a result of this instability leading normal alleles to become expanded (Laffita-Mesa et al., 2012).

2.5. Ataxin-2 structure and functions

The *ATXN2* gene encodes ataxin-2 (Uniprot: Q99700-1), a ubiquitous protein that reaches its highest levels of expression in the nervous system, particularly in the cerebral cortex, basal ganglia, and cerebellum. Additionally, an already heightened expression of ataxin-2 in Purkinje cells further increases with age (Huynh et al., 1999). Regarding its subcellular location, ataxin-2 can be found diffused within the cytoplasm, in the ER (van de Loo et al., 2009), Golgi apparatus (Huynh et al., 2003), stress granules (SGs) (Nonhoff et al., 2007) and, in pathological conditions, inclusions (Egorova and Bezprozvanny, 2019).

Ataxin-2 is a large protein with low sequence complexity, which shares no structural or functional similarities with other glutamine-rich proteins associated with neurological diseases apart from the polyQ tract (Ordway et al., 1997).The canonical isoform corresponds to a 140 kDa protein, comprising 1,312 amino acids in the case of the most frequent variant in the global population, with 22 glutamines (figure 1.2). Ataxin-2 is a highly basic protein, except for an acidic region containing 46 amino acids (aa 254-475). It is predicted that this region defines two conserved globular domains named Lsm (Like Sm domain; aa 254-345), containing two RNA splicing motifs (Sm1 and Sm2; aa 230-233 and 283-286, respectively), and LsmAD (Lsm-associated domain; aa 353-475). Both domains are localized in the N-terminal portion of ataxin-2, downstream of the polyQ stretch (Albrecht et al., 2004; Huynh et al., 2000; Neuwald and Koonin, 1998). They confer the ability for ataxin-2 to bind RNA and, as an RNA-binding protein (RBP), ataxin-2 is expected to participate in RNA metabolism and/or regulation of translation. A study supporting this idea determined that ataxin-2 stabilizes target messenger RNAs (mRNAs). Ataxin-2 was reported to physically interact with uridine-rich elements within the 3'-UTR of its target mRNAs through the Lsm domain, consequently increasing protein abundance (Yokoshi et al., 2014). The LsmAD is located downstream of the Lsm domain, and it was found to harbor an endoplasmic reticulum (ER) exit signal (aa 426-428) required for ataxin-2 exportation from the ER, as well as a clathrin-mediated trans-Golgi signal (aa 414-416) required for the clathrin-mediated cleavage from the ER, Golgi apparatus or plasma

membrane (Huynh et al., 2003). In addition, the LsmAD also contains a predicted site for caspase-3 cleavage (aa 396-399), consistent with the production of an ataxin-2 fragment with 41.2 kDa that appears to be more abundant in human SCA2 brains. However, whether this truncation is important for SCA2 pathogenesis is still elusive (Huynh et al., 2000; Matos et al., 2017). Ataxin-2 also comprises two proline-rich Src homology 3 (SH3) domain binding motifs, SBM1 (aa 117-126) and SBM2 (aa 587-596), which are thought to interact with proteins harboring SH3 domains, including endophilins. Since endophilins are part of the endocytic machinery, it is believed that ataxin-2 may play a role in endocytosis (Nonis et al., 2008). Finally, the C-terminal region of ataxin-2 contains a poly(A)-binding protein (PABP) interacting motif (PAM2; aa 908-925). The PAM2 domain enables the physical interaction between ataxin-2 and PABP, a protein belonging to the translation initiation complex, which promotes mRNA circularization during mRNA translation (Bravo et al., 2005). The ataxin-2/PABP interaction functions as a true regulator of translation, because ataxin-2 counteracts mRNA circularization by destabilizing the translation initiation complex, when binding to PABP. As an example, re-establishing ataxin-2 levels in SCA3 mice downregulates ataxin-3 and mitigates the disease, while overexpressing PABP or ablating ataxin-2 PAM2 domain does not produce such effects (Nobrega et al., 2015).

Investigating the biologic functions of ataxin-2 has been revealed to constitute a real challenge. Currently, it is known that ataxin-2 participates in distinct cellular processes but, in a global perspective, its concrete role is not very well understood. To this date, ataxin-2 functions have been inferred through three different methods: (i) by observing the cellular and molecular impact of modulating ataxin-2 expression, either by overexpressing or silencing the protein, (ii) by using bioinformatic tools to detect structural similarity between ataxin-2 and other known proteins and identify already characterized motifs and domains, and (iii) by characterizing ataxin-2 intermolecular interactions. In regard to the first approach, ataxin-2 was suggested to regulate the presence of R-loops – triple-stranded nucleic acids encompassing a DNA-RNA hybrid and a single-stranded non-template DNA, which can be tolerated or cleared by cellular components – because ataxin-2-depleted cells tend to present an accumulation of these structures (Abraham et al., 2016; Salvi et al., 2014). Using the second method, ataxin-2 was proposed to function as an RNA regulator because of the structural similarities between its Lsm domain and the members of the LSm protein family, which is a family of RBPs (Tharun, 2009). On the other hand, since ataxin-2 interacts with PABP, and PABP is a translational regulator, it was inferred (and later verified) that ataxin-2 may also be involved in this same cellular process (Bravo et al., 2005). By taking advantage of these three methods, diverse biological functions have been proposed for ataxin-2 (figure 1.3), of which some were experimentally confirmed.

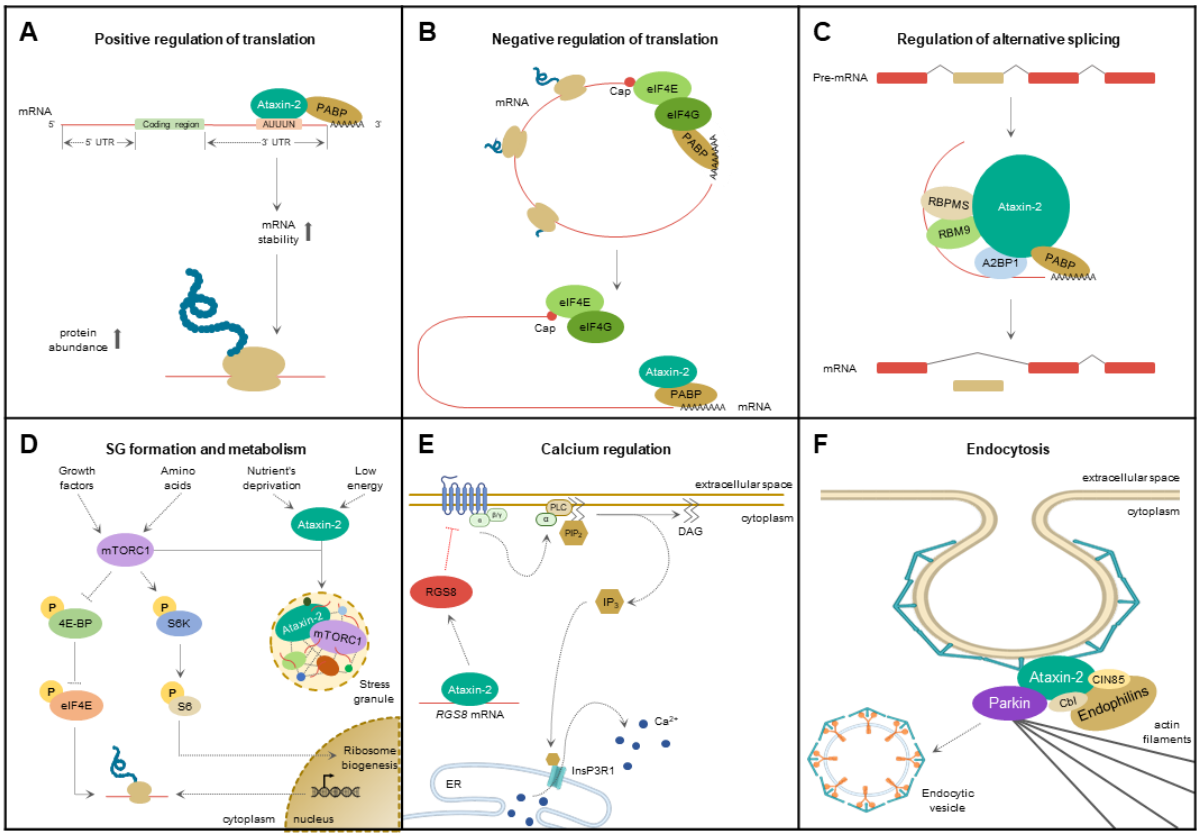

Figure 1.3 – Biologic functions of ataxin-2. Ataxin-2 was suggested to participate in many distinct cellular processes, including (A) the positive regulation of mRNA translation by stabilizing mRNAs, and (B) the negative regulation of mRNA translation by impairing the formation of the translation initiation complex. (C) Ataxin-2 may possibly regulate RNA splicing by interacting with proteins involved in this mechanism. (D) Ataxin-2 regulate metabolism upon sequestration of mTORC1 into SGs. (E) Ataxin-2 may negatively regulate mGluR1 by stabilizing RGS8 mRNA, thus increasing its abundance. (F) Ataxin-2 may be involved in endocytosis by interacting with endophilins, Cbl, and CIN85, which was shown to influence the internalization rate of EGFR.

2.6. Ataxin-2 interacting partners and associated biological functions

Due to the long list of ataxin-2 interacting partners, at least 182 experimentally confirmed to the present date (BioGRID ID: 112218), research into ataxin-2 functions has been particularly focused on studying its interactions.

Ataxin-2 physically interacts with proteins involved in alternative splicing, including A2BP1, the RNA-binding motif protein 9 (RBM9), as well as with the RNA-binding protein with multiple splicing (RBPMS). This molecular partners support the putative role of ataxin-2 in modulating RNA alternative splicing, by forming a complex with RBM9, RBPMS, A2BP1, PABP and the target RNA itself (Lim et al., 2006; Magana et al., 2013). Ataxin-2 has also been implicated in the suppression of mRNA translation by promoting the assembly of SGs and P-bodies, which are dynamic cellular components involved in mRNA triage (Marcelo et al., 2021; Nonhoff et al., 2007). Normally, SGs assemble as a response to different stress stimuli and

disassemble when the stimuli are no longer present. Meanwhile, RBP-bound mRNAs can be recruited to SGs, preventing mRNA translation, or released from these structures, re-entering a state of active translation (Anderson and Kedersha, 2006). In a similar manner, P-bodies can also regulate mRNA translation by sequestering and releasing mRNAs (Brengues et al., 2005), with the particularity that mRNA degradation may as well occur within these structures, promoted either by mRNA deadenylation or decapping mechanisms (Cougot et al., 2004; van Dijk et al., 2002). The DEAD box protein 6 (DDX6) is an RNA helicase that participates in both P-bodies and SGs assembly and is also an interacting partner of ataxin-2. It was suggested that ataxin-2 can interfere with SGs and P-bodies dynamics, as its modulation was able to destabilize these structures. In detail, the overexpression of ataxin-2 was shown to alter the subcellular location of DDX6 and impair the assembly of P-bodies, while its depletion disabled the formation of SGs, suggesting that ataxin-2 is required for SGs assembly (Nonhoff et al., 2007). Altogether, it is suggested that an adequate intracellular concentration of ataxin-2 is required for the normal functioning of these cellular structures. However, the molecular mechanisms through which ataxin-2 articulates with P-bodies and SGs dynamics are not well understood.

Staufen-1 (STAU1) is an RBP involved in SGs dynamics that binds double-stranded RNA and which was found to be present in mutant ataxin-2 aggregates in human SCA2 fibroblasts (Paul et al., 2018; Thomas et al., 2009). Furthermore, STAU1 is not only a regulator of RNA metabolism, but also participates in mRNA transport in neuronal dendrites (Kiebler et al., 1999; Kim et al., 2005; Kim et al., 2007b; Tang et al., 2001). The physical interaction between ataxin-2 and STAU1 is further evidence for the presumed role of ataxin-2 in multiple steps of RNA regulation, as well as in SGs dynamics (Paul et al., 2018). Moreover, increased levels of STAU1 expression can stimulate apoptosis as a response to multiple ER stressors, such as misfolded proteins (Gandelman et al., 2020). Interestingly, both animal models and fibroblasts derived from SCA2 patients present heightened steady-state levels of STAU1 expression, suggesting an association between expression of possibly misfolded expanded ataxin-2 and increased levels of STAU1, which may contribute to neuronal loss in SCA2 (Paul et al., 2018).

The RBPs TAR DNA-binding protein 43 (TDP-43) and fused in sarcoma (FUS) are mostly nuclear proteins that may harbor ALS-associated mutations, in which cases they assemble into SGs (Dewey et al., 2012). As mentioned before, a link between ataxin-2 with intermediate-length polyQ expansions and an increased risk of developing ALS has been established (Elden et al., 2010). A possible explanation for this association is based on the fact that ataxin-2 interacts with both TDP-43 and FUS, the former interaction occurring in an RNA-dependent manner (Elden et al., 2010; Farg et al., 2013). It was reported that intermediate-

length ataxin-2 can promote TDP-43 and mutant FUS mislocalization to the cytoplasm, decreasing their nuclear abundancy (Elden et al., 2010; Farg et al., 2013). Additionally, ataxin-2 co-localizes with ALS-associated mutant forms of TDP-43 and FUS in SGs (Nihei et al., 2012). It is likely that intermediate-length ataxin-2 can stably interact with TDP-43 and FUS, mislocate them to the cytoplasm and, consequently, recruit them into SGs, causing an ALS pathological situation.

The mammalian target of rapamycin (mTOR) signaling pathway controls cell growth, metabolism, and energy homeostasis by sensing the availability of nutrients and the energetic status of the cell. Its main function is to control protein synthesis by stimulating the initiation of mRNA translation, but since this is an energy-demanding anabolic process, it only occurs when nutrients are abundant and in the absence of bioenergetic deficits (Albert and Hall, 2015). Briefly, when these criteria are met, mTOR assembles with its partners, forming the mTOR complex 1 (mTORC1). After that, mTORC1 phosphorylates the eukaryotic initiation factor 4E (eIF4E)-binding protein 1 (4E-BP1) and the ribosomal S6 kinase (S6K). On one hand, the phosphorylation of 4E-BP1 leads to its inactivation and consequent release of eIF4E, which induces the cap-dependent translation initiation of mRNAs. At the same time, the phosphorylation of S6K activates its kinase activity, which then phosphorylates the ribosomal S6 protein at multiple sites to stimulate the transcription of ribosomal subunits (Albert and Hall, 2015). Recently, it was suggested that ataxin-2 regulates food intake and body weight by acting as a nutritional and energetic sensor, in a very complex network (Carmo-Silva et al., 2017). Nutrient deprivation and cellular bioenergetic deficits elicit the transcriptional activation of ataxin-2, increasing the abundance of the protein, which in turn inhibits mTORC1 signaling in direct and/or indirect manners. The direct mechanism of mTORC1 inhibition consists of its sequestration by ataxin-2 into SGs, hampering downstream signaling in this pathway (Takahara and Maeda, 2012). Indirectly, ataxin-2 inhibits the mTORC1 pathway by promoting reduced phosphorylation of 4E-BP1 and S6, consequently inhibiting the initiation of translation and ribosomal biogenesis, respectively (Lastres-Becker et al., 2016). Altogether, ataxin-2 seems to contribute to the slowing of the cell's anabolic state under starvation-induced stress.

Ataxin-2 has also been implicated in the regulation of calcium-mediated signaling through its interaction with regulator of G protein signaling 8 (RGS8) mRNA. RGS8 is a brain-specific regulator of G protein-coupled receptors (GPCRs), showing high levels of expression in cerebellar Purkinje cells. RGS8 acts by stimulating the GTPase activity of the GPCR alpha subunit, turning it into its GDP-bound inactive form and, thus, blocking signal transduction. Consequently, calcium release into the cytosol is stopped (Saitoh et al., 2003). It is believed that, in Purkinje cells, ataxin-2 regulates RGS8 mRNA, presumably by stabilizing it, which in turn negatively regulates the metabotropic glutamate receptor subtype 1 (mGluR1)-mediated

signaling, preventing potential consequences of excitotoxicity caused by exacerbated intracellular levels of calcium (Paul et al., 2014).

Ataxin-2 was also found to interact with parkin, an E3 ubiquitin ligase associated with Parkinson's disease (PD) (Huynh et al., 2007), and with cyclin-dependent kinase 5 (Cdk5) (Asada et al., 2014). Parkin and Cdk5 seem to regulate the steady-state protein levels of both the wild-type and the polyQ-expanded ataxin-2, through ubiquitination and phosphorylation, respectively. These post-translational modifications signal ataxin-2 for degradation by the proteasome, thus inducing ataxin-2 turnover. Interestingly, both parkin and Cdk5 act more efficiently on the polyQ-expanded protein, with Cdk5 decreasing mutant ataxin-2 levels to a greater extent (~60% reduction), when compared to the wild-type form (~25% reduction) (Asada et al., 2014; Huynh et al., 2007). On the other hand, parkin itself is phosphorylated by Cdk5, reducing its ubiquitin ligase activity (Avraham et al., 2007). This interaction may suggest the existence of a crosstalk between the two distinct mechanisms of ataxin-2 clearance. However, despite the apparent triad of interactions between ataxin-2, parkin and Cdk5, it is still not clear whether the two pathways are related, concerning ataxin-2 turnover.

Ataxin-2 has been further implicated in endocytosis and cytoskeleton organization due to the physical interactions it establishes with endophilins A1 and A3, E3 ubiquitin ligase Cbl, adaptor Cbl-interacting protein of 85 kDa (CIN85), and protein kinase Src. Endophilins A1 and A3 are part of a protein complex that facilitates the formation of the plasma membrane curvature at sites where endocytosis is occurring. As an example, upon stimulation of the epidermal growth factor receptor (EGFR), endophilins A assemble with Cbl, CIN85, and Src, to promote EGFR internalization. A study revealed that ataxin-2, participates in this process. This participation of ataxin-2 was found to delay EGFR's internalization as ataxin-2-knockout cells present a faster internalization rate of the receptor. Ataxin-2 was thus considered a regulator of endocytosis, acting as part the endocytic machinery (Nonis et al., 2008). Endocytosis occurs through the activation of a ubiquitination-regulated protein complex coupled with actin filaments. The ubiquitination-mediated activation of endocytosis is presumably driven by parkin, since parkin ubiquitinates endophilins, as well as its major binding partners dynamin and synaptojanin-1, which are also involved in endocytosis (Cao et al., 2014). Furthermore, parkin also targets the epidermal growth factor receptor substrate 15 (Eps15) for ubiquitination, another protein involved in endocytosis (Fallon et al., 2006). The fact that parkin is so functionally present in endocytosis, together with the interaction between ataxin-2 and parkin, further supports the role of ataxin-2 in the process.

Endophilin A1 was shown to promote actin polymerization in dendritic spines (Yang et al., 2018). Since ataxin-2 interacts with endophilin A1, it is reasonable to consider that it may

also be involved in the regulation of the actin cytoskeleton. This hypothesis was addressed much earlier, in a study using *Drosophila melanogaster*, where it was suggested that the ataxin-2 homolog regulates actin filament formation, indirectly, in a dose-dependent manner (Satterfield et al., 2002). Later, it was revealed that ataxin-2 interacted with plastin in the brains of mice, a protein known to bind to actin filaments and promote the assembly of actin bundles (Ralser et al., 2005). Another study suggested that ataxin-2 may be necessary for the regulation of microtubule dynamics, because *Caenorhabditis elegans* mutants for the ataxin-2 ortholog displayed enhanced microtubule nucleation at the centrosome, but short microtubule formation towards the cellular cortex (Stubenvoll et al., 2016). Taking all observations together, proper regulation of the cytoskeleton by ataxin-2 may be fundamental to maintain not only the physical structure of the cell but also to support normal cellular trafficking.

2.7. Expanded ataxin-2 and SCA2 molecular pathogenesis

The resulting polyQ-expanded ataxin-2, with 32 or more glutamines, displays altered biological functions as a result of the protein's gain and/or partial loss-of-function, ultimately leading to the development of SCA2 (Velazquez-Perez et al., 2017). Currently, whether the *ATXN2* mutation represents a loss-of-function or gain-of-function mutation is still a matter of debate (Egorova and Bezprozvanny, 2019). On one hand, the absence of functional ataxin-2 disturbs mRNA-related metabolic processes including mRNA stability, translation, and degradation (Nonhoff et al., 2007). It also enhances the mTORC1-mediated ribosomal biogenesis and translation initiation (Lastres-Becker et al., 2016; Takahara and Maeda, 2012), leading to nutritional and metabolic alterations, and promotes neuronal toxicity due to impaired regulation of the intracellular calcium release via *RGS8* downregulation (Dansithong et al., 2015; Paul et al., 2014). However, opposing to its wild-type form, the polyQ-expanded ataxin-2 tends to aggregate into inclusion bodies (Seidel et al., 2017) and gains the ability to directly interact with InsP3R1 (Liu et al., 2009).

For many years, extensive research has been conducted to clarify the molecular mechanisms underlying SCA2 pathogenesis, for understanding the disease at the molecular level will help identify relevant targets for the development of efficient treatments. In general, the mechanisms of pathogenesis proposed for SCA2, resulting from the abnormal expansion of ataxin-2, include: protein aggregation, impairment of autophagy, deleterious mRNA processing, RNA-mediated toxicity, enhanced oxidative stress, cell signaling alterations, and disturbances in calcium homeostasis.

2.7.1. Protein aggregation

The abnormal expansion of the polyQ tract of ataxin-2 shifts its conformation to a β-sheet-rich structure, rendering ataxin-2 more prone to form insoluble aggregates with amyloid fibrillar morphology, which accumulate in neurons as inclusion bodies (Takeuchi and Nagai, 2017). Protein aggregation is a common histopathological feature observed in all polyQ diseases, and aggregates can either be cytoplasmic or intranuclear. In SCA2, they are mainly found in the cytoplasm, but intranuclear aggregates have also been reported (Seidel et al., 2012). The presence of ubiquitin-positive protein aggregates is a common feature of polyQ diseases (Gutekunst et al., 1999), but ubiquitinated intranuclear aggregates are rare in SCA2; they were most frequently found in pontine neurons, but only in 1-2% of cells, and were absent from Purkinje neurons (Koyano et al., 1999). Moreover, aggregates from human SCA2 brain samples were found to contain other proteins, including ataxin-1, ataxin-3, and the TATA box-binding protein (Uchihara et al., 2001).

Whether polyQ aggregates are able to induce neuronal death is still controverse among the polyQ diseases research community because, while some studies report a positive correlation between the presence of polyQ aggregates and neurodegeneration (Cooper et al., 1998; Martindale et al., 1998), others suggest that intracellular aggregates may be cytoprotective (Gutekunst et al., 1999; Kuemmerle et al., 1999). The hypothesis whereby polyQ aggregates are neurotoxic is supported by the fact that some proteins that are critical for neuronal survival can be sequestered into inclusion bodies (Chai et al., 2002; Nucifora et al., 2001). However, it has been suggested that large macromolecular inclusions are cytoprotective, whereas smaller intermediate species, such as mutant polyQ-containing oligomers and misfolded monomers, which are formed during the aggregation process, are the actual cause of toxicity (Arrasate et al., 2004; Takahashi et al., 2008).

2.7.2. Impairment of autophagy

The clearance of polyQ-containing aggregates occurs through autophagy (Jimenez-Sanchez et al., 2012), a selective lysosomal-mediated degradation process, which is involved in maintaining protein homeostasis. Generally, apart from autophagy, the degradation of misfolded proteins can also occur through the ubiquitin-proteasome system (UPS), however, proteins containing long polyQ tracts are not efficiently degraded by eukaryotic proteasomes (Venkatraman et al., 2004). Furthermore, important UPS components can be sequestered to polyQ-containing aggregates, hindering the degradation of misfolded polyQ proteins (Park et al., 2013). Hereupon, in a polyQ disease context, protein turnover may rely on autophagy, as it can degrade both aggregated and soluble forms of expanded proteins (Ravikumar et al.,

2002). However, autophagy impairment seems to be common among polyQ diseases such as HD, SBMA, SCA1, SCA3, SCA7, and SCA17 (Cortes and La Spada, 2015). Despite the fact that autophagy impairment has not yet been reported in SCA2, strong evidence suggests that it does occur, since fibroblasts from SCA2 patients show an accumulation of the autophagic markers sequestosome-1 (p62/SQSTM1) and light chain 3 isoform II (LC3-II), indicating a reduction in the autophagic flux (Paul et al., 2018). If autophagy is indeed impaired in SCA2 and considering that the UPS may as well be dysfunctional, in combination, both may pose a severe obstacle in the maintenance of cellular proteostasis.

2.7.3. Deleterious mRNA processing

The ataxin-2-binding protein 1 (A2BP1), also known as RNA-binding protein fox-1 homolog 1 (RBFOX1; Uniprot: Q9NWB1), is an ataxin-2 interacting partner that binds to its C-terminus (Shibata et al., 2000). A2BP1 is an RBP involved in the alternative splicing of the subunit 1 of N-methyl-D-aspartate (NMDA) receptors (GluN1) (Lee et al., 2009). NMDA receptors can modulate excitatory synaptic transmission in several brain regions, including the hippocampus, where they participate in long-term potentiation and learning (Rigby et al., 2002). Distinct splice variants of the GluN1 subunit of NMDA receptors can impact excitatory synapses differently. For instance, the excision of exon 5 from the transcript encoding the GluN1 subunit results in an overproduction of excitatory synapses that can render neuronal populations more prone to excitotoxicity (Liu et al., 2019). Interestingly, under certain circumstances, the splicing regulator A2BP1 can target exon 5 of the GluN1 subunit of NMDA receptors (Lee et al., 2009), suggesting that A2BP1 could predispose neurons to excitotoxicity. Moreover, although ataxin-2 is ubiquitously expressed, A2BP1 expression is more restricted and, interestingly, one of A2BP1 isoforms is strongly expressed in the cerebellum, particularly in Purkinje cells. Since both ataxin-2 and A2BP1 are strongly expressed in Purkinje cells, which are the most affected cells in SCA2, and considering that they interact, this raises the possibility that ataxin-2 may act as a regulator of A2BP1. In this manner, mutant ataxin-2 could lose the ability to interact with A2BP1 and thus promote excitotoxicity, which could possibly explain the cell type-specific neuronal death observed in SCA2 neuropathology (Shibata et al., 2000). However, despite the tempting speculation, further research would be needed to clarify this scenario.

2.7.4. RNA-mediated toxicity

Apart from the protein-derived neuronal toxicity observed in SCA2, there is strong evidence that an aberrant natural antisense transcript (NAT)-based process may also be involved in SCA2 pathogenesis. NATs are antisense RNAs transcribed from the opposite, non-template, DNA strand, which can regulate gene expression at multiple levels and their dysregulation has been associated with disease development (Wanowska et al., 2018). The *ATXN2* locus was shown to be transcribed bidirectionally, originating the mRNA encoding ataxin-2 and an antisense transcript called *ATXN2-AS*. SCA2-associated *ATXN2-AS* transcripts contain an abnormally expanded CUG sequence and were found to be present in *post-mortem* human SCA2 patients brains, as well as in patient-derived fibroblasts, induced pluripotent stem cells, and neural stem cells (Li et al., 2016). The same study reported that the abnormally expanded *ATXN2-AS* transcript was toxic in a cellular model of SCA2 and it was able to form RNA foci in the cerebellar Purkinje cells of SCA2 mice and in *post-mortem* human brains. Similar to myotonic dystrophy type 1 and HD-like 2, the RNA foci detected in the brains of SCA2 patients were found to sequester the muscleblind-like protein 1 (MBNL1), a splicing regulator of the amyloid-beta precursor protein (APP) and GluN1 (Jiang et al., 2004; Li et al., 2016; Rudnicki et al., 2007). The sequestration of MBNL1 into RNA foci is consistent with the presence of misspliced forms of APP and GluN1 in the brains of SCA2 patients, a pattern of missplicing resembling that one found in Alzheimer's disease (AD) (Li et al., 2016). Taking all observations together, RNA-mediated toxicity, in combination with putatively toxic oligomers, may explain the neurodegeneration observed in those cases where protein aggregation did not correlate with cell death (Arrasate et al., 2004; Gutekunst et al., 1999; Kuemmerle et al., 1999; Takahashi et al., 2008). In this manner, it is possible that the *ATXN2-AS* transcript contributes to SCA2 pathogenesis, representing an additional pathogenic mechanism that synergizes with the deleterious effects of mutant ataxin-2, subsequently promoting neuronal death.

2.7.5. Enhanced oxidative stress

PTEN-induced kinase 1 (PINK1) is a mitochondrially targeted serine/threonine kinase thought to play a neuroprotective role by preventing mitochondrial dysfunction-mediated damage, oxidative stress, and apoptosis (Deas et al., 2009; Matsuda et al., 2013). Global transcriptome analyses performed by deep RNA-sequencing suggest that ataxin-2 may positively regulate PINK1 by interfering with its mRNA processing, as it was shown that ataxin-2-knockout mice present severely reduced expression of PINK1, whereas blood samples from SCA2 patients show an increase of its expression (Sen et al., 2016). Enhanced expression

levels of PINK1 in SCA2 may indicate disturbances in mitochondrial health and an aberrant response to oxidative stress. Supporting this hypothesis, fibroblasts from SCA2 patients were shown to aberrantly express two antioxidant enzymes: (i) mRNA and protein levels of Cu/Zn superoxide dismutase (SOD1) enzyme were found to be increased, while (ii) the catalase enzyme was significantly downregulated (Cornelius et al., 2017). The superoxide anion is a toxic byproduct originating from mitochondrial oxidative phosphorylation, which is converted into hydrogen peroxide (H_2O_2) by the SOD1 enzyme. H_2O_2 is also a highly toxic reactive oxygen species, which needs to be further decomposed into water and oxygen by the catalase enzyme (Lin and Beal, 2006). The fact that SOD1 levels are increased in SCA2, together with the decreased expression of the catalase enzyme, means that high amounts of H_2O_2 are produced but its conversion into non-toxic molecules is impaired. Consequently, H_2O_2 may accumulate, suggesting that these abnormalities could contribute to increased oxidative stress and consequent cell death (Cornelius et al., 2017).

2.7.6. Cell signaling alterations

Considering the importance that cell signaling has in development, cell repair and communication, neurogenesis and the overall maintenance of cellular homeostasis, it is expected that disturbances in cell signaling mechanisms may underly diverse pathological processes and contribute to neurodegeneration (Egorova and Bezprozvanny, 2019). In fact, alterations in the activity of signaling proteins have been described in distinct types of ataxia (Brown et al., 2018; Verbeek et al., 2008) and, since SCAs share some common mechanisms of pathogenesis, it could be expected that signaling disturbances are also a feature of SCA2. In fact, SCA2 mouse models display severely reduced levels of metastasis suppressor protein 1 (MTSS1), a suppressor of the Src family of non-receptor tyrosine kinases (SFK). These are signaling proteins involved in nervous system homeostasis and are associated with neurodegenerative diseases. It was found that decreased levels of MTSS1 lead to increased SFK signaling, consequently reducing the arborizations of Purkinje cells and lowering their basal firing rates. The aberrant SFK-mediated signaling may ultimately lead to neuronal death, thus contributing to SCA2 pathogenesis (Brown et al., 2018).

2.7.7. Disturbances in calcium homeostasis

Calcium ions act as second messengers and are thus fundamental for cell signaling. Moreover, certain regulatory proteins and enzymes depend on calcium to exert their functions. However, high levels of calcium within the cytosol can disturb neuronal signaling and cellular

homeostasis, leading to synaptic loss and neuronal death. Therefore, intracellular calcium levels have to be tightly controlled, in order to assure the functioning of calcium-dependent proteins, but also avoid excitotoxicity (Egorova and Bezprozvanny, 2019).

Transcriptome analyses performed by deep RNA-sequencing, complemented with Western blot analyses, revealed a decrease in RGS8 mRNA levels and even more severely reduced steady-state protein levels, both in the cerebellum of a SCA2 animal model and in lymphoblastoid B cells from SCA2 patients. This can be explained by the impaired interaction between RGS8 mRNA and the polyQ-expanded ataxin-2, as determined by RNA immunoprecipitation (Dansithong et al., 2015). The absence of negative regulation of the mGluR1 signaling may lead to increased calcium concentration in the cytosol, thus prompting excitotoxicity and neuronal death.

On the other hand, polyQ-expanded ataxin-2, but not its wild-type form, interacts with the type 1 inositol 1,4,5-trisphosphate receptor (InsP3R1) in the ER membrane. This aberrant interaction leads to an increased sensitivity to inositol 1,4,5-trisphosphate (IP3), hyperactivation of InsP3R1 and, consequently, high amounts of calcium are released from the ER into the cytosol (Liu et al., 2009). The overloaded calcium ions may be pumped into the mitochondria, leading to mitochondrial swelling and further rupture of its outer membrane. Finally, mitochondrial rupture could release cytochrome *c* into the cytosol, triggering apoptosis and leading to neuronal death (Egorova and Bezprozvanny, 2019; Liu et al., 2009).

2.8. Region-selective neurodegeneration in SCA2

The typical pattern of brain damage in anatomically interconnected areas of the brain, in SCA2, suggests the existence of one or more mechanisms through which neurodegeneration progresses in space. It is reasonable to hypothesize that SCA2 may spread along the brain from one anatomical region to the next, in a stepwise manner, similar to that which has been proposed for AD and PD pathogenesis (Braak and Del Tredici, 2011; Dunning et al., 2012; Jucker and Walker, 2011). In fact, neurodegeneration in SCA2 was suggested to occur in directly anatomically interconnected brain areas, following the neuronal fibers described by tracing studies in non-human primates (Braak and Del Tredici, 2011; Dunning et al., 2012; Jucker and Walker, 2011; Rub et al., 2000).

Possible explanations for neuron-neuron propagation may include mechanisms of transsynaptic and interneuronal spread of aggregates of disease-associated proteins, through tunneling nanotubes, for example, or the propagation of such proteins in a prion-like manner (Goedert et al., 2010; Jucker and Walker, 2011). The evaluation of spatiotemporal expansion

of the neurodegenerative processes in SCA2 could permit an accurate reconstruction of the mechanisms involved and allow the identification of the origin of SCA2 pathology. Importantly, these regions may be potential targets for therapeutic interventions, which could halt or delay the spreading of SCA2, by impairing the stepwise cascade of neurodegeneration (Rub et al., 2013).

3. Intercellular communication

Every cell, from the simplest bacterium to the most complex eukaryotic cell, monitors its intracellular and extracellular environment, processes the acquired information, and responds accordingly to the detected conditions. The ability to respond to physical and chemical changes within the environment was developed by unicellular organisms, long before multicellular life emerged. For example, although bacteria live mostly independent lives, they can communicate with each other and accumulate at higher populational density in response to chemical signals secreted by their neighbors. This process is called *quorum sensing* and allows bacteria to coordinate their behavior and carry out colony-wide functions, such as transferring genetic material between individuals or forming biofilms. By communicating with one another, bacteria are able to increase their survival chances and maintain the existence of their species (Alberts, 2015).

During the evolution of multicellular organisms, intercellular communication achieved a high degree of complexity. Individual cells began to associate as groups, in which survival of the whole organism is often privileged in detriment of that of individual cells. Mechanisms of intercellular communication continued evolving, forming extremely complex signaling networks that allowed the collaboration and coordination of different cell types and, later, different tissues (Alberts, 2015). The communication between distinct cell types and tissues became so fundamental for the development and homeostasis of multicellular organisms that a possible failure in the communication network can lead to disease states (Müller and Schier, 2011).

3.1. Types of intercellular communication

Most cells in multicellular organisms emit and receive signals. These intercellular signals are mainly extracellular signaling molecules that can travel long distances and target cells far away from where the signal was emitted, or they can remain within the milieu near the emitter cell and signal to immediate neighbors. Signaling molecules, such as particular proteins, bind to and activate specific receptors on the cell surface, or inside the cytoplasm,

triggering signaling cascades that ultimately stimulate effector proteins, the ones actively promoting alterations in the cell's behavior (Alberts, 2015).

Typical short-range communication comprises three distinct types of signaling methods: juxtacrine or contact-dependent, paracrine and autocrine signaling (Alberts, 2015). Juxtacrine signaling occurs when the signaling molecules remain bound to the surface of the signaling cell, influencing only the cells with which it establishes direct contact. This type of intercellular communication provides a mechanism for strict spatial control and is especially important, for example, during development and immune responses, occurring through the Notch signaling pathway during neural development (Chitnis, 1995) or through the physical interaction between T cells and antigen-presenting cells at immunological synapses, respectively (Dustin and Choudhuri, 2016).

Sometimes, cells synthesize diffusible molecules known as paracrine factors. These molecules can travel small distances (40-200 μm) through the extracellular milieu and interact with neighboring cells to influence their behavior. This type of interaction is called paracrine signaling and is involved in several stages of development. The most common paracrine factors include members of the fibroblast growth factor, Hedgehog, Wnt and transforming growth factor β families (Barresi and Gilbert, 2020).

Autocrine signaling is a particular type of paracrine interaction where an individual cell is both the emitter and the receiver of the signal. In other words, the cell secretes a molecule for which it has its own receptor (Barresi and Gilbert, 2020). Autocrine interactions are not very common and are mostly associated with cancer, in which the cells often secrete extracellular signals to stimulate their own survival and proliferation (Alberts, 2015). Although rare, this type of self-interaction also occurs in physiological conditions. For example, placental cytotrophoblasts require explosive proliferation for the formation of the placenta and, for that reason, they secrete platelet-derived growth factor, whose receptor is present in the membrane of cytotrophoblasts (Goustin et al., 1985).

To coordinate the behavior of cells that lie in distant parts of the organism, some signaling molecules have to travel long distances. Large multicellular organisms like humans evolved mechanisms of long-range intercellular communication, including specialized cell types. For example, neurons project their axons far away and contact their target cells at specialized sites called synapses. In the case of chemical synapses, upon stimulation by other nerve cells lying more upstream, neurons send action potentials along their axons, which will trigger the secretion of neurotransmitters into the synaptic cleft, in case it targets another nerve cell, or into a neuromuscular junction, in case it targets a muscle fiber. Neurotransmitters will act as chemical signals that will be delivered specifically to their matching receptors within the

postsynaptic membrane or the muscle fiber's sarcolemma. The response originating from the synaptic signaling depends on the neurotransmitter being secreted (Alberts, 2015).

Endocrine signaling consists of targeting distant cells through the secretion of signaling molecules, known as hormones, into the bloodstream. Hormones can travel far and wide and, thus, are able to act on target cells, in any region of the body (Alberts, 2015). As an example, insulin is a hormone secreted by the β cells of the pancreas that then travels through the circulatory system until it reaches its target organs (liver, skeletal muscle and adipose tissue), where it stimulates glucose uptake and glycogenesis (Baron and Van Obberghen, 1995).

Non-conventional mechanisms of intercellular communication have recently captivated the interest of researchers all around the world, from the moment it was noticed that not only individualized signaling molecules can alter a cell's behavior. Interestingly, multimolecular structures composed of lipids and nucleic acids can be transferred from one cell to another by distinct mechanisms. Moreover, those molecules can actively change a cell's behavior, for example, by stimulating GPCRs or by modifying the target cell's expression pattern, respectively (Hannun and Obeid, 2008; Maas et al., 2017; Okajima, 2002; Sherer and Mothes, 2008). One of such intercellular communication mechanisms, promoting both lipid and genetic material transferring between cells, consists of the natural release of lipid bilayer-delimited particles called extracellular vesicles (EVs). The role of EVs as agents of intercellular communication will be detailed in depth in the following topics.

3.2. Extracellular vesicles

3.2.1. Historical background

EV is a general term used when referring to membrane-enclosed structures that are naturally released from cells, which can be found in almost every bodily fluid, including blood, urine, semen, saliva, cerebrospinal fluid (CSF) and breast milk (Admyre et al., 2007; Boukouris and Mathivanan, 2015; Cheng et al., 2014; Madison et al., 2017; Michael et al., 2010). The initial understanding of membrane shedding came from studies in reticulocytes, which are precursors of mature erythrocytes that shed about one third of their membranes during maturation. During this maturation process, the transferrin receptors at the surface of reticulocytes were found to be endocytosed, preceding the formation of multivesicular endosomes, also called multivesicular bodies (MVBs). After endocytosis, the transferrin receptors were found at the surface of small vesicles (approximately 50 nm in diameter), with the same orientation as if they were at the cell's surface. These small vesicles were contained inside of MVBs, for which they became known as intraluminal vesicles (ILVs). A critical finding

arose in the 1980s, when two research groups showed, independently, that the transferrin receptors were exocytosed into the extracellular space, contained within the surface of small vesicles. The authors then suggested that the MVBs fused with the plasma membrane, releasing ILVs containing the transferrin receptor by exocytosis (Harding et al., 1983; Pan et al., 1985). Johnston and colleagues then coined the term “exosomes” to describe the vesicles formed inside MVBs that are released into the extracellular milieu (Johnstone et al., 1987).

Research within the EV’s field remained dormant for over a decade because EV release was initially considered solely a system for “waste disposal”, through which cells could get rid of toxic molecules or were able to remove protein/membrane components during differentiation, as it is the case of the transferrin receptor disposal from reticulocytes. It was not until 1996, when EVs resembling exosomes were suggested to play an important role as intercellular messengers. At that time, researchers revealed that B cells were able to release major histocompatibility complex class II (MHC-II)-enriched exosomes, which were able to present antigens to T cells and, consequently, induce MHC-II-restricted T cell responses (Raposo et al., 1996). The idea that EVs could act as antigen presenters to stimulate immune responses quickly roused interest, especially within the cancer research field. In 1998, researchers isolated EVs from tumor peptide-pulsed dendritic cells and delivered those EVs to murine models with established tumors. As a result, EVs seemed to prime specific cytotoxic T cells *in vivo*, which led to tumor growth suppression or eradication (Zitvogel et al., 1998). Facing such promising results, human phase I clinical trials were rapidly performed in 2005, following the same rationale: EVs derived from autologous dendritic cells were administered to metastatic melanoma patients. This study highlighted the feasibility of large-scale EVs production and showed that EVs administration is safe in metastatic melanoma patients. However, only one patient exhibited a partial response to the EV-based treatment (Escudier et al., 2005).

Up to this point, studies focusing on EVs proteome were dominant (Potolicchio et al., 2005; Simpson et al., 2008; Xiao et al., 2009), and it was shown that EVs could interact with cell surface receptors, similar to ligand-receptor interactions, to present antigens, for example (Raposo et al., 1996). Alternatively, EVs could attach to or fuse with the target cell membrane, or even be endocytosed by the recipient cell. In all cases, delivery of EV surface proteins into the recipient cell, and perhaps proteins contained within EVs, would be expected to occur (Clayton et al., 2004; Denzer et al., 2000; Morelli et al., 2004). EV-mediated protein transfer between cells could putatively alter the receiver’s behavior and, for that reason, researchers were keen to determine which proteins would potentially be transferred between cells. However, in 2007, a huge discovery struck the EV research community: it was demonstrated that EVs can also mediate the transfer of functional RNAs, especially mRNAs and microRNAs

(miRNAs), from one cell to another (Valadi et al., 2007). This finding allowed the emergence of an ongoing research line as, in that study alone, mRNAs from approximately 1300 genes were detected. Additionally, the fact that many miRNAs may also be present and that different cell types secrete EVs with different compositions suggests an overwhelming set of possibilities and combinations that can occur within an organism. An even higher level of complexity emerges when the cell targeting possibilities of a particular type of EV are considered. Thus, the almost-never-ending questions in the EVs field are: what is the composition of a particular type of EV deriving from a particular cell type? And what cells can be targeted by that EV? Some researchers devoted their efforts to answer these questions, at least in part. For instance, some types of cancer cells release EVs with their own molecular signature. The emitting source can be determined by understanding the EVs signature. For this reason, researchers believe that EVs possess great potential as biomarkers of disease (Skog et al., 2008; Taylor and Gercel-Taylor, 2008). On the other hand, by understanding the potential targets, one may take advantage of EVs to deliver therapeutic molecules, such as synthetic drugs or nucleic acids, to a particular cell type (Guo et al., 2019; Lamichhane et al., 2016).

3.2.2. Classification and nomenclature

EV is an umbrella term used when referring to every lipid bilayer-containing structure released from cells. Since the early stages of EVs research, researchers have struggled with the classification criteria and nomenclature for EVs, because, regardless of the classification method being used, there always seems to be a gray zone where different classes of EVs overlap. Sometimes it is challenging to differentiate subsets of EVs, and ambiguous classification criteria can occasionally cause uncertainties. For this reason, numerous methods are currently being used to catalogue EVs.

EVs can be named based on their cellular origin; for example, dexosomes and prostasomes are EVs derived from dendritic cells and prostate epithelial cells, respectively (Morse et al., 2005; Ronquist and Brody, 1985). However, EVs are usually classified based on their mechanisms of biogenesis, composition, and biophysical properties, such as their size. By using these three criteria simultaneously, researchers have tried to reach a consensus regarding the nomenclature of EVs, which can be divided into three major subtypes: exosomes, ectosomes or shedding microvesicles (MVs), and apoptotic bodies. A common feature between these three subtypes of EVs is the existence of a lipid bilayer membrane surrounding a specific cargo of biomolecules, which can be either proteins, RNA, DNA, and bioactive lipids (Malkin and Bratman, 2020; Sagini et al., 2018; Tian et al., 2021; Veziroglu and

Mias, 2020). Among these EV subsets, exosomes constitute the most well-studied type (Mathivanan et al., 2021).

Besides the three subtypes of EVs mentioned above, other subsets of EVs have been described in the literature, differing in size, composition, and mechanisms of biogenesis. Such not-so-common subtypes of EVs include exomeres (<50 nm), migrasomes (500-3,000 nm), and large oncosomes (1,000-10,000 nm). However, for simplicity, this thesis will only focus on exosomes and MVs, which will be referred together as EVs.

Exosomes are very small vesicles measuring 30-150 nm in size. They are formed as a result of the inward budding of the endosomal membrane and accumulate as ILVs inside MVBs (Théry et al., 1999). These large MVBs can have two different fates: they can either fuse with lysosomes for degradation of their cargo, or they can follow the exocytic pathway and fuse with the plasma membrane. In this latter scenario, ILVs are released into the extracellular space and are referred to as exosomes (Kalra et al., 2016). The molecular mechanisms determining the fate of MVBs and those regulating the sorting of specific cargo into ILVs remain poorly understood (Simons and Raposo, 2009). Nevertheless, the endosomal sorting complexes required for transport (ESCRT) machinery is thought to play a role in some parts of these mechanisms, since ESCRT complexes assemble at the endosomal membrane, promoting its bending and the scission reaction away from the cytoplasm (Colombo et al., 2013; Schmidt and Teis, 2012). However, ILVs may be formed through ESCRT-independent mechanisms, which are thought to involve the tetraspanin family of transmembrane proteins (Jankovičová et al., 2020) or the conversion of sphingomyelin to ceramide pathway (Trajkovic et al., 2008). The mechanisms of exosomal biogenesis will be covered in the following topic.

In contrast to exosomes, MVs are a heterogeneous population of larger vesicles with 100-1,000 nm in diameter, which result directly from the outward budding of the plasma membrane (Mathivanan et al., 2021). Like exosomes, MVs carry a molecular signature that allows the identification of their cellular source (Keerthikumar et al., 2015), but the mechanisms of MVs formation and release are also poorly understood. Recurring evidence has shown that the release of MVs occurs due to both vertical and lateral reorganization of the actin cytoskeleton and depends on the lipid content of the plasma membrane. This leads to local alterations in the membrane's curvature and consequent shedding of MVs (Pollet et al., 2018; Tricarico et al., 2017). Prior to the outward budding of the plasma membrane, cells increase the accumulation of calcium. The intracellular overload of calcium is important for the release of MVs because the activation of calcium-dependent proteases, such as calpain, is essential for cytoskeletal breakdown, which leads to disrupted attachment of the budding region to the plasma membrane (Taylor et al., 2020).

3.2.3. Mechanisms of EV formation and release

The biogenesis mechanisms of EVs involve a series of interactions between protein complexes and lipids on the cell surface or endosomal membrane. Even though lipids play an important role on EV formation, only a few studies have tried to identify the specific lipid constituents of EVs that mediate their biogenesis process (Haraszti et al., 2016; Laulagnier et al., 2004; Subra et al., 2007). For this reason, most of the knowledge on EV formation was acquired based on the EV's proteome, which allowed to determine particular markers that highly represent specific organelles from where EVs originate (Kowal et al., 2016). For instance, exosomes originate from the endocytic pathway, suggesting that they share some membrane constituents with other organelles involved in endocytosis, such as the plasma membrane and the endosome. Concordantly, exosomes are enriched in transmembrane tetraspanins, such as the clusters of differentiation CD9, CD63 and CD81, as well as endosomal ESCRT components like the tumor susceptibility gene 101 (TSG101) (Andreu and Yáñez-Mó, 2014; Pathan et al., 2019). However, other EV subtypes apart from exosomes may be difficult to identify based on their proteomic profile, because markers or enriched proteins for other EVs are still poorly characterized (Mathivanan et al., 2021).

The primary signal for the formation of EVs and the loading of their cargo is the cargo itself (Carnino et al., 2020). Although exosomes and MVs originate from separate organelles they share similar mechanisms of cargo loading. Cargo clustering at the site of origin, as well as clustering of several membrane proteins and lipids, induces the curvature of the membrane and triggers the endosomal membrane invagination or plasma membrane budding processes that lead to the formation of exosomes and MVs, respectively (Anand et al., 2018).

3.2.3.1. Biogenesis of exosomes

The invagination of the plasma membrane gives rise to endocytic vesicles that fuse with early endosomes. At some point, the endosome's content will be degraded by lysosomes, sorted into recycling endosomes, or secreted into the extracellular space (figure 1.4) (Gruenberg, 2001). The remaining early endosomes can mature and transform into late endosomes, also known as MVBs, accumulating ILVs resulting from the inward budding of the endosomal membrane (Stoorvogel et al., 1991). During ILVs formation, cytosolic proteins, nucleic acids, and lipids are sorted into these small vesicles. MVBs can either fuse with lysosomes for degradation of their cargo, or they can fuse with the plasma membrane, releasing ILVs as exosomes into the extracellular milieu (Kalra et al., 2016).

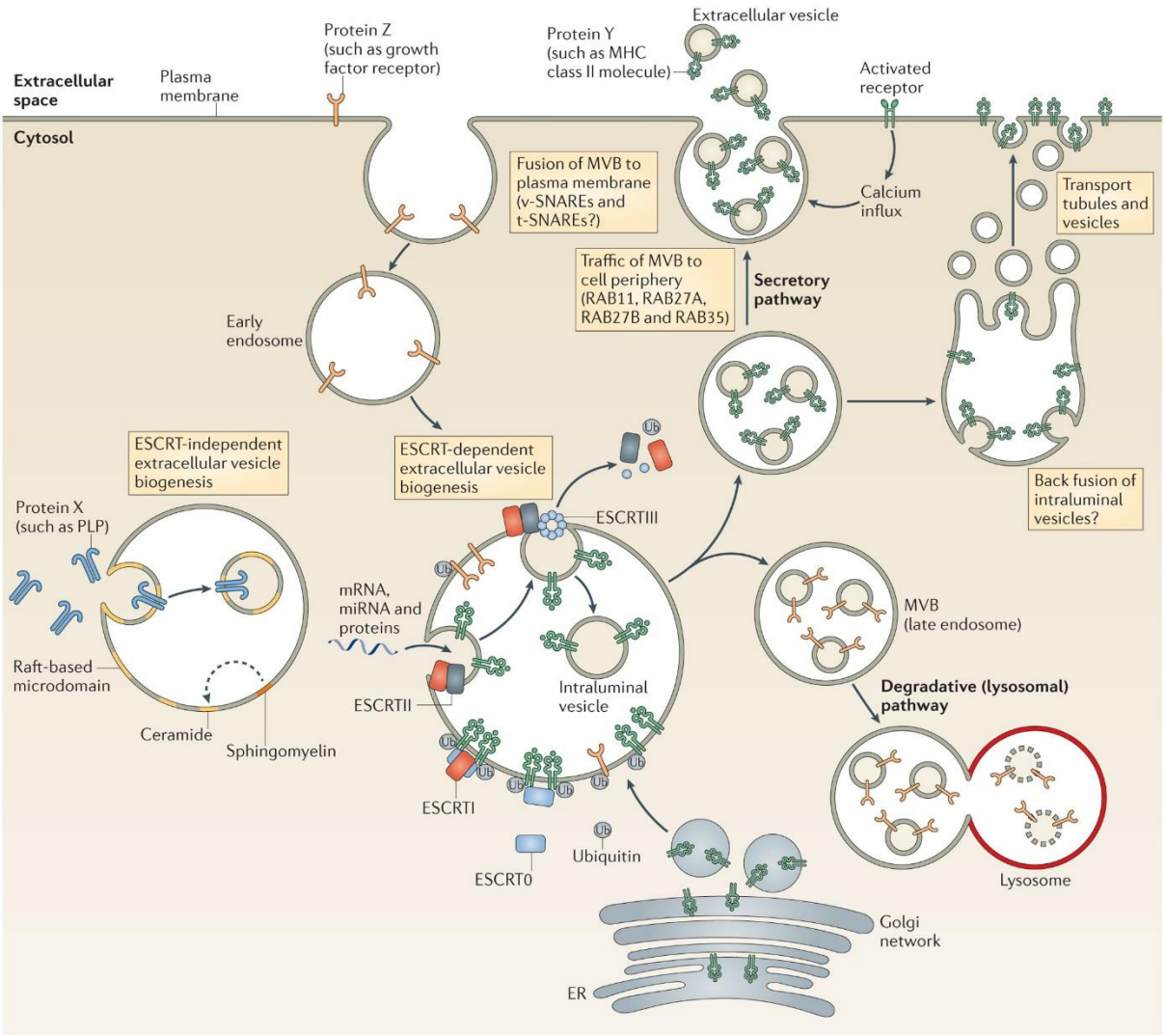

Figure 1.4 – Mechanisms of exosome biogenesis. Invaginations of the early endosomal membrane begin the exosome biogenesis process, which can occur in an ESCRT-dependent or -independent manner. In one of the ESCRT-independent pathways, sphingomyelin is converted into ceramide by nSMase, which bends the membrane with a negative curvature. In the ESCRT-dependent pathway, ESCRT-0 identifies ubiquitinated cargo and recruits ESCRT-I, which in turn recruits ESCRT-II with the concomitant inward budding of the endosomal membrane. Then, ESCRT-II recruits ESCRT-III, which facilitates membrane neck scission. ESCRT-III recruits the accessory VPS4, which drives membrane's fission and catalyzes ESCRT-III disassembly. The formed MVBs can either be sorted for lysosomal degradation or undergo SNARE-mediated exocytosis with concomitant release of exosomes. From Robbins and Morelli, 2014.

Exosomal biogenesis begins with the formation of ILVs within MVBs, a process that can be either dependent or independent on ESCRT complexes. The following two topics will address both pathways.

3.2.3.1.1. ESCRT-dependent pathway

The ESCRT machinery consists of more than 30 proteins that assemble to form highly conserved multi-protein complexes that mediate ILV formation. The ESCRT machinery comprises four distinct ESCRT complexes (ESCRT-0, -I, -II, and -III), which associate with each other and their accessory proteins: vacuolar protein sorting-associated protein 4 (VPS4), vacuolar protein sorting-associated protein VTA1 homolog (VTA1), and ALIX (McCullough et al., 2013). The relevance of the ESCRT-dependent pathway in the biogenesis of exosomes was revealed in an extensive study involving the knockdown of 23 constituents of ESCRT complexes by RNA interference (RNAi). It was shown that the absence of specific ESCRT subunits and accessory proteins could lead to alterations in exosome secretion, as well as in their cargo constitution, highlighting that some components are essential for exosome formation and release (Colombo et al., 2013). From this point on, the functions of other ESCRT components began to be revealed, allowing a better understanding of the overall ESCRT-dependent mechanism for exosomal biogenesis.

The ESCRT-0 subunit called hepatocyte growth factor regulated tyrosine kinase substrate (HRS) can bind, through its FYVE domain, to phosphatidylinositol 3-phosphate (PI3P), a phospholipid highly abundant in the early endosomal membrane, and recruit the rest of the ESCRT-0 complex (Kutateladze, 2006). The ESCRT-0 complex is thought to mediate exosomal cargo loading, at least in part, because its subunits HRS and signal transducing adaptor molecule 1 (STAM1) can interact with each other and thus sequester mono-ubiquitinated cargo (Bache et al., 2003b; Takahashi et al., 2015). Along with other post-translational modifications described, ubiquitination seems to act as a primary signal to mediate intraluminal cargo loading (Burke et al., 2014; Carnino et al., 2020). The ESCRT-0 subunit HRS also contains a PSAP motif, which allows its association with the TSG101 subunit of ESCRT-I. In this manner, ESCRT-0 recruits ESCRT-I to the early endosomal membrane (Bache et al., 2003a; Pornillos et al., 2003). ESCRT-I is also thought to sort ubiquitinated cargo into ILVs through its mono- and di-ubiquitin binding activity conferred by its ubiquitin-associated protein 1 (UBAP1) subunit (Agromayor et al., 2012). Subsequently, the vacuolar protein sorting-associated protein 28 homolog (VPS28) subunit of ESCRT-I interacts with the GLUE domain of the vacuolar protein-sorting-associated protein 36 (VPS36), which is a subunit of ESCRT-II. ESCRT-I thus mediates the recruitment of ESCRT-II, which is accompanied by the inward budding of the endosomal membrane (Teo et al., 2006; Wollert and Hurley, 2010). The VPS36 and VPS22 subunits of ESCRT-II then interact with the charged multivesicular body protein 6 (CHMP6) subunit of ESCRT-III, which facilitates the endosomal membrane neck scission (Babst et al., 2002a; Babst et al., 2002b; Wollert and Hurley, 2010). On the other hand, ESCRT-III may also be recruited by the accessory protein ALIX, which

interacts simultaneously with its CHMP4B subunit, via Bro1 domain, and TSG101 subunit of ESCRT-I (Katoh et al., 2003; McCullough et al., 2008; Strack et al., 2003). Finally, the CHMP2 and CHMP3 subunits of ESCRT-III self-assemble into a subcomplex and recruit the accessory VPS4 ATPase, which assembles with ESCRT-III and its co-factor VTA1. Hereupon, VPS4 catalyzes the disassembly of ESCRT-III, presumably combined with the membrane's fission, and redistributes the ESCRT-III components throughout the cytoplasm for further rounds of ILV formation (Babst et al., 2002a; Babst et al., 2002b; Yang and Hurley, 2010).

An additional ESCRT-dependent pathway was described for exosomal biogenesis, one which does not require ubiquitination reactions nor all the ESCRT complexes. Many of the signaling events that occur at the cell surface require the assistance of heparan sulfate (Rapraeger et al., 1991; Schlessinger et al., 2000). Syndecans are single transmembrane proteins thought to act as co-receptors and supply most of the heparan sulfate to the cell's surface (Bishop et al., 2007). Syndecans harbor a short cytoplasmic domain, which can bind cytosolic factors, such as syntenin (Grootjans et al., 1997). Syntenin binds ALIX which, as mentioned above, interacts with TSG101 and CHMP4B. When syndecans are endocytosed to the endosome, the cytosolic syndecan-syntenin-bound ALIX can recruit ESCRT-I (via TSG101) and ESCRT-III (via CHMP4B), which mediate the endosome's membrane inward budding and abscission. Interestingly, ESCRT-II does not seem to be required for syndecan-syntenin-ALIX-mediated exosomal biogenesis, because RNAi targeting CHMP6 (the ESCRT-III component to which ESCRT-II binds for recruitment) has no apparent effects on syndecan-syntenin-ALIX-mediated exosomes (Baietti et al., 2012).

3.2.3.1.2. ESCRT-independent pathways

The formation of MVBs still occurs even in the absence of major components of the ESCRT machinery, indicating that ILVs can also derive from ESCRT-independent mechanisms. Nevertheless, it was reported that the ablation of ESCRT components leads to the formation of larger MVBs, encapsulating a reduced number of ILVs, and ILVs themselves appear to be irregularly shaped and sized (Stuffers et al., 2009). Additionally, exosomes secreted from oligodendroglial precursor cells lacking functional ESCRT constituents are enriched in cholesterol, ceramide, and sphingomyelin (Trajkovic et al., 2008). Indeed, it was suggested that cholesterol and sphingomyelin cluster into lipid rafts to initiate the ESCRT-independent formation of ILVs. When lipid rafts are formed, the neutral sphingomyelinase (nSMase) cleaves sphingomyelin, producing ceramide (Ando et al., 2015; Trajkovic et al., 2008). Structurally, ceramide has a conical shape, meaning that when several molecules of ceramide accumulate into microdomains, the endosomal membrane spontaneously adopts a

negative curvature, beginning the inward budding process that will drive ILVs biogenesis (Castro et al., 2014; Janmey and Kinnunen, 2006; Trajkovic et al., 2008). Accordingly, inhibiting nSMase with either RNAi or small molecules like GW4869 leads to reduced amounts of secreted exosomes by impairing the conversion of sphingomyelin into ceramide and, consequently, ILV formation (Menck et al., 2017b).

Tetraspanins are also believed to participate in the biogenesis of exosomes, as well as in the regulation of cargo sorting into ILVs. This assumption arose from the fact that tetraspanins are highly enriched within the membranes of EVs, and changes in their expression were seen to impact EV formation and the EV's proteome. Due to the enrichment of tetraspanins on EVs membranes, they are often used as EV markers, especially for exosomes. The most commonly used markers are CD9, CD37, CD63, CD81 and CD82 (Andreu and Yáñez-Mó, 2014). However, the mechanisms through which tetraspanins regulate EV's formation are far from being understood.

Tetraspanins are transmembrane proteins comprising four transmembrane domains, which have been found to be present in many metazoan cells (Stipp et al., 2003). Tetraspanins can associate between themselves, forming homo- or heterodimers, or they can interact with a plethora of other transmembrane or membrane-associated proteins such as integrins, immunoglobulins and matrix metalloproteinases. In either case, by performing such interactions, tetraspanins begin to cluster in microdomains called tetraspanin-enriched microdomains (Barreiro et al., 2005; Berditchevski, 2001; Charrin et al., 2003; Mazurov et al., 2013; Rubinstein et al., 1996; Stipp et al., 2001; Yáñez-Mó et al., 2009). Tetraspanins were suggested to be involved in the ESCRT-independent pathways for the biogenesis of exosomes, because CD63, one of the major tetraspanin markers of exosomes, was reported to sort the premelanosome protein into ILVs of melanosomes, during the ESCRT-independent pathway, but not upon the canonical ESCRT-dependent formation of ILVs (van Niel et al., 2011). The emerging evidence of the enrollment of tetraspanins in the biogenesis of exosomes has been obtained by modulating the expression of tetraspanins. For instance, the knockdown of CD63 in B lymphocytes led to an increased production of exosomes by these cells (Petersen et al., 2011). Moreover, the overexpression of the tetraspanin TSPAN6 in the brain of a mouse model of AD resulted in the size augmentation of endosomes and an increased number of ILVs, therefore increasing exosome secretion (Guix et al., 2017).

Tetraspanins also regulate the release of EVs directly from the plasma membrane. For example, CD81 and CD82 are mostly expressed in the plasma membrane and were shown to be involved in the formation of membrane protrusions such as microvilli. On one hand, CD81 was reported to induce the formation of microvilli, whilst CD82 exerts the opposite effect (Bari

et al., 2011). Because both CD81 and CD82 are present in the plasma membrane, and since exosomes derive from the endocytic pathway, these two tetraspanins are also commonly used as exosomal markers (Andreu and Yáñez-Mó, 2014).

Tetraspanins CD9 and CD63 were found within the microprotrusions of activated platelets (Brisson et al., 1997; Israels and McMillan-Ward, 2007). For this reason, it was suggested that the tetraspanin-enriched domains within activated platelets, formed by the enrichment of CD9 and CD63, could lead to altered morphology of the plasma membrane, presumably by altering cytoskeletal organization through their interactions with Rho GTPases (Bari et al., 2011; Hemler, 2005; Richardson et al., 2011; Zhang et al., 2011a). Since CD9 and CD63 may as well follow the endocytic pathway, these two tetraspanins are also commonly used as exosomal markers (Andreu and Yáñez-Mó, 2014).

Besides impacting exosomal biogenesis, tetraspanins were also suggested to act as protein cargo sorters into ILVs. For example, CD9-knockdown and CD151-overexpressing prostate cancer cells-derived EVs presented alterations in their proteome. These proteomic alterations were shown to be important to enhance the cells' migratory and invasive capabilities in non-cancer cells, suggesting that EVs may function not only as intercellular communicators in physiological conditions, but they may also act as disease spreading agents (Brzozowski et al., 2018).

Still considering the putative role of tetraspanins in cargo sorting, the protein-protein interaction network of tetraspanin-enriched microdomains seems to deeply influence the exosomal protein content, because 45% of the exosomal proteome corresponds to interacting partners of the components of those microdomains. Additionally, specific tetraspanin-associated proteins, such as Rac, are excluded from exosomes derived from CD81-deficient animals, meaning that CD81 is crucial for the loading of Rac into ILVs (Perez-Hernandez et al., 2013). Following the same rationale, CD81 and CD9 seem to be required for sorting β-catenin into ILVs, so that β-catenin-loaded exosomes can modulate the Wnt signaling activity in dendritic cells (Chairoungdua et al., 2010).

There are further examples supporting the importance of tetraspanins in the biogenesis of exosomes, as well as in the regulation of cargo sorting. However, while the roles of tetraspanins in these mechanisms are currently emerging, most of the biological functions of the tetraspanins protein family remain poorly understood.

3.2.3.1.3. Exosomal release

Secretion of exosomes into the extracellular space is a tightly controlled process (Hannafon and Ding, 2013). When MVBs are formed, they can either be targeted for lysosomal degradation or they can fuse with the plasma membrane and release their content as exosomes (Kowal et al., 2014). Trafficking and exocytosis of MVBs are governed mostly by Rab GTPases, cytoskeleton components such as microtubules and actin, and soluble N-ethylmaleimide-sensitive fusion factor attachment protein receptor (SNARE) proteins (Kowal et al., 2014; Rodriguez-Boulan et al., 2005).

Rab GTPases are key proteins in intracellular vesicular trafficking that act as regulatable switches, recruiting effector molecules such as sorting adaptors, tethering factors, kinases, phosphatases, and motor proteins when in their active GTP-bound form. Rab proteins participate in vesicular budding, intracellular movement of MVBs, and they guide vesicles to disembark into their respective targets, which may be lysosomes or the plasma membrane. In this last scenario, Rab GTPases would be potential mediators of MVB's fusion and exosomal secretion (Stenmark, 2009). Accordingly, knockdown of RAB5A, RAB9A and RAB2B was shown to decrease the release of exosomes into the extracellular environment (Ostrowski et al., 2010). Moreover, early sorting of endosomal compartments destined for exocytosis was shown to be mediated by RAB11 and RAB35, indicating that these two proteins may participate in MVB's trafficking towards the plasma membrane (Stenmark, 2009). In fact, both RAB11 and RAB35 were suggested to mediate MVB's tethering and docking at the plasma membrane, which is supported by the fact that RAB11 GDP-locked mutants and RAB35 inhibition results in the intracellular accumulation of endosomal vesicles and impairs the secretion of exosomes (Hsu et al., 2010; Savina et al., 2005; Savina et al., 2002). Other Rab proteins, such as RAB27A and RAB27B, have also been implicated in MVB's docking at the plasma membrane. Interestingly, silencing of RAB27B redistributed MVBs towards the perinuclear region of the cell, suggesting that RAB27B may be essential for MVB's trafficking towards the plasma membrane (Ostrowski et al., 2010).

The final step of exosomal secretion involves the fusion of MVBs with the plasma membrane. Similarly to other processes involving the fusion of membranes, such as the release of synaptic neurotransmitters, release of exosomes seems to involve SNARE proteins (Jahn and Scheller, 2006). Stable SNARE complexes need to be assembled for exocytosis to occur, implying that the MVB's membrane contains v-SNAREs, while the plasma membrane includes t-SNAREs (Yang et al., 2019). Regulators of exocytosis of the v-SNARE category include the vesicle-associated membrane protein 2 (VAMP2), VAMP3, VAMP7, and VAMP8, whereas the synaptosome-associated protein 23 (SNAP23) has been characterized as part of

the t-SNAREs (Zhu et al., 2015). The release of exosomes was shown to occur upon phosphorylation of SNAP23, which promotes the assembly of the SNARE complex (Wei et al., 2017). The SNARE complex promotes the approaching of the two membranes and, subsequently, the MVB's limiting membrane fuses with the plasma membrane, releasing the contained exosomes into the extracellular environment (Hessvik and Llorente, 2018). The mechanisms of exosomal secretion, and especially the role of Rab proteins in the process, are still under active investigation.

3.2.3.2. Biogenesis of microvesicles

The biogenesis of MVs begins with coordinated alterations in the distribution of phospholipids within the plasma membrane and is followed by the contraction of cytoskeletal constituents (figure 1.5) (Kalra et al., 2016). The alterations in the phospholipid distribution during MV's biogenesis are mediated by floppases and scramblases, which allow lipid movements towards the outer leaflet of the plasma membrane or bi-directionally, respectively. When the intracellular calcium concentration increases, floppases and scramblases are activated in response. Phosphatidylserine (PS) is typically restricted to the inner leaflet of the plasma membrane. However, at the beginning of the membrane's outward budding, PS is externalized to the outer surface by floppases and scramblases. The externalization of PS alters the biochemical and biophysical properties of the budding membrane, destabilizing the plasma membrane-cytoskeleton anchorage, thus facilitating the shedding of MVs (Albrecht et al., 2005; Bevers and Williamson, 2016; Hankins et al., 2015; Oram and Vaughan, 2000; Taylor et al., 2020). Additionally, GTP-bound ADP-ribosylation factor 6 (ARF6) is activated and initiates a signaling cascade that will ultimately promote actin-myosin contraction, causing the abscission of the shedding MVs from the plasma membrane. In detail, GTP-bound ARF6 activates phospholipase D, which recruits and activates extracellular signal-regulated kinase (ERK), at the plasma membrane. ERK then phosphorylates myosin light chain kinase (MLCK), activating it. Subsequently, MLCK phosphorylates myosin light chains, thereby inducing actin-myosin contraction and ultimately leading to MV's release (Muralidharan-Chari et al., 2009).

The MV's biogenesis process seems to share some common mechanisms associated with exosomal formation, namely through the ESCRT machinery. Arrestin domain-containing protein 1 (ARRDC1) is an adaptor protein that enables MV's formation. The protein harbors PSAP and PPXY motifs that allow it to interact with TSG101 from ESCRT-I and ALIX, respectively. During this process, ARRDC1 may interact with the E3 ubiquitin-protein ligase neural precursor cell expressed developmentally down-regulated protein 4 (NEDD4), also via PPXY motifs, suggesting that MVs biogenesis also includes a ubiquitin-based cargo sorting

mechanism (Anand et al., 2018; Nabhan et al., 2012; Rauch and Martin-Serrano, 2011). Ultimately, ESCRT-III would be expected to be recruited to mediate the membrane neck abscission along with the VPS4 complex, since ESCRT-III can either be directly recruited by ALIX, or indirectly by TSG101 from ESCRT-I, which would recruit ESCRT-II prior to ESCRT-III. However, even though ARRDC1 interacts with ALIX and TSG101, the recruitment of ESCRT-III through this pathway has not yet been confirmed. Nevertheless, ARRDC1-mediated microvesicles release requires both TSG101 and VPS4. The fact that ESCRT-III was not found to be involved in ARRDC1-mediated MVs release suggests an alternative mechanism through which the VPS4 complex is recruited, but, so far, it remains elusive (Kuo and Freed, 2012; Nabhan et al., 2012).

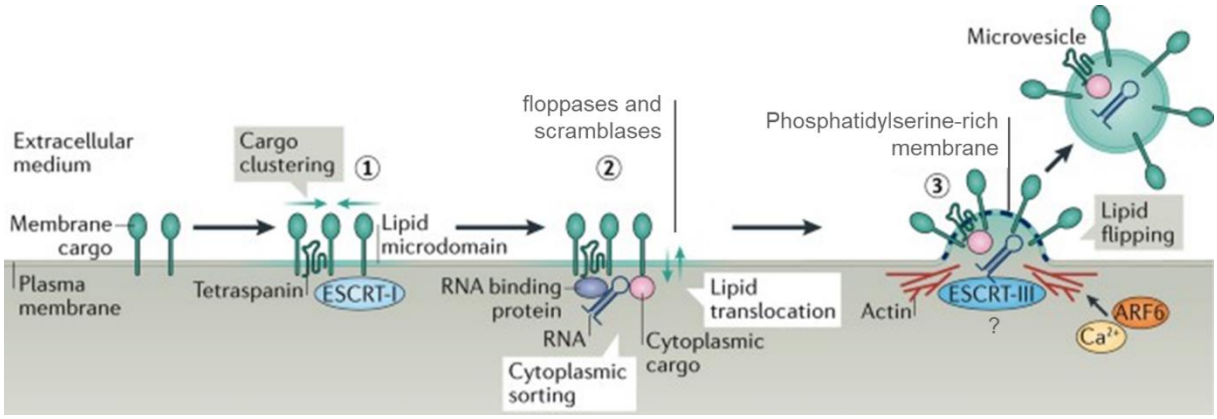

Figure 1.5 – Mechanisms of microvesicles biogenesis. Floppases and scramblases translocate phosphatidylserine to outer leaflet of the plasma membrane, causing destabilization between the membrane and cytoskeleton anchorage. ARF6 leads to cytoskeletal contraction, facilitating the abscission of the shedding MV, and calcium activates calcium-dependent proteases for cytoskeletal breakdown and consequent release of MVs. Adapted from van Niel et al., 2018.

3.2.4. Isolation and characterization of EVs

Generally, EVs can be isolated and purified from cell culture media or body fluids (Admyre et al., 2007; Asea et al., 2008; Caby et al., 2005; Houali et al., 2007; Pisitkun et al., 2004; Poliakov et al., 2009). Nevertheless, isolation of EVs from biofluids is challenging due to their composition complexity, because, apart from EVs, they can contain cell debris, proteins, lipoproteins, nucleic acids, among other types of biomolecules. The complex composition of biofluids contributes to their higher viscosity, trapping EVs and hindering their isolation procedures (Théry et al., 2006). For this reason, it is common practice to dilute samples in phosphate buffered saline (PBS) and consider important factors during EV isolation, such as sample collection and handling, or the centrifugation time and speed, because these should

be optimized according to the material source being used for EV isolation (Théry et al., 2006; Witwer et al., 2013; Yuana et al., 2015).

Usually, mammalian cells are cultured in the presence of fetal bovine serum (FBS), which is itself highly enriched in EVs. For this reason, when studying EVs derived from a specific cell culture, it is important to be aware that serum-derived EVs pose a risk of contamination that can influence the results obtained. Therefore, to overcome this technical difficulty, EVs should be harvested in serum-free conditions or, if a particular cellular type requires FBS to grow, EV-depleted FBS should be used instead (Shelke et al., 2014; Théry et al., 2006). Another technical detail to be considered when cells are cultured with FBS-supplemented media is the presence of diverse RNA species of bovine origin. These can be associated with either vesicles or proteins that are only partially removed when depleting the medium from bovine EVs, and could produce incorrect results during downstream analyses (Wei et al., 2016).

Another important consideration when working with EVs is the potential loss of sample, which can be due to EV's binding onto the walls of storage vials, to vesicular disruption caused by repetitive freeze-thaw cycles, or to the use of an inappropriate storage buffer (Jeyaram and Jay, 2017; Lőrincz et al., 2014). However, little is known about the optimal conditions for EV preservation, either before or after the isolation procedure, and this poses a real challenge when thinking of EVs as therapeutic agents for clinical applications (Deville et al., 2021; Lőrincz et al., 2014; Park et al., 2018).

Taking all things together, issues can arise in every step of the EV isolation procedure, from cell culturing to EV purification and storage, and all can influence the yield and quality of the isolated EVs. Therefore, it is crucial to be aware of such issues when outlining, performing, and interpreting experiments.

3.2.4.1. Isolation methods

When isolating EVs, there are some considerations that should be taken: first, the isolation method should yield high amounts of EVs, and second, extra-vesicular contaminants should be depleted, while maintaining the integrity and biophysical properties of the vesicles. However, a flawless isolation method does not exist, and, for that reason, active research is being made in this regard, in order to develop new procedures or improve the protocols already available (Liangsupree et al., 2021).

EVs derived from culture cells can be isolated by different methods, but pre-clearance steps are common to all of them (Brennan et al., 2020; Veerman et al., 2021). These pre-

clearance steps are employed to deplete the supernatants from floating cells, large debris, and apoptotic bodies, and are usually accomplished by performing low-speed centrifugations at 300 x *g* and 2,000 x *g*. Similar steps are used when isolating EVs from biofluids, although with increased time and speed due to the fluids' viscosity (Théry et al., 2006). After the pre-clearance steps, EVs can be isolated through various methods, of which the most often used are detailed bellow and summarized in table 1.2.

Table 1.2 – EV isolation methods principles, advantages, and disadvantages

ISOLATION METHOD	ISOLATION PRINCIPLE	ADVANTAGES	LIMITATIONS
DIFFERENTIAL CENTRIFUGATION	EV separation based on particle density, size, and shape	Commonly used; standardized; vesicle enrichment as pellet; EV subtypes isolation by density gradient centrifugation	Vesicle aggregation; protein and soluble factors contamination; low recovery; laborious
POLYMER-BASED PRECIPITATION	EV precipitation using polymers altering solubility	Easy and inexpensive; high yield; effective with small amounts of starting material; preservation of bioactivity	Co-precipitation of protein contaminants and polymeric material; not suitable for large scale studies; long incubation times
SIXE-EXCLUSION CHROMATOGRAPHY	EV isolation by gel filtration chromatography based on size	Inexpensive; reproducible; high yield and purity; preservation of integrity and activity	Specific equipment; not suitable for large scale studies; long run times
IMMUNOAFFINITY CAPTURE-BASED TECHNIQUES	EV immuno-purification using magnetic beads conjugates with antibodies direct toward specific EV surface markers	Sensitivity; specificity; high purity; EV subtypes isolation	Expensive; antibody cross-reactivity; low yield

Adapted from (Chiriacò et al., 2018)

3.2.4.1.1. Differential centrifugation

EVs are most commonly isolated by differential centrifugation because it is a non-expensive method that allows the isolation of a satisfactory amount of EVs and it is relatively simple to perform, as long as an ultracentrifuge is available (Gardiner et al., 2016; Théry et al., 2006). The differential centrifugation method consists of performing successive centrifugations with increasing time and speed from one step to the following, and it is based on the sedimentation rate principle, meaning that larger EVs will sediment with shorter and lower-speed centrifugations (Ohlendieck, 2010). The pre-clearance steps described above are most commonly followed by a 0.22 µm filtration to eliminate MVs but, and the MV-free medium is centrifuged at 100,000 x *g* or above to concentrate exosomes. At this point, the sample

containing the exosomes also contains a high degree of contaminants, so a PBS wash is often introduced to increase the purity of the exosomes obtained (Théry et al., 2006). Alternatively, in case MVs isolation is intended, the pre-cleared supernatant can be spun at 10,000 x *g* to pellet MVs, followed by a re-suspension step with PBS (Mohammadi et al., 2020).

Despite its extensive use, the limitations of differential centrifugation are evidenced by relatively low yields of EVs, with membrane disruptions and EV aggregation caused by the extremely high speeds to which the samples are subjected (Linares et al., 2015). Moreover, this method usually results in the co-isolation of contaminant biomolecules, including bovine proteins in those cases in which FBS is used. Also, differential centrifugation is time-consuming and has poor scalability because the maximum volume of medium from which EVs can be isolated is determined by the rotor's capacity (Brennan et al., 2020). Additionally, the spinning time and the rotor type can affect the purity and yield of the EVs obtained, meaning that differential centrifugation is a method that can require exhaustive optimization (Cvjetkovic et al., 2014). For these reasons, alternative methods have been developed to improve the quality and yield of isolated EVs.

3.2.4.1.2. Size exclusion chromatography

Size exclusion chromatography (SEC) became a popular alternative to differential centrifugation as it allows to obtain higher yields of EVs with increased purity and it does not affect the vesicles' integrity (Mol et al., 2017; Nordin et al., 2015). SEC is used to purify EVs based on their size. Briefly, the sample is loaded on top of a column filled with porous polymer beads of various sizes. As the EV-containing solution passes through the column, larger particles that do not fit in the bead pores pass by faster and are eluted in earlier fractions. On the other hand, smaller particles that can fit inside the porous beads are retained for a longer period, meaning that they are eluted in latter fractions. SEC is able to separate distinct subpopulations of EVs (Willms et al., 2016), but it is not a scalable technique and, therefore, implementing it in clinical applications would be challenging.

3.2.4.1.3. Polymer co-precipitation

Polymer co-precipitation is based on the incubation of EV-containing samples with hydrophilic polymers. These reagents cause the precipitation of EVs by reducing their hydration and, consequently, their solubility. The precipitated EVs can then be subjected to low-speed centrifugation for harvesting. Available commercial kits such as ExoQuick and Exo-Spin are based on polymer co-precipitation, and they allow to bypass the need for lengthy

ultracentrifugation. However, these kits are too expensive for large-scale isolation of EVs and they produce heterogeneous results because the solubility is decreased equally for EVs and proteins, meaning that polymer co-precipitation methods can isolate any subtype of EVs, as well as contaminating biomolecules (Shao et al., 2018).

3.2.4.1.4. Immunoaffinity enrichment

Immunoaffinity enrichment of EVs consists of targeting EV surface markers with specific antibodies and perform a pull-down assay to purify marker-positive EVs. Typically, magnetic beads are coated with antibodies against MHC-II, when isolating EVs from antigen-presenting cells, or CD9, CD63 or CD81, when isolating EVs from non-immune cells. One of the advantages of using this technique consists in the fact that bead-EV complexes can be directly analyzed by flow cytometry, Western blot, or electron microscopy without the need for separating the beads from the EVs. Additionally, immunoaffinity enrichment does not require ultracentrifugation. However, it is important to note that this technique is based on specific proteins present on the vesicle's surface, which may only allow the isolation of a subpopulation of marker-positive EVs and, consequently, downstream analyses may not reflect the EV population as a whole (Théry et al., 2006).

3.2.4.2. Characterization methods

It is fundamental to characterize EVs following isolation, not only to confirm their presence in the prepared samples, but also to identify their cargo (proteins, RNA, DNA, or lipids), (Théry et al., 2018). However, technical difficulties associated with the isolation methods may be reflected during the characterization procedures. For instance, disruption and aggregation of EVs due to the extremely high speeds used during ultracentrifugation may be detected upon electron microscopy visualization and pose a challenge when characterizing EVs by their size and morphology (Linares et al., 2015). Therefore, not only are the EVs isolation and purification protocols in constant development, but novel characterization methods and EV markers are continuously introduced, to better understand the physicochemical and molecular properties of EVs. Currently, the international society for extracellular vesicles (ISEV) recommends the combined use of different characterization methods due to the overlapping features that exist between distinct EV subtypes (Théry et al., 2018). For this reason, it is very common for researchers to characterize EVs based on their size, morphology, and molecular markers, in conjunction. The methods most often used for the characterization of EVs are detailed below.

3.2.4.2.1. Physical characterization

Physical features of EVs have been widely used in their characterization and include the size and morphology of the vesicles. By using microscopy-based techniques, for example, it is possible to distinguish small and large EVs, which can suggest the presence of distinct subpopulations of EVs, such as exosomes and MVs (Shao et al., 2018). However, there has been some controversy when characterizing EVs based on their size, due to the existing overlap in some categories. For example, during the exosomal biogenesis process, some larger exosomes may be produced and, in contrast, smaller MVs may as well be released into the extracellular environment, hence the need for additional characterization methods (Brennan et al., 2020). This section briefly surveys some of the physical methods through which EVs can be characterized.

Transmission electron microscopy

Transmission electron microscopy (TEM) is a highly popular technique for characterizing EVs based on their size and morphology (Théry et al., 2006). For example, exosomes measure between 30-150 nm and present a typical cup shape, whilst MVs tend to be larger (100-1,000 nm) and rounder, and, in contrast to exosomes, usually do not show such a high electron density in their middle zone (Collino et al., 2017; Malenica et al., 2021; Zabeo et al., 2017). In TEM, heavy metal stains such as uranyl acetate can be used to generate contrast in lipid membranes, which further improves EVs imaging (Ting-Beall, 1980). Importantly, TEM can also be coupled with immunogold labeling against EV surface markers such as tetraspanins, to provide additional molecular characterization (Chuo et al., 2018).

Scanning electron microscopy

Scanning electron microscopy (SEM) is a useful technique in EV research that provides surface topography information in a three-dimensional perspective (Shao et al., 2018). Apart from the size and surface topography of EVs, SEM also provides information regarding their elemental composition, usually enriched in carbon (Malenica et al., 2021). Under SEM, EVs usually present a smooth spherical shape but, sometimes, agglomeration of EVs can occur due to a drying process carried out before SEM analysis (Sokolova et al., 2011).

Atomic force microscopy

Atomic force microscopy (AFM) is a well-established high-resolution imaging technique used for EV characterization (Sharma et al., 2010; Yuana et al., 2010). AFM consists of a mechanical cantilever that passes over a surface and “feels” its topography. When going over an EV, the cantilever deflects, indicating the EVs presence, as well as its topography. Furthermore, AFM can also record energy dissipation while the cantilever scans the EV sample, providing information about the EV’s stiffness and adhesion properties. Under AFM, EVs show a round morphology and their height is also measured, allowing the user to distinguish large and small EVs (Sharma et al., 2010).

Dynamic light scattering

Dynamic light scattering (DLS) measures the light scattered from an EV suspension when a laser beam strikes the sample (Lawrie et al., 2009). As EVs suspended in a medium present Brownian motion, i.e., random movements, the intensity of the scattered light from all EVs in the suspension fluctuates over time. The amount of light scattered is directly proportional to the vesicle’s size, meaning that larger EVs scatter more light than the smaller ones. By measuring the fluctuations in the scattered light’s intensity over time, DLS instruments can retrieve a distribution of EV’s sizes and measure the EV’s average size in a sample (Szatanek et al., 2017).

Nanoparticle tracking analysis

Nanoparticle tracking analysis (NTA) is based on the optical tracking of individual EVs, which provides the size distribution of vesicles, as well as information on their total concentration (Dragovic et al., 2011; Gardiner et al., 2013). Its principle is like that of DLS: a laser beam strikes the EV sample, which scatters the light as EVs undergo Brownian motion. Simultaneously, a camera records the path of individual EVs and determines their mean velocity and diffusivity. However, in contrast to the above-mentioned method, which measures the light scattering of all vesicles in bulk, NTA detects individual EV scattering. By doing so, NTA retrieves not only an accurate size distribution of an EV sample, but also the number of EVs present in that sample (Shao et al., 2018).

3.2.4.2.2. Molecular characterization

Physical characterization of EVs is usually coupled with the characterization of their molecular content, in particular of the proteins that are present. EV-associated proteins derive mainly from the plasma membrane and cytosol, due to their mechanisms of biogenesis and cargo sorting. However, they lack proteins derived from other intracellular organelles such as Golgi apparatus, ER, mitochondria, and nucleus (Kowal et al., 2016; Raimondo et al., 2011; Théry et al., 2018). Accordingly, ISEV recommends careful characterization of EVs based on their constituting proteins, requiring at least three distinct protein markers for their characterization: (i) a transmembrane or membrane-associated protein, (ii) a cytosolic protein, and (iii) a protein derived from other organelles not associated with EVs, serving as a negative control (Théry et al., 2018). The detection of specific EV protein markers is conventionally performed by techniques such as Western blot and enzyme-linked immunosorbent assay (ELISA). However, both require large sample volumes, which can be difficult to obtain using some of the EVs isolation methods that are available (Théry et al., 2006). Unlike Western blot and ELISA, which detect targeted proteins, mass spectrometry can be advantageous since it not only enables the unbiased detection of EV markers for characterization, but also allows to perform high throughput studies of the EV's proteome upon modulation of specific pathways. Furthermore, mass spectrometry can also be used for lipidomic characterization of EVs besides their proteome analysis, which has been shown to be of particular interest since the lipidomic profiles of EVs may serve as biomarkers of disease (Kreimer et al., 2015; Pocsfalvi et al., 2016; Skotland et al., 2017).

In mammals, transmembrane or membrane-associated proteins can be found within exosomes and MVs, however, specific markers can differ between these two subtypes of EVs (Théry et al., 2018). As mentioned before, exosomes are highly enriched with tetraspanins, (Mathivanan et al., 2021). Hence, CD9, CD63 and CD81 have been widely used as exosomal markers, although tetraspanins are not expressed in exosomes alone. On the other hand, MVs are enriched with plasma membrane-associated proteins such as integrins, selectins and CD40 ligands, or even transmembrane protein receptors and adhesion proteins such as EGFR and cell adhesion molecules, respectively (Al-Nedawi et al., 2009; Graner et al., 2009; Im et al., 2014; Tauro et al., 2013; Théry et al., 2018).

Intravesicular proteins include cytosolic proteins that can be associated with the mechanisms of EV biogenesis, protein sorting, or vesicular trafficking, such as TSG101, ALIX, annexins and Rab GTPases. Since cytoskeletal proteins also play a role in EV's biogenesis, trafficking and release, actins, myosins and tubulins can also be detected within them. Some cytosolic proteins that do not associate directly with EVs biogenesis or trafficking can also

localize promiscuously inside the vesicles. These include cytosolic chaperones (for example, heat-shock proteins), metabolic enzymes (such as glyceraldehyde 3-phosphate dehydrogenase), and ribosomal proteins (Choi et al., 2015; Théry et al., 2018).

The use of negative markers is recommended by ISEV to track co-isolated non-EV components and thus assess the purity of the EV sample. Negative markers include proteins that are associated with intracellular organelles other than those involved in the endocytic pathway from where EVs originate, such as the nucleus (histones, lamins), mitochondria (cytochrome *c*), ER (calnexin), and Golgi apparatus (Golgin subfamily A member 2) (Théry et al., 2018).

3.2.5. Mechanisms of extracellular vesicles cellular uptake

While transiting through the extracellular matrix, EVs protect their cargo from enzymatic degradation until it is released into the recipient cell (Mulcahy et al., 2014). Functional cargo transported within EVs, especially mRNAs and miRNAs, can induce phenotypic alterations in the target cells by regulating gene expression, either through *de novo* translation or post-transcriptional regulation of target mRNAs (Valadi et al., 2007). It is well-established that EVs are involved in normal physiological processes, such as antigen presentation to immune cells to trigger an immune response (Raposo et al., 1996). However, alterations in EV's activity and cargo may be a feature of certain pathologies, including cancer and neurodegenerative diseases (Emmanouilidou et al., 2010; Ogorevc et al., 2013). Given the involvement of EVs in normal physiological processes and disease, it is not only fundamental to understand the molecular mechanisms through which EVs are released by their donor cells, but also the processes involved in their uptake by recipient cells (Mulcahy et al., 2014).

There is a plethora of evidence demonstrating that EVs are taken up into recipient cells and that they then induce a cellular response. For instance, EVs can deliver small interfering RNAs (siRNA), knocking down the expression of target genes in the recipient cells (Alvarez-Erviti et al., 2011). Moreover, luciferase-expressing cells produce bioluminescence when they internalize EVs loaded with the luciferin substrate. This evidence implied that the cytosolic content from EVs established direct contact with the cytoplasmic compartment of the target cell, either by EV-plasma membrane fusion or through other possible uptake pathways (Montecalvo et al., 2012).

The internalization of EVs into recipient cells has been studied using several techniques. EV uptake can be directly visualized using fluorescence microscopy tools such as fluorescent lipophilic dyes that stain EV membranes, or with engineered proteins such as

tetraspanins fused with fluorescent proteins (Fabbri et al., 2012; Feng et al., 2010). Upon delivery of fluorescently labelled EVs, recipient cells can then be analyzed by confocal microscopy or flow cytometry. Other techniques that can be employed to study EV uptake are based on the use of antibodies to test the putative enrolment of specific ligands or receptors. Additionally, chemical inhibitors can also be used to block uptake pathways and assess the impact it might have on the internalization of EVs. By employing these different techniques, the studies performed in the last years have provided important hints on the routes through which EVs can be internalized into recipient cells (figure 1.6) (Mulcahy et al., 2014).

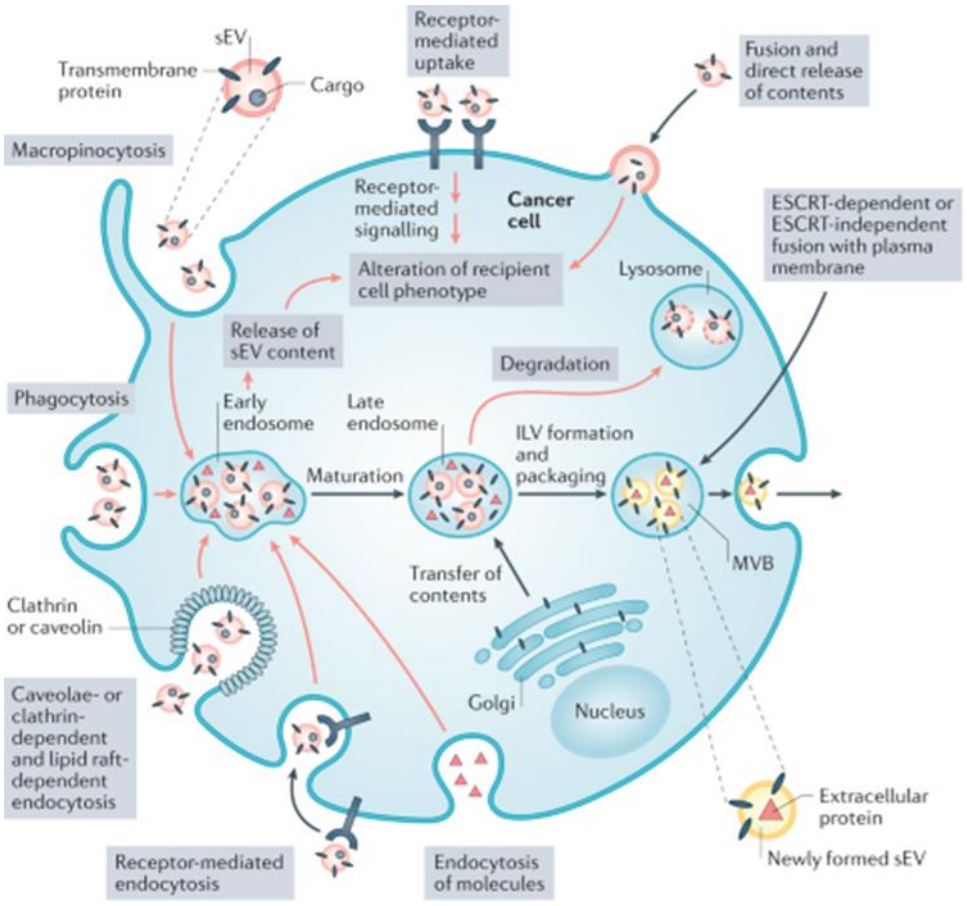

Figure 1.6 – Mechanisms for EV uptake within recipient cells. There are a number of biological mechanisms that extracellular vesicles (EVs) use to bind to and/or be internalized by recipient cells. The inhibition of dynamin-2 suggests EVs can be taken up by clathrin- or caveolin-mediated endocytosis. Moreover macrophages showed co-localization between EVs and clathrin, and the ablation of caveolin-1 impairs EV internalization. Microglia internalizes EVs by macropinocytosis, which is impaired by Rac1 inhibition. EV uptake can also occur through phagocytosis in dendritic cells. Apart from endocytic mechanisms, EVs derived from melanoma cells can directly fuse with the plasma membrane and release their cargo within the recipient cell's cytoplasm. Adapted from Moller and Lobb, 2020.

3.2.5.1. Endocytosis

Several studies suggest that internalized EVs usually undergo the endocytic pathway and end up being taken up into endosomal compartments (Escrevente et al., 2011; Montecalvo et al., 2012; Morelli et al., 2004). EV uptake was shown to be a rapid energy-requiring process, whereby EVs can be found inside the recipient cells as early as 5 minutes after their introduction into the medium (Escrevente et al., 2011; Morelli et al., 2004). Further evidence for the involvement of the endocytic pathway in taking up EVs was obtained when inhibiting endocytosis in recipient cells with cytochalasin D, a metabolite known to induce depolymerization of actin filaments (Flanagan and Lin, 1980; Lamaze et al., 1997; Montecalvo et al., 2012). EV uptake was significantly reduced in several cell types upon treatment with cytochalasin D, suggesting that endocytosis may indeed contribute to the internalization of EVs. However, EV uptake was not completely abolished, suggesting the existence of alternative pathways mediating this process (Escrevente et al., 2011; Montecalvo et al., 2012; Morelli et al., 2004).

Endocytosis is a broad term comprising several molecular internalization mechanisms, including, for example, macropinocytosis, phagocytosis, and clathrin-mediated endocytosis (Doherty and McMahon, 2009). The roles of these particular endocytic processes in EV uptake have been studied using inhibitors to block specific pathways, antibodies that impede interactions between ligands and receptors, and resorting to RNAi technology to downregulate particular genes involved in these mechanisms (Escrevente et al., 2011; Feng et al., 2010; Fitzner et al., 2011; Montecalvo et al., 2012).

3.2.5.1.1. Clathrin-mediated endocytosis

Clathrin-mediated endocytosis is a cellular process where clathrin-coated vesicles form to internalize a range of transmembrane receptors and their ligands. Clathrin molecules assemble at the inner leaflet of the plasma membrane and deform it until the membrane collapses into a vesicular bud, with subsequent formation of an intracellular vesicle. Inside the cytoplasm, the intracellular vesicle undergoes clathrin uncoating and subsequently fuses with the early endosome, where it releases its contents (Kirchhausen, 2000).

EV uptake has been suggested to occur through clathrin-mediated endocytosis, because the inhibition of clathrin-coated pits formation with chlorpromazine was shown to decrease the internalization of EVs into recipient cells (Escrevente et al., 2011; Wang et al., 1993). Other studies led to the same conclusion through the inhibition of dynamin-2 (Barrès et al., 2010; Herskovits et al., 1993; Vallee et al., 1993), a GTPase that forms a collar-like

structure at the neck of deeply invaginated clathrin-coated pits, which is important for membrane scission and consequent clathrin-coated vesicle release (Chappie et al., 2010; Marks et al., 2001). Inhibition of dynamin-2 impaired clathrin-mediated endocytosis and prevented EV uptake (Barrès et al., 2010; Escrevente et al., 2011; Herskovits et al., 1993; Vallee et al., 1993; Wang et al., 1993). Moreover, a small percentage of EVs co-localize with clathrin during their internalization into macrophages (Feng et al., 2010). Altogether, these studies suggest that EV uptake occurs, to some extent, through clathrin-mediated endocytosis. However, since the internalization of EVs was not completely abolished upon the inhibition of clathrin-mediated endocytosis, it is likely that other pathways are responsible for this process.

3.2.5.1.2. Caveolin-dependent endocytosis

Caveolin-dependent endocytosis consists in the formation of small cave-like invaginations of the plasma membrane called caveolae, which can become internalized into the cytoplasm, like clathrin-coated vesicles. Caveolae form from glycolipid rafts in the plasma membrane, hence they are rich in cholesterol and sphingolipids (Anderson, 1998; Kurzchalia and Parton, 1999; Nabi and Le, 2003). The formation of caveolae is dependent on the protein caveolin-1 (Doherty and McMahon, 2009), which forms clusters within the plasma membrane. Here, oligomers of caveolins are formed, originating caveolin-rich rafts in the cell's membrane. The enrichment of cholesterol in these rafts, along with the attachment of caveolin oligomers to the plasma membrane through their scaffolding domains, as well as the assistance of dynamin-2, enable the formation and release of caveolar endocytic vesicles (Doherty and McMahon, 2009; Nabi and Le, 2003; Parton and Simons, 2007).

Dynasore is a specific inhibitor that blocks the activity of dynamin-2 (Newton et al., 2006), and dynasore-treated cells show a decreased capacity to internalize both exosomes and MVs, suggesting that EV uptake can be mediated by caveolin-dependent endocytosis (Menck et al., 2013; Nanbo et al., 2013). However, dynamin-2 is also a key participant in the clathrin-mediated endocytosis, thus these experiments cannot rule out the hypothesis that EV uptake may as well be influenced by the activity of clathrin-coated vesicles (Mettlen et al., 2009). Further evidence for the enrolment of caveolin-dependent endocytosis on EV uptake was obtained with the knockdown of the *CAV1* gene, which encodes caveolin-1. The downregulation of *CAV1* significantly impaired the internalization of EVs (Nanbo et al., 2013) but, paradoxically, *Cav1*-knockout mouse embryonic fibroblasts showed an increased uptake of EVs (Svensson et al., 2013). These results suggest that caveolin-dependent endocytosis may indeed mediate EV uptake, although the role of this mechanism may vary between cell types and EV's origin (Mulcahy et al., 2014).

3.2.5.1.3. Macropinocytosis

Macropinocytosis is another pathway of endocytosis that begins with the formation of invaginated membrane ruffles, which then pinch off into the cytosolic compartment. Ruffled extensions protrude from the plasma membrane towards the extracellular space, engulfing the target cargo as well as part of the extracellular fluid. Then, the membrane protrusions fuse with themselves or back with the plasma membrane and the target cargo is internalized (Doherty and McMahon, 2009; Swanson, 2008). Mechanistically, macropinocytosis is similar to phagocytosis, with the particularity that the former does not require direct contact with the internalized material. Macropinocytosis is dependent on cholesterol, actin, Na^+/H^+ exchanger activity, and Ras-related C3 botulinum toxin substrate 1 (Rac1), a small GTPase associated with cytoskeletal reorganization among many other functions (Grimmer et al., 2002; Ridley, 2006). The Na^+/H^+ exchanger at the plasma membrane transports H^+ out of the cell and promotes Na^+ influx into the cytosol, causing an increase in the cytosolic pH. These alterations in the cytosolic pH are suitable for the functioning of activated Rac1, a pH-sensitive protein that is recruited by cholesterol to sites of macropinocytosis (Grimmer et al., 2002; Koivusalo et al., 2010).

The inhibition of Na^+/H^+ exchange by amiloride results in the acidification of the submembranous region, which in turn impedes the activity of Rac1 and compromises actin remodeling, leading to the impairment of micropinocytosis. It was shown that this causes a reduction of oligodendrocyte-derived EV uptake by microglia (Fitzner et al., 2011; Koivusalo et al., 2010). Accordingly, the direct inhibition of Rac1 with NSC23766 also led to decreased uptake of EVs by microglia (Fitzner et al., 2011). However, other studies did not find an association between macropinocytosis and EV uptake, suggesting that it might be a minor pathway for the internalization of EVs, or a cell-specific mechanism (Feng et al., 2010; Mulcahy et al., 2014; Nanbo et al., 2013).

3.2.5.1.4. Phagocytosis

Phagocytosis is a process through which opsonized materials, usually with large dimensions, are internalized into recipient cells. In contrast to macropinocytosis, phagocytosis requires direct contact with the materials being internalized. It is a receptor-mediated process consisting of progressive invaginations of the plasma membrane accompanied by enveloping membrane extensions called pseudopods (Doherty and McMahon, 2009; Swanson, 2008).

Phosphoinositide 3-kinases (PI3Ks) are pivotal players in the phagocytic pathway , since they participate in the delivery of membranes to the extending pseudopods (Stephens et

al., 2002). The PI3K inhibitors wortmannin and LY294002 were shown to impair phagocytosis and, consequently, reduce EV uptake in a dose-dependent manner. Additionally, EVs were found to co-localize with fluorescent phagosome tracers (Feng et al., 2010). Further evidence showed that EVs can be internalized by phagocytosis as acceptor dendritic cells emit red fluorescence when receiving EVs labelled with pHrodo, a red fluorescent dye that emits strong fluorescence at the phagosome's pH (Montecalvo et al., 2012). Taking all these considerations together, it seems rational to accept that EV uptake might also occur via phagocytosis.

3.2.5.2. Cell surface membrane fusion

Apart from endocytosis, another potential mechanism for EV uptake is the direct fusion between the EVs membrane and the plasma membrane of recipient cells (Parolini et al., 2009). In this process, two distinct lipid bilayers are brought into proximity and the two outer leaflets of both membranes contact with each other and establish a local hemifusion connection, referred to as the hemifusion stalk. Then, the stalk expands, originating the hemifusion diaphragm, where a fusion pore is subsequently formed. At this point, the two hydrophobic cores mix, the two cytoplasmic compartments communicate with each other, and a single consistent structure is formed (Chernomordik and Kozlov, 2008; Chernomordik et al., 1987; Jahn et al., 2003). The protein families involved in this mechanism are the same as the ones promoting MVB's fusion with the plasma membrane for exosomal release: the SNARE and Rab protein families (Jahn and Südhof, 1999).

The most common method used to study the fusion of membranes is fluorescent lipid dequenching. Fluorescently labeled membranes present decreased fluorescence intensity due to the quenching phenomenon that occurs when the fluorescent dyes are in proximity of a quencher molecule. However, when the fluorescently labeled membranes fuse with non-labeled membranes, the fluorescent dyes disperse due to the lipids dynamics and an intense fluorescent signal can be detected (François-Martin and Pincet, 2017). By employing fluorescent lipid dequenching, melanoma cells-derived EVs labeled with quenched fluorescent dyes were shown to fuse with the recipient cell's membrane, at least to some extent. Additionally, this fusion was enhanced under acidic conditions. This may suggest that the fusion between EVs and recipient cells may be limited to acidic conditions, which is a feature of endosomes, where EV's fusion usually takes place (Parolini et al., 2009).

Most of the research addressing the mechanisms of EV uptake support the endocytic pathways as primary routes for this process, however, some studies have shown that a fusion-based mechanism cannot be ruled out. Therefore, it is important that future research

addresses this mechanism to ascertain the extent to which EV uptake occurs via direct membrane fusion under physiological conditions (Mulcahy et al., 2014).

3.2.5.3. Cell-specific EV uptake

One question currently vexing the EV research community is whether EV uptake is a cell type-specific process. Some studies performed with fluorescently labeled EVs suggest that they can be internalized by virtually every cell type tested (Svensson et al., 2013; Zech et al., 2012), while others report EV uptake in a cell type-specific manner and suggest that EV uptake can only occur in very specific conditions, when EVs and target cells share the right combination of ligands and receptors. Peritoneal exudate cells were shown to internalize pancreatic adenocarcinoma-derived EVs more efficiently than granulocytes and T cells (Zech et al., 2012). Another example states that the inhibition of integrin-mediated receptor internalization hampers EV uptake in macrophages and dendritic cells (Atay et al., 2011; Morelli et al., 2004), but the same results were not observed in microglia (Fitzner et al., 2011). These examples suggest that distinct mechanisms are responsible for the communication between EVs and cells, and different combinations of EVs are used by different cell types for communication (Mulcahy et al., 2014). It is important to note that heterogeneity in the donor and recipient cells, EVs themselves, the experimental design, as well as the context of experiments can all influence the results obtained and may account for the discrepancies observed between studies (Mulcahy et al., 2014).

3.2.6. EVs in neurodegenerative diseases

Neurodegenerative diseases represent a group of neurological disorders, usually associated with the aging process, which manifest as a dysfunction of the nervous system and progressive neuronal loss (Martin, 1999). The most common neurodegenerative diseases include AD, PD, multiples sclerosis (MS), ALS, HD, and prion diseases. Notwithstanding large differences in clinical manifestation and prevalence, these diseases share many common features besides their chronic and progressive nature and association with the aging process. These common features include neuronal death in particular areas of the brain, damage within the synaptic network, and selective brain mass loss (Ross and Poirier, 2004). Moreover, the progressive accumulation of misfolded protein aggregates into well-organized structures of amyloid nature is thought to be at the root of neurodegenerative diseases (Ross and Poirier, 2004; Soto, 2003). Although distinct neurodegenerative diseases are associated with different protein aggregates, the process of protein misfolding is remarkably similar (Soto, 2003).

The importance of intercellular communication mechanisms in the context of neurodegenerative diseases has recently been drawing attention and, beyond the complex molecular events occurring within a cell, the impact that these can have on neighboring or distant cells is being actively investigated. The growing interest in studying the mechanisms of communication between cells in neurodegenerative diseases derives mostly from the fact that communication often occurs through the extracellular environment, which is also the region where it is easier to intervene, either by using a therapeutic tool to modify a disease or by collecting samples to diagnose or evaluate disease progression. EVs, especially exosomes, were many times referred to as communicating mediators in physiological conditions, but during the last decade they have also been emerging as common players in neurodegenerative diseases. The clearance and disposal of byproducts and harmful molecules, along with the intercellular transmission of nucleic acids, cytokines, enzymes, and aggregated or misfolded proteins, are some of the mechanisms being studied as part of neurodegenerative pathophysiology. Although most of the advances regarding the roles of EVs in neurodegenerative diseases derive from *in vitro* experiments, the findings are in line with the prion-like disease spreading hypothesis recently proposed to explain some of the features of these diseases (Soria et al., 2017).

Prions are infectious agents consisting of misfolded proteins which adopt an aberrant conformation and can transmit their misfolded state to normal variants of the same protein and aggregate among themselves into oligomers and fibrils. The prion hypothesis postulates that these infectious particles act as proteopathic seeds, which trigger a chain reaction of refolding and self-aggregation, ultimately spreading the pathophysiological status to healthy cells and leading to neurodegeneration (Prusiner, 1982). Some known human diseases originating from this mechanism include Creutzfeldt-Jakob disease and Gerstmann-Straussler-Scheinker syndrome (Collinge, 2001). In a similar manner, other neurodegenerative diseases are also characterized by the accumulation of misfolded proteins, as is the case of β-amyloid (Aβ) and tau in AD, and α-synuclein (α-syn) in PD. The accumulation of these protein aggregates occurs concomitantly with the spreading of the pathology to neuroanatomically connected regions. These similarities gave rise to the hypothesis that AD and PD, as well as other proteinopathies, share a common spreading mechanism, which became known as the “prion-like” hypothesis (Jucker and Walker, 2013).

In 2004, cells expressing the prion protein (PrP) were found to secrete both the PrP^{C} (normal) and PrP^{Sc} (aberrant) forms in association with exosomes, supporting the idea of an exosome-mediated propagation of prion diseases (Fevrier et al., 2004). Four years later, PrP^{C} was found to be associated with EVs in the CSF of sheep, linking for the first time the pathogenesis of prion disease and EV-mediated communication (Vella et al., 2008). The

mechanisms underlying the interplay between prions and exosomes began to be unveiled very recently, therefore they are still poorly understood. However, it appears that the conversion of PrP^{C} into PrP^{Sc}, as well as its packaging into exosomes, is associated with the biogenesis mechanisms of these small vesicles (Vella et al., 2007; Yim et al., 2015). Moreover, the aberrant form PrP^{Sc} seems to be able to alter the structure of exosomes as well as their cargo (Bellingham et al., 2012; Coleman et al., 2012). The increased secretion of exosomes enhanced the infectiousness of PrP^{Sc} (Guo et al., 2016), strongly suggesting that prions can take advantage of EV-mediated communication mechanisms for neuropathological propagation into distinct areas of the brain, contributing for disease spreading.

The β-cleavage of APP was shown to occur in early endosomes with subsequent secretion of exosomes containing Aβ into the extracellular environment (Rajendran et al., 2006). Since APP is also expressed at the plasma membrane, it is highly probable to be contained within the membrane of MVs as well. Therefore, it was suggested that EVs could mediate Aβ propagation. However, there were no further reports concerning the link between exosomal secretion and Aβ spreading. On the other hand, C-terminal fragments of APP were detected in exosomes, both *in vitro* and *in vivo*, suggesting that the exosomal secretory pathway may not be so related with the direct spreading of Aβ, but may rather be more strongly associated with its generation (Perez-Gonzalez et al., 2012; Sharples et al., 2008). The β-secretase-1 enzyme is known to participate in Aβ fragments formation upon β-cleavage of APP, consequently leading to Aβ aggregation and amyloid plaques formation in the extracellular space (Zhang et al., 2011b). The expression of APP and β-secretase-1 in endosomes suggest that Aβ may be contained withing MVBs. However, conflicting reports have emerged regarding the stabilization of Aβ toxic species within these compartments. For instance, some studies suggest that exosomes serve as nucleation hubs for the formation of plaques by enhancing the aggregation of Aβ (Dinkins et al., 2014; Falker et al., 2016). This hypothesis suggests a neuroprotective role for exosomes, as they would putatively eliminate toxic Aβ oligomers in favor of the more stable and less toxic fibrils. In contrast, other authors suggest the opposite, where exosomes promote the disassembly of stable species into neurotoxic oligomers. However, it was suggested that the pathological role of exosomes may depend on the originating cell type, specifically regarding a neuronal or myeloid origin, based on the hypothesis that the composition of the exosome's lipid membrane might affect Aβ aggregation in different manners (Joshi et al., 2014; Yuyama et al., 2012).

Apart from the association between Aβ and exosomes, hyperphosphorylated tau, the primary component of neurofibrillary tangles in AD, was also found in exosomes derived from the CSF of AD patients (Saman et al., 2012). Moreover, overexpressed tau was shown to be secreted within EVs and transmitted through the extracellular space in *in vitro* studies (Chai et

al., 2012; Lee et al., 2012; Liu et al., 2012; Simón et al., 2012). Additionally, the inhibition of exosomal release impairs the propagation of tau, both *in vitro* and *in vivo* (Asai et al., 2015). Altogether, these observations suggest a role for exosomes in the spreading of tauopathy within the brain of AD patients.

Dementia with Lewy bodies (DLB) and PD are neuropathologically characterized by the presence of Lewy bodies, which are inclusion bodies composed of aggregated proteins including α-syn (Spillantini et al., 1997). The monomeric and oligomeric forms of α-syn exist in constant equilibrium, but mutations within this protein and other factors can disturb the aggregation dynamics and shift the balance towards fibrillization (Dehay et al., 2015). In PD, the neurodegenerative process was shown to spread to distinct neuroanatomically interconnected regions of the CNS (Braak et al., 2003), and the pathogenic trait of misfolded α-syn is thought to disseminate in a prion-like manner (Lee et al., 2010; Olanow and Prusiner, 2009). Indeed, it was shown that α-syn species are present in exosomes derived from the CSF of PD and DLB patients, and such exosomes were revealed to stimulate α-syn aggregation (Stuendl et al., 2016). Nevertheless, it is still not clear whether exosomes are able to spread α-syn to other brain regions (Soria et al., 2017).

The α-syn protein is present in synaptic vesicles and, although its functions are poorly understood, α-syn was suggested to participate in synaptic vesicle trafficking and subsequent neurotransmitter release (Logan et al., 2017). The role of α-syn in this cellular process led researchers to hypothesize a possible link between α-syn and exosomes due to its intrinsic function within the exocytic machinery at the pre-synaptic terminal (Bendor et al., 2013). Indeed, not only α-syn was detected in exosomes, but also the exosomal environment with reduced pH was shown to accelerate α-syn aggregation (Grey et al., 2015).

In multiple system atrophy (MSA), oligodendrocytes accumulate α-syn in aggregates designated as glial cytoplasmic inclusions (GCIs). The formation of GCIs in oligodendrocytes is accompanied by demyelination and extensive loss of dopaminergic neurons throughout the brain. The aggregation of α-syn in oligodendrocytes has been extensively studied in transgenic MSA models overexpressing α-syn under the control of various oligodendrocyte-specific promoters, but the association between α-syn aggregation in these cells and neuronal death has not yet been elucidated (Fernagut and Tison, 2012). Moreover, it is unknown if oligodendrocytes can synthesize α-syn *de novo* in a disease context, since α-syn is a predominantly neuronal protein. Following this rationale, neurons could be the source of α-syn found in oligodendrocytes. In fact, there are reports indicating that exosomes can mediate the communication between neurons and oligodendrocytes, supporting the hypothesis that α-syn could originate in neurons and be taken up by the latter cells (Bakhti et al., 2011; Krämer-

Albers et al., 2007). Additionally, genetic material such as miRNAs is also shared between neurons and oligodendrocytes via exosomes (Frühbeis et al., 2013), and miRNAs were shown to be altered in MSA (Schafferer et al., 2016; Ubhi et al., 2014). All of these observations support that EV-mediated communication is a process potentially involved in the pathogenesis of MSA.

Misfolding of SOD1 into aberrant conformations has been identified as the central cause of both familiar and sporadic forms of ALS (Bosco et al., 2010). SOD1 was shown to be associated with exosomes and can be transmitted between neuronal cells, hence propagating the pathogenic trait to recipient cells (Grad et al., 2014). Moreover, SOD1-loaded exosomes are also secreted by astrocytes, which can induce selective toxicity into recipient motor neurons, indicating that the transfer of mutant SOD1 mediated by exosomes is pathogenic (Basso et al., 2013).

EVs may also mediate the transfer of toxic molecules between different species. An interesting work showed that mutant huntingtin-containing exosomes derived from human HD patient-derived fibroblasts and the human neuroblastoma cell line SH-SY5Y were taken up by mouse neural stem cells, when in co-culture. Furthermore, the intracerebroventricular delivery of human HD fibroblasts-derived exosomes into newborn wild-type mice triggered HD motor features and neuropathology, as determined by the loss of the neuronal marker dopamine- and cAMP-regulated neuronal phosphoprotein (DARPP-32) (Jeon et al., 2016). Because HD belongs to the group of polyQ diseases, and since it is frequently accepted that these disorders share common pathogenic mechanisms (although the symptoms and the regional patterns of neurodegeneration are not shared among them) (Nóbrega and Pereira de Almeida, 2018), it would be important to address the possibility that EV-mediated toxicity and disease spreading is feature of other polyQ disorders.

Even though EVs participate in the propagation of misfolded proteins such as Aβ and tau, probably the relevance of EVs in proteinopathies is not limited to the intercellular transmission of proteopathic seeds. Indeed, there is still debate about whether the transmission of the misfolded protein itself is sufficient to cause neurodegeneration *per se*, or if other factors external to the EV-mediated transmission of these proteins could induce aberrant folding in selectively vulnerable neurons (Walsh and Selkoe, 2016). Proteopathic seeds can be found all over the brain, still supporting the spreading of these seeds, presumably mediated by EVs; however, only selective regions of the brain display protein aggregation and neurodegeneration, meaning that other still unknown factors can be the cause of this regional selectivity for neuronal death (Alibhai et al., 2016).

During the last decade, the scientific community witnessed an increase in the number of publications regarding EVs. Initially considered as waste disposal mechanisms, recent evidence caught the researchers' attention and a growing interest in this field has been noticed since then. Currently, EVs are considered important mediators of intercellular communication by internalizing, transporting, and transferring all types of biomolecules, including nucleic acids, proteins, and lipids. The *in vitro* studies performed so far provided useful data to understand the biogenesis mechanisms and physiological roles of EVs, but their role in neurodegenerative diseases as disease-spreading agents is far from being understood. This is in part due to the lack of *in vivo* studies. Several questions remain unanswered, but those of particular interest are: what are the molecular signatures of particular types of EVs that can be isolated from patients and used as biomarkers? Can the EV secretory pathway constitute a therapeutic target? Do EVs efficiently propagate pathogenic traits *in vivo*? Hopefully, future studies will shed light on the relevance of EVs in neurodegenerative diseases.

4. Objectives

EVs have emerged as intercellular communicating agents able to transfer presumably all types of cargo, including nucleic acids, enzymes, lipids, metabolites and, importantly, disease-associated proteins. Nevertheless, EVs enrollment in SCA2 pathogenesis was never addressed. Since EVs seem to be common players in mediating the transport of misfolded proteins in neurodegenerative diseases such as HD, which is thought to share common pathogenic mechanisms with other polyQ diseases, we hypothesized that EVs could also mediate disease spreading in SCA2, explaining, in part, the regional progression of neurodegeneration.

Therefore, the aim of this work was to determine if ataxin-2 can spread between cells in association with EVs, and whether this process can be associated with SCA2 phenotypical changes. To accomplish this general goal, two major tasks were outlined. The first task of this work aimed to ascertain whether the human ataxin-2 protein and/or mRNA would be intercellularly transferred *in vitro* by (i) assessing the possible transfer of ataxin-2 through the conditioned medium of ataxin-2-transfected cells into naïve recipient cells, (ii) by determining the presence or absence of the ataxin-2 protein and/or mRNA within exosomes and MVs, and (iii) by investigating the ability for ataxin-2-loaded EVs to cause ataxin-2 accumulation in naïve recipient cells. The second task aimed at evaluating the ability of intracerebroventricularly-delivered ataxin-2-loaded EVs in targeting the mutant protein to several brain regions of wild-type mice and induce formation of aggregate-like structures.

CHAPTER 2 – MATERIALS AND METHODS

Plasmids

The pEGFP-ataxin-2-(Q22) and pEGFP-ataxin-2-(Q58) plasmids were kindly provided by Dr. Stefan M. Pulst (Department of Neurology, University of Utah, Salt Lake City, Utah, USA). These plasmids encode a human form of ataxin-2, respectively with 22 or 58 glutamines, N-terminally fused in frame with enhanced green fluorescent protein (eGFP), under the control of a CMV promoter, and contains a neomycin resistance cassette.

The pEGFP-Q74 plasmid was a gift from David Rubinsztein (Department of Medical Genetics, Cambridge Institute for Medical Research, Addenbrooke's Hospital, UK; Addgene plasmid #40262). This plasmid encodes a portion of the exon 1 of human huntingtin with 74 glutamines, N-terminally fused in frame with eGFP, under the control of a CMV promoter, and contains a neomycin resistance cassette.

The mCherry-CD81-10 plasmid was a gift from Michael Davidson (Florida State University, Tallahassee, Florida, USA; Addgene plasmid #55012). It codifies a human form of the tetraspanin CD81, N-terminally fused in frame with mCherry, which is under the control of a CMV promoter, and contains a neomycin resistance cassette controlled by an SV40 promoter.

Extracellular vesicles-depleted medium production

Polypropylene copolymer (PPC) ultracentrifuge tubes (Thermo Scientific™ Nalgene™, USA) containing Dulbecco's Modified Eagle's Medium High Glucose with L-Glutamine (DMEM HG 4.5 g/L; BioConcept, Switzerland), 3.7 g/L sodium bicarbonate ($NaHCO_3$; Fisher Scientific, USA) and 10 mM 4-(2-hydroxyethyl)-1-piperazineethanesulfonic acid (HEPES; Fisher Scientific, USA), supplemented with 20% (v/v) fetal bovine serum (Gibco, USA), 100 U/mL penicillin and 100 µg/mL streptomycin (Gibco, USA) were centrifuged in an Avanti JXN-30 high-speed centrifuge (Beckman Coulter,USA), using a JA-30.50 Ti rotor, at 100,000 x *g* and 4 ºC, for 18 hours, in order to pellet extracellular vesicles originating from FBS. Afterwards, the supernatant was decanted into 50 mL syringes and filtered through a 0.22 µm filter into sterile containers, where it remained at 4 ºC until further use. On usage, EV-depleted medium was diluted in serum-free DMEM HG containing 100 U/mL penicillin and 100 µg/mL streptomycin (Gibco, USA), in a 1:1 proportion, reaching a final concentration of 10% (v/v) EV-depleted FBS.

Cell culture, transfection, and conditioned medium transferring

The mouse neuroblastoma Neuro-2A (N2a) cell line was cultured in normal DMEM HG with L-Glutamine, supplemented with the components described above. The cells were maintained in 175 cm^2 flasks at 37 ºC, in an incubator with a 5% CO_2 humidified atmosphere. Every 2/3 days, the culture medium was changed as cells were split upon reaching 80-90% average confluence.

For transfection, N2a cells were either seeded in 12-well plates or 100 mm culture dishes. For the 12-well plates, cells were transfected with 500 ng of plasmid DNA and 3 µL of polyethylenimine (PEI, 1 mg/ml, Polysciences Inc., USA) per well; for the 100 mm culture dishes, 7.3 µg of DNA and 44 µL of PEI (1 mg/mL) were used instead. Twenty-four hours following transfection, the cells were rinsed with prewarmed phosphate-buffered saline (138 mM NaCl, 2.7 mM KCl, 11.76 mM phosphate buffer, pH 7.4; NZYTech, Lisbon) to wash out dead cells and debris, as well as FBS-derived EVs. Then, EV-depleted culture medium was added to the cells, in order to collect N2a-derived EVs, during the two following days. N2a-derived EV-conditioned media from the 12-well plates were diluted in fresh EV-depleted medium, for nutritional support, and then transferred to new N2a cultures. Following a 24 h-incubation, the cells were fixed and analyzed for the detection of eGFP-ataxin-2. N2a-derived EV-conditioned media from the 100 mm culture dishes were collected and pooled for downstream EV isolation and purification procedures.

Extracellular vesicles isolation and characterization

Extracellular vesicles were isolated and purified by differential ultracentrifugation as previously described (Menck et al., 2017a; Thery et al., 2006), with minor modifications. Briefly, approximately 200 mL of N2a-derived EV-conditioned media were spun at 300 x *g* for 10 min to remove dead cells and large debris. The supernatants were collected and again centrifuged at 2,000 x *g* for 20 min to eliminate any possible apoptotic bodies and smaller debris. To harvest large EVs, such as microvesicles, the supernatants from the previous step were transferred to PPC ultracentrifuge tubes (Thermo Scientific™ Nalgene™, USA) and spun at 10,000 x *g* for 30 min, in an Avanti JXN-30 high-speed centrifuge (Beckman Coulter, USA), using a JA-30.50 Ti rotor. The supernatants were collected for isolating exosomes while the resulting pellets containing microvesicles were resuspended and pooled in 1 mL of PBS to wash any contaminants. The microvesicles suspension was then centrifuged at 14,000 x *g* for 35 min, in a microcentrifuge. The contaminant-free microvesicles pellet was then resuspended in 18-250 µL of PBS and stored at -80 ºC until use. Exosomes were pelleted by

ultracentrifugation at 100,000 x *g* for 70 min, using a JS-24.38 Swinging-Bucket rotor. Exosomes were then resuspended in PBS to wash any contaminating proteins and pooled for a last ultracentrifugation at 100,000 x *g* for 70 min. The resulting pellet containing the purified exosomes was resuspended in 18-250 µL of PBS, and exosomes were stored at -80ºC until use. All of the centrifugations were performed at 4 ºC, and samples were manipulated inside a laminar flow hood to maintain aseptic conditions.

The EVs parent cells were additionally collected for the characterization of exosomes and to be used as a positive control of transfection, in further experiments. EVs were characterized based on their size, morphology, and well-established exosome molecular markers, such as the tetraspanin CD9 and Alix.

Protein isolation, quantification, and Western blotting

EVs parent cells were rinsed twice with ice-cold PBS and lysed on ice in radioimmunoprecipitation assay (RIPA) buffer (Merck Millipore, Germany), supplemented with a mini protease inhibitor cocktail tablet (Roche, Switzerland). Cell lysates were then sonicated on a Bioruptor® Pico sonication device (Diagenode, Belgium) for 5 cycles, each with 30 seconds ON and 30 seconds OFF. The insoluble material from the sonicated samples was removed by centrifugation at 20,000 x *g* and 4 ºC, for 20 min. The protein samples from EVs parent cells were then diluted 1:10 in PBS. The total protein concentration was determined for EVs and their parent cells by the Bradford method using a ready-to-use Bradford reagent (NZYTech, Lisbon), as previously described (Thery et al., 2006). Briefly, bovine serum albumin (BSA) standards were prepared in PBS by performing serial dilutions, ranging the BSA concentration from 4 µg/mL to 500 µg/mL. Next, 10 µL of each standard was loaded per well into a 96-well plate. Then, 5 µL of EV samples were added to 5 µL of PBS and 2 µL of total lysates from EVs parent cells were added to 8 µL of PBS, in each well. A blank was also established by using 10 µL of PBS. At last, 200 µL of the ready-to-use Bradford reagent were added to each well and the absorbance was measured at 590 nm, within 10 min. All measurements were performed in two replicates of each sample.

Samples were reduced and denatured by adding 4x reducing Laemmli SDS sample buffer (Alfa Aesar, USA) or simply denatured with 4x non-reducing SDS sample buffer [0.25 M Tris-HCl (pH 6.8), 8% (v/v) sodium dodecyl sulfate (SDS), 30% (v/v) glycerol, and 0.02% (w/v) bromophenol blue], when indicated, and by heating them at 95 ºC, for 5 min. After that, samples were stored at -20 ºC until further use.

Sample volumes corresponding to equal amounts of total protein mass were loaded per well of a 4-12.5% gradient SDS-polyacrylamide gel and separated by electrophoresis. Proteins were electrotransferred at 750 mA in CAPS buffer [0.1 M CAPS (pH 11.0), 10% (v/v) methanol] into polyvinylidene difluoride (PVDF) membranes (Millipore, USA). The membranes were blocked with 5% low-fat milk in Tris-buffered saline [1.37 M NaCl, 200 mM Tris base (pH 7.6)] containing 0.1% (v/v) Tween-20 (TBS-T), for one hour at room temperature. The membranes were incubated overnight with the primary antibody diluted in blocking solution, at 4 ºC (Table 2.1). Then, the membranes were washed three times in TBS-T and incubated with the respective polyclonal horseradish peroxidase-conjugated secondary antibody, for one hour, at room temperature (Table 2.1). Immunoreactive bands were visualized by chemiluminescence with the Amersham™ ECL™ Prime Western Blotting Detection Reagent (GE Healthcare, USA) in a ChemiDoc™ XRS+ System (Bio-Rad, USA).

Table 2.1 – Antibodies used in Western blot procedures

	Antibody name	Species	Dilution	Incubation	Manufacturer
Primary antibody	anti-AIP1 (Alix) (clone 49/AIP1)	mouse monoclonal	1 : 500	ON, 4 ºC	BD Biosciences (USA)
	anti-CD9 (clone MM2/57)	mouse monoclonal	1 : 1,000	ON, 4 ºC	Millipore (USA)
	anti-calnexin	rabbit polyclonal	1 : 1,000	ON, 4 ºC	Millipore (USA)
	anti-ataxin-2 (clone 22/Ataxin-2)	mouse monoclonal	1 : 1,000	ON, 4 ºC	BD Biosciences (USA)
Secondary antibody	anti-mouse IgG HPC	sheep polyclonal	1 : 10,000	2 h, RT	GE Healthcare (USA)
	anti-rabbit IgG HPC	sheep polyclonal	1 : 10,000	2 h, RT	GE Healthcare (USA)

Abbreviations: **IgG –** immunoglobulin, **HPC** – horseradish peroxidase-conjugated, **ON –** overnight, **RT** – room temperature

Transmission and scanning electron microscopy

TEM and SEM analyses were performed at the Centro de Instrumentación Científica (CIC, University of Granada, Spain). Briefly, for both TEM and SEM, exosome samples were negatively stained with uranyl acetate as follows: a 30 µL drop of the exosomes sample was placed on a carbon-coated 300-mesh grid and exosomes were allowed to adsorb for 5 min at room temperature. The grids were then washed several times in drops of ultrapure water for 1 min. Adsorbed exosomes were negatively stained in droplets of 1% (w/v) uranyl acetate for 1 min. The exceeding uranyl acetate solution was removed with filter paper, and the samples were dried at room temperature for 6 min. The preparations were examined with a LIBRA 120 PLUS transmission electron microscope (Carl Zeiss SMT, Germany) at an acceleration voltage of 120 kV, and with the HITACHI, S-510 scanning electron microscope.

Atomic force microscopy

AFM analyses were performed at the Centro de Instrumentación Científica (CIC, University of Granada, Spain). Briefly, purified exosomes were diluted 1:50 in deionized water. A 10 µL drop of the exosomes suspension was adsorbed to freshly cleaved mica sheets for 10 min at room temperature. Then, the mica sheets were rinsed with deionized water to remove salt precipitates and completely dried under a gentle stream of argon gas. The preparations were examined with an NX20 atomic force microscope (Park Systems, South Korea), and images were acquired and analyzed using the PARK SYSTEMS XEI software (Park Systems, South Korea). Measurements were carried out using ACTA silicon cantilevers (40 $N \cdot m^{-1}$), in the non-contact mode.

Extracellular vesicles size characterization

Extracellular vesicles size distribution was determined using a Malvern Zetasizer® Nano ZS instrument (Malvern Instruments S.A., UK). In a polystyrene cuvette, 40 µL of EV samples were diluted in 1 mL of ultrapure water and their sizes were measured by dynamic light scattering at 25 °C, with a scattering angle of 173°. Measurements were performed in triplicate for two independent experiments.

RNA extraction and RT-PCR analysis

Total RNA from EVs and their parent cells was purified using a combination of phase separation and the NZY Total RNA Isolation kit (NZYTech, Lisbon). Briefly, 250 µL of EV suspensions were lysed in 500 µL of QIAzol™ Lysis Reagent (Qiagen, Germany). Subsequently, 200 µL of chloroform were added and the mixture incubated at room temperature for 5 min. For complete phase separation, the samples were centrifuged at 12,000 x *g* and 4 ºC, for 15 min. The upper aqueous phase was transferred into a new microcentrifuge tube (~ 500 µL) and mixed with isopropanol (1.25x volume) for RNA precipitation. Samples were then transferred into a spin column, and the following steps were carried out with the NZY Total RNA Isolation kit, according to the manufacturer's instructions. Finally, the RNA concentrations were determined with the NanoDrop2000c spectrophotometer (Thermo Fisher Scientific, USA).

The cDNAs were obtained by converting 100 ng of purified RNA, using the iScript cDNA Synthesis kit (Bio-Rad, USA). Reverse transcription reactions were performed in a thermocycler at 25 ºC for 5 minutes, 46 ºC for 20 minutes, and 95 ºC for 1 minute. A standard polymerase chain reaction (PCR) was performed using the DreamTaq™ DNA polymerase kit (Thermo Scientific, USA). A reaction mastermix was prepared according to the manufacturer's instructions, containing the appropriate concentration of each pair of primers (Table 2.2), and the PCR procedure was performed in a final volume of 25 µL, containing 5 µL of each cDNA. The PCR parameters were also set according to the polymerase manufacturer's instructions, as follows: initial denaturation at 95 ºC for 3 min, followed by 30 cycles at 95 ºC for 30 seconds, 60 ºC for 30 seconds, and 72 ºC for 1 min, corresponding to denaturation, annealing and extension steps, respectively. The protocol also included a final extension step at 72 ºC for 10 min. The resulting amplicons were submitted to a 2% (w/v) agarose gel electrophoresis at 120 V, for 45 min, which was subsequently scanned using the ChemiDoc™ XRS+ System (Bio-Rad, USA).

Table 2.2 – Primers used in PCR procedures

Gene	Primer sequence	Final concentration	amplicon	Manufacturer
hATXN2	N.d.	1X	~ 85 bp	Qiagen (Germany)
ACTB	**Fwd**: 5'-GGAGACGGGGTCACCCACAC-3'	0.25 µM	315 bp	Invitrogen™ (USA)
	Rev: 5'-AGCCTCAGGGCATCGGAACC-3'	0.25 µM		

Abbreviations: **N.d. –** not disclosed, **Fwd** – forward primer, **Rev –** reverse primer

Mass spectrometry

Mass spectrometry analyses were performed by the Instituto de Patologia e Imunologia Molecular da Universidade do Porto (IPATIMUP). The detected proteins were identified based on the UniProt database.

Flow cytometry

For functional assays regarding EV uptake, N2a cells were seeded in 6-well plates and 42 µL of EV suspensions were diluted in EV-depleted medium and added to the cell cultures, 12 h and 24 h prior to flow cytometry analyses. Cells were rinsed twice in ice-cold PBS and subsequently resuspended in 0.5% (w/v) BSA/PBS at a density of approximately 1.0 x 10^6 cells/mL. The cells suspensions were transferred into sterile flow cytometry tubes, passing through a 35 µm strainer cap to avoid cell doublets. Samples were analyzed in a FACSCalibur flow cytometer (Becton-Dickinson, USA), using a 488 nm argon laser. For each condition, approximately 10,000 cells were assayed and scanned for eGFP fluorescence using a 530/30 bandpass filter. To distinguish the cells from debris, data was manually gated based on size, measured by forward scatter height (FSC-H), and subsequently plotted as a function of the eGFP fluorescence intensity, using the channel FL1-H, to determine EV uptake. The analyses were performed using FlowJo 7.6.1 (Becton-Dickinson, USA).

Immunocytochemistry

N2a cells were seeded on 0.1% (w/v) porcine gelatin pre-coated glass coverslips. On the following day, approximately 5 µg of total protein of EVs were diluted in EV-depleted medium and added to N2a cells. Cells were harvested at three distinct time points: 24 h, 48 h,

and 72 h following EV exposure. Subsequently, cells were rinsed twice in ice-cold PBS and fixed with 4% (w/v) paraformaldehyde in PBS (PFA/PBS) for 15 min. After two more washes with PBS, the cells were permeabilized with 0.1% (v/v) Triton X-100™ (Thermo Fisher Scientific, USA) in PBS for 5 min at room temperature. The cells were once again rinsed with PBS and then blocked with 3% (w/v) BSA/PBS for 1 h at room temperature, followed by an overnight incubation with the primary antibody (Table 2.3), at 4 ºC. After incubation, the cells were washed twice with PBS and incubated with the respective secondary antibody (Table 2.3), for 2 h at room temperature. Finally, cells were rinsed twice with PBS and the coverslips were mounted on glass microscope slides with Fluoromount-G™ Mounting Medium with 4′,6-diamidino-2-phenylindole (DAPI; Invitrogen™, USA).

Table 2.3 – Antibodies used in immunocytochemistry assays

	Antibody name	Species	Dilution	Incubation	Manufacturer
Primary antibody	anti-GFP (clone 1GFP63)	mouse monoclonal	1 : 1,000	ON, 4 ºC	BioLegend® (USA)
Secondary antibody	Alexa Fluor™ 488 anti-mouse IgG	goat polyclonal	1 : 200	2 h, RT	Invitrogen™ (USA)

Abbreviations: **IgG** – immunoglobulin, **ON** – overnight, **RT –** room temperature

Animal maintenance

C57BL/6J mice (Charles River Laboratories) were housed in a temperature-controlled room maintained on a 12 h light/12 h dark cycle. Food and water were provided *ad libitum*. The experiments were carried out in accordance with the European Community directive (2010/63/EU) for the care and use of laboratory animals. The researchers received certified training (FELASA course) and approval to perform the experiments from the Portuguese authorities (Direção Geral de Alimentação e Veterinária) in the project Neuropath (421/2019).

Extracellular vesicles *in vivo* delivery

EVs obtained from cells transfected with eGFP-ataxin-2-(Q58) and mCherry-CD81 were delivered *in vivo* to ten-week-old mice, through intracerebroventricular injection. First, the animals were anesthetized with an intraperitoneal injection of a combination of ketamine

(Nimatek 70 mg/Kg; Dechra Pharmaceuticals, UK) and medetomidine (Domitor® 0.7 mg/Kg; Orion Corporation, Finland). When completely anesthetized, the mice were properly placed and fixed on a stereotaxic device, and their scalps were incised to expose the skull, following the surgical procedure described previously (Nobrega et al., 2013). Using the bregma point at the surface of the skull as coordinate zero, the cranium was unilaterally perforated to inject EVs in the brain's right lateral ventricle. The coordinates used were defined according to the Mouse Brain Atlas online tool, which is based on Paxinos and Franklin's mouse brain atlas (Paxinos and Keith B. J. Franklin, 2007): anteroposterior = -0.2 mm, mediolateral = 0.9 mm, dorsoventral = -2.3 mm. The injections were performed using a Hamilton precision syringe (26G needle) and 3 µL of EVs (0.1-0.3 µg/µL of total protein) per animal, at a flow rate of 1 µL/min. After the injections, the needle was kept in place for 5 min to prevent EV reflux. The animals were kept for 24 h post-injection before being sacrificed for posterior analyses.

Brain tissue collection

The mice were euthanized with a lethal intraperitoneal injection of ketamine/medetomidine (120 mg/Kg and 1.2 mg/Kg, respectively), and transcardially perfused with 50 mL of 4% (w/v) PFA/PBS. The whole brains were removed and incubated in 4% PFA/PBS for 3 days and, subsequently, in 20% (w/v) sucrose/PBS for 24 h to dehydrate the tissue. Later, the brains were completely dried and frozen at -80 ºC.

Histological processing and immunohistochemistry

The whole brains were cut into 30 µm sagittal sections using the cryostat model CryoStar™ NX50 (Thermo Fisher Scientific, USA). The brain sections were stored at 4 ºC, free-floating in 0.02% (w/v) sodium azide/PBS, until further use.

Fifteen parasagittal sections covering the whole brain and cerebellum from each mouse were collected for immunohistochemical processing. First, the sections were washed in PBS to remove sodium azide and, subsequently, permeabilized and blocked with a PBS solution containing 0.1% (v/v) Triton X-100™ and 10% (v/v) normal goat serum for 1 h, under smooth agitation. The slices were posteriorly incubated overnight with the primary antibodies diluted in blocking solution (Table 2.4), at 4 ºC, under agitation. On the following day, the brain sections were washed three times in PBS, for 10 min each, and then incubated with the respective secondary antibodies (Table 2.4) for 2 h, under smooth agitation, at room temperature. The slices were again washed three times in PBS and, subsequently, mounted with Fluoromount-

G™ Mounting Medium with DAPI (Invitrogen™, USA) onto gelatin-coated glass microscope slides.

Table 2.4 – Antibodies used in immunohistochemistry assays

	Antibody name	Species	Dilution	Incubation	Manufacturer
Primary antibody	anti-GFP (clone 1GFP63)	mouse monoclonal	1 : 1,000	ON, 4 ºC	BioLegend® (USA)
	anti-CD81 (clone 5A6)	mouse monoclonal	1 : 1,000	ON, 4 ºC	BioLegend® (USA)
	anti-calbindin-D-28K (clone CB-955)	mouse monoclonal	1 : 1,000	ON, 4 ºC	Sigma-Aldrich® (USA)
	anti-SQSTM1/p62	rabbit polyclonal	1 : 1,000	ON, 4 ºC	Cell Signaling (USA)
	anti-ubiquitin (clone P4D1)	mouse monoclonal	1 : 1,000	ON, 4 ºC	Cell Signaling (USA)
Secondary antibody	Alexa Fluor™ 488 anti-mouse IgG	goat polyclonal	1 : 200	2 h, RT	Invitrogen™ (USA)
	Alexa Fluor™ 594 anti-mouse IgG	goat polyclonal	1 : 200	2 h, RT	Invitrogen™ (USA)
	Alexa Fluor™ 647 anti-mouse IgG	goat polyclonal	1 : 200	2 h, RT	Invitrogen™ (USA)

Abbreviations: **IgG – i**mmunoglobulin, **ON** – overnight, **RT** – room temperature

Widefield and confocal fluorescence microscopy

Widefield fluorescence images were acquired with an Axio Imager.Z2 microscope (Carl Zeiss, Germany) equipped with an AxioCamHR3 digital camera, using the Plan-Apochromat 63x/1.40 Oil DIC M27 and alpha Plan-Apochromat 100x/1.46 Oil DIC (UV) M27 objectives and the AxioVision imaging software (Carl Zeiss, Germany).

Confocal fluorescence imaging was performed with an LSM 710 confocal microscope (Carl Zeiss, Germany) equipped with a Plan-Apochromat 63x/1.40 Oil DIC M27 objective, using the Super-Resolution mode and the ZEN Black software (Carl Zeiss, Germany). eGFP-atxn2^{Q58} and DAPI signals were revealed by exciting with 488 nm argon (25 mW) and

405-30 diode (30 mW) lasers, respectively. Z-series optical sections were obtained with a step-size of 0.16 µm. Z-series are displayed as maximum Z-projections or as 3D image reconstructions, and gamma, brightness, and contrast were adjusted identically for compared image sets, using the ImageJ 1.53c software (National Institutes of Health, USA). For the quantification of eGFP-atxn2^{Q58} aggregates number and volume, five random cells were blindly selected per each experimental group and submitted to 3D analysis, using the ImageJ's "3D Object Counter" plugin. For the quantification of the number of eGFP-atxn2^{Q58} aggregates per cell, the voxels' intensity was thresholded to 1131 in all experimental conditions, considering a size range of 20-500.000 voxels for detected objects. Concerning the quantification of the average volume of aggregates per cell, the intensity's threshold was maintained, but the size interval was set to 25-500.000 voxels for detected objects. Because of the great bias observed in the distribution of the volume of individual aggregates due to the greater abundance of small aggregates, only the 25 larger aggregates from each experimental group were considered for analysis.

Statistical analyses

The EV uptake experimental results are represented as the average number or volume of aggregates per cell (n=5 cells per experimental group), and as the mean ± standard error of the mean of the average number or volume of aggregates per cell and per time point. Data was analyzed using one-way analysis of variance followed by the Tukey's multiple comparisons *post hoc* test. The threshold of significance was set at p<0.05. All analyses were performed using GraphPad Prism version 7.04 (GraphPad Software, La Jolla, USA).

Chapter 2

CHAPTER 3 – RESULTS

Ataxin-2 is transported between cells through the extracellular medium

Similarly to other neurodegenerative diseases, SCA2 patients display region-selective neurodegeneration that propagates to other neuroanatomical regions with the progression of the disease (Mascalchi et al., 2014). However, the reason for the disease spreading in SCA2, as well as in other neurodegenerative diseases is not completely clear. In the last years, neuron-neuron propagation of misfolded proteins has been linked to the progression of many neurodegenerative diseases, including AD, PD, and HD, and such propagation was suggested to be associated with EVs, especially exosomes, the most studied subtype of EVs (Jeon et al., 2016; Perez-Gonzalez et al., 2012; Saman et al., 2012; Stuendl et al., 2016).

The fact that HD is a polyQ disorder that has been associated with exosome-mediated spreading raises the question of whether this is a common mechanism among polyQ diseases, since it is believed that they share common pathogenic mechanisms (Nóbrega and Pereira de Almeida, 2018). This question is particularly intriguing in the case of SCA2, since ataxin-2 is a cytosolic protein that has been shown to be associated with the endocytic pathway (Nonis et al., 2008), the same from which exosomes originate. However, the transfer of ataxin-2 between cells has never been described until the present date.

In culture, EVs are secreted to the culture medium. As a first approach to determine if ataxin-2 was transported in EVs, we aimed to determine if the transfer of conditioned media (CM) between different cell cultures could lead to the detection of ataxin-2 in the recipient cells. Mouse neuroblastoma N2a cells were transfected with pEGFP-ataxin-2-(Q22), encoding the human wild-type form of ataxin-2 fused with eGFP, or with pEGFP-ataxin-2-(Q58), encoding the mutant form with 58 glutamines. Ataxin-2-transfected cells were cultured in EV-depleted medium for EV harvesting. CM were collected 48 h later and transferred to non-transfected N2a cell cultures (figure 3.1A). Both wild-type and mutant forms of ataxin-2 were detected in non-transfected recipient cells 24h later, as indicated by the presence of eGFP-positive cells (figure 3.1B). This suggests that both wild-type and expanded ataxin-2 can be transferred from transfected cells to non-transfected cells, through the extracellular medium. Similar results were obtained when using media from cells expressing mutant huntingtin, a protein already described to spread in association with exosomes (figure S3.1) (Jeon et al., 2016).

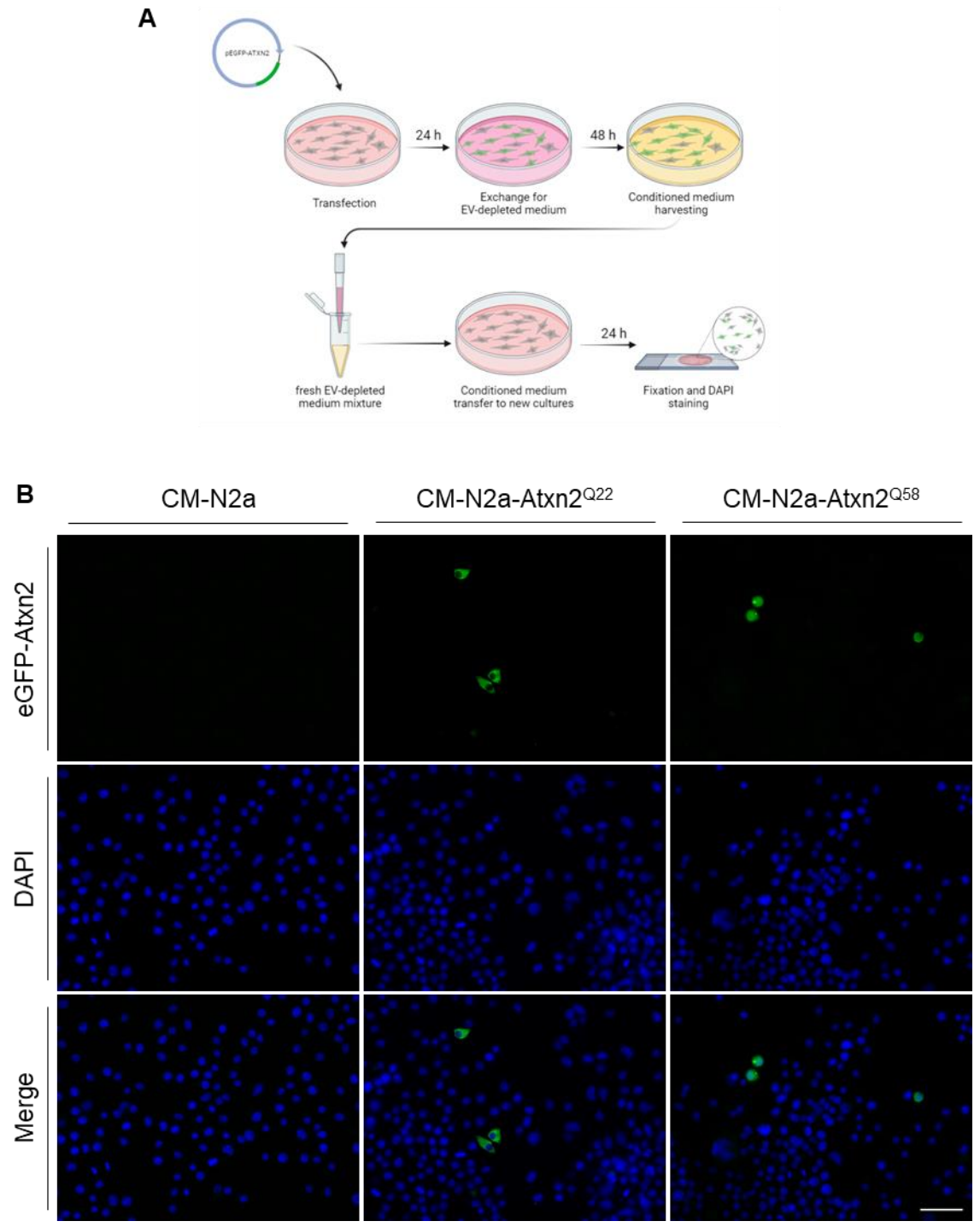

Figure 3.1 – Human ataxin-2 is detected in recipient cells upon the transfer of CM from N2a cells transfected with pEGFP-ataxin-2. **(A)** Schematic representation of the experimental design: both wild-type and mutant pEGFP-ataxin-2 plasmids were used to transfect N2a cells, using PEI. Cells were then cultured for 24 h in EV-free medium, for posterior EV harvesting. Non-transfected N2a recipient cells were cultured in CM (mixed with fresh EV-free medium for nutritional support) for 24 h and then fixed and DAPI-stained for observation. **(B)** Both wild-type and mutant forms of eGFP-ataxin-2 were detected in non-transfected N2a recipient cells (green). N2a recipient cells cultured in CM derived from non-transfected cells were used as negative control. DAPI-stained nuclei can be observed in blue. Scale bar, 50 µm. Results are representative of four independent experiments.

Characterization of extracellular vesicles from cells overexpressing ataxin-2

Upon obtaining evidence that ataxin-2 can be transferred from one cell to another, we then aimed to investigate by which means such transport was mediated. Since ataxin-2 is recruited to the plasma membrane to participate in the endocytic pathway (Nonis et al., 2008), we hypothesized that exosomes and MVs could serve as carriers for mutant ataxin-2. Therefore, MVs and exosomes were isolated from pEGFP-ataxin-2-(Q58)-transfected N2a cells (N2a-MV^{Q58} and N2a-Exo^{Q58}, respectively) by differential centrifugation, and characterized based on their physical features and molecular markers.

DLS analyses confirmed the presence of two distinct populations of EVs with average sizes of 208.4 ± 4.5 nm and 530.7 ± 109.0 nm in diameter, presumably corresponding to exosomes and MVs, respectively (figure 3.2A). The polydispersity index (PdI) indicated that the population of larger EVs was heterogeneous in size (0.460 ± 0.072), which is a typical feature of MVs. In contrast, the population of smaller EVs seemed more homogenous (0.262 ± 0.092), which is characteristic of exosomal fractions. The morphology of smaller EVs was further analyzed by electron microscopy and scanning probe microscopy. TEM, SEM, and AFM analyses indicated that these vesicles were indeed small in size and most of them measured less than 200 nm in diameter (figure 3.2B-E). Furthermore, TEM analysis revealed that the small vesicles displayed a cup-like shape (figure 3.2B).

The smaller vesicles were further subjected to molecular analysis and found to be enriched in exosomal markers, such as ALIX and CD9, relative to cell lysates obtained from the parent cells (figure 3.3A). Additional exosomal markers were also detected by mass spectrometry analyses in the small vesicles, including CD63, CD81, and TSG101, among others (figure 3.3B). Gene ontology enrichment analysis showed that the small EVs were particularly enriched in proteins with catalytic (38.1%) and binding (41.6%) activities. Within the latter category, EV-associated proteins such as cytoskeletal-, enzyme-, signaling receptor-, clathrin-, and SNARE-binding proteins were among the most frequently present proteins within the small vesicles' proteome, suggesting that EVs were successfully isolated (figure 3.3C).

Taking all things together, the results obtained suggest that the EV isolation protocol was successful and that the process yielded two distinct populations of EVs. On one hand, the heterogeneous population of large EVs displayed an average diameter size consistent with the values reported for MVs (100-1,000 nm) (Mathivanan et al., 2021). On the other hand, the second population of vesicles were much smaller in size and presented the typical morphology of exosomes, as well as exosomal markers.

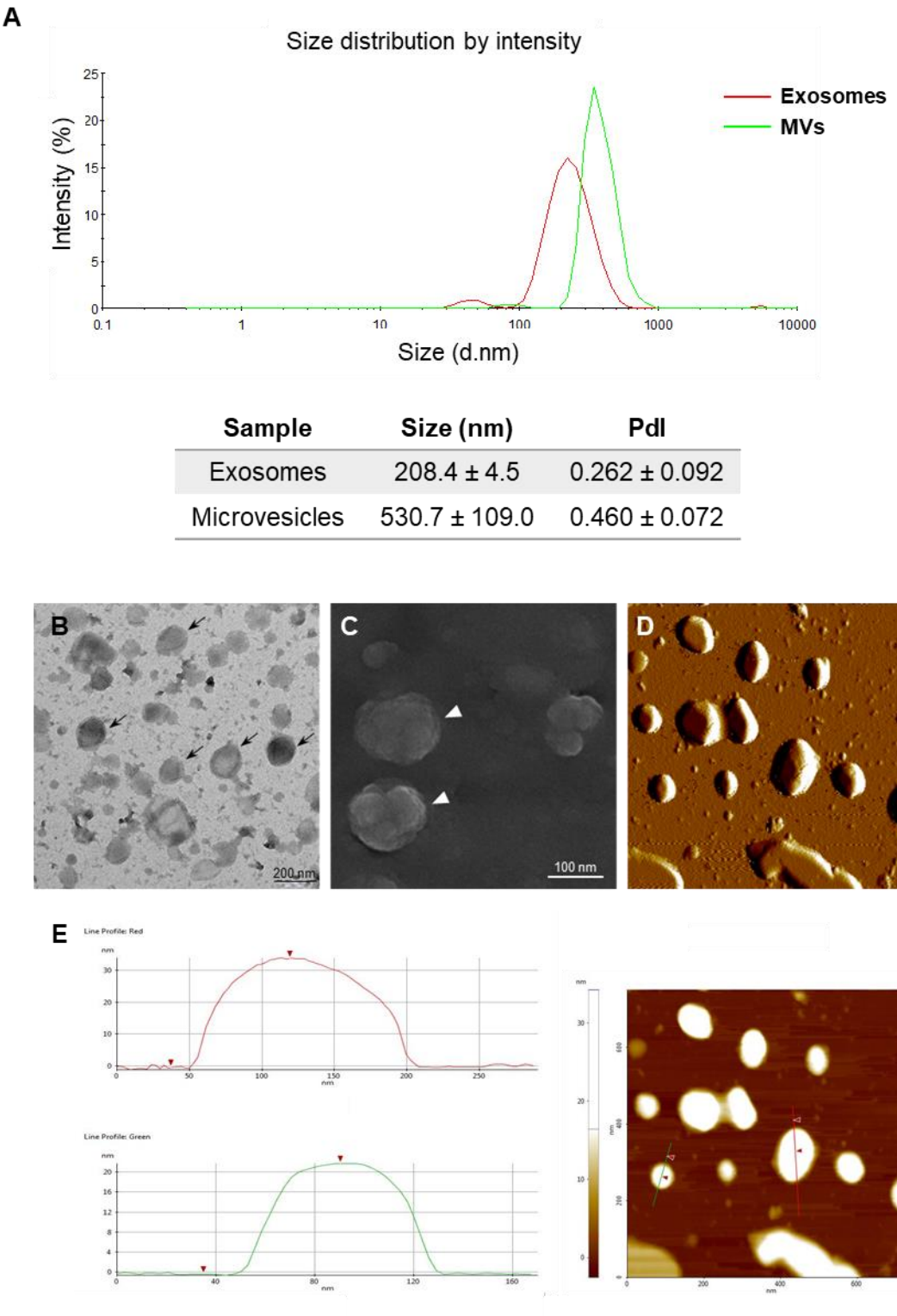

Sample	Size (nm)	PdI
Exosomes	208.4 ± 4.5	0.262 ± 0.092
Microvesicles	530.7 ± 109.0	0.460 ± 0.072

Figure 3.2 – Physical characterization of EVs derived from N2a-atxn2Q58 cells. EVs were isolated from pEGFP-ataxin-2-(Q58)-transfected N2a cells, following a differential centrifugation method, and were physically characterized based on their size and morphology. **(A)** Size distribution by intensity obtained upon DLS analyses on two different samples of EVs. Two different populations of EVs were detected by DLS, with average diameter sizes of 208.4 ± 4.5 and 530.7 ± 109.0 nm. The PdI values indicate that the population of larger EVs (0.460 ± 0.072) is more heterogenous than the population of smaller vesicles (0.262 ± 0.092). Results are representative of two independent experiments. **(B)** TEM micrograph of the population of smaller vesicles indicates that the vesicles, limited by a lipid bilayer, display a cup-like shape and diameter consistent with the reported features of exosomes (black arrows).

Scale bar, 200 nm. **(C)** SEM micrograph of the population of smaller vesicles, displaying their size and topography in a three-dimensional perspective (white arrowheads). **(D** and **E)** AFM analysis of the population of smaller vesicles displaying their topography (D) and individual diameter (E). EVs on a mica surface revealed some degree of heterogeneity in size and shape. Acquisition areas were 750 x 750 nm^2. Results are representative of one isolation experiment.

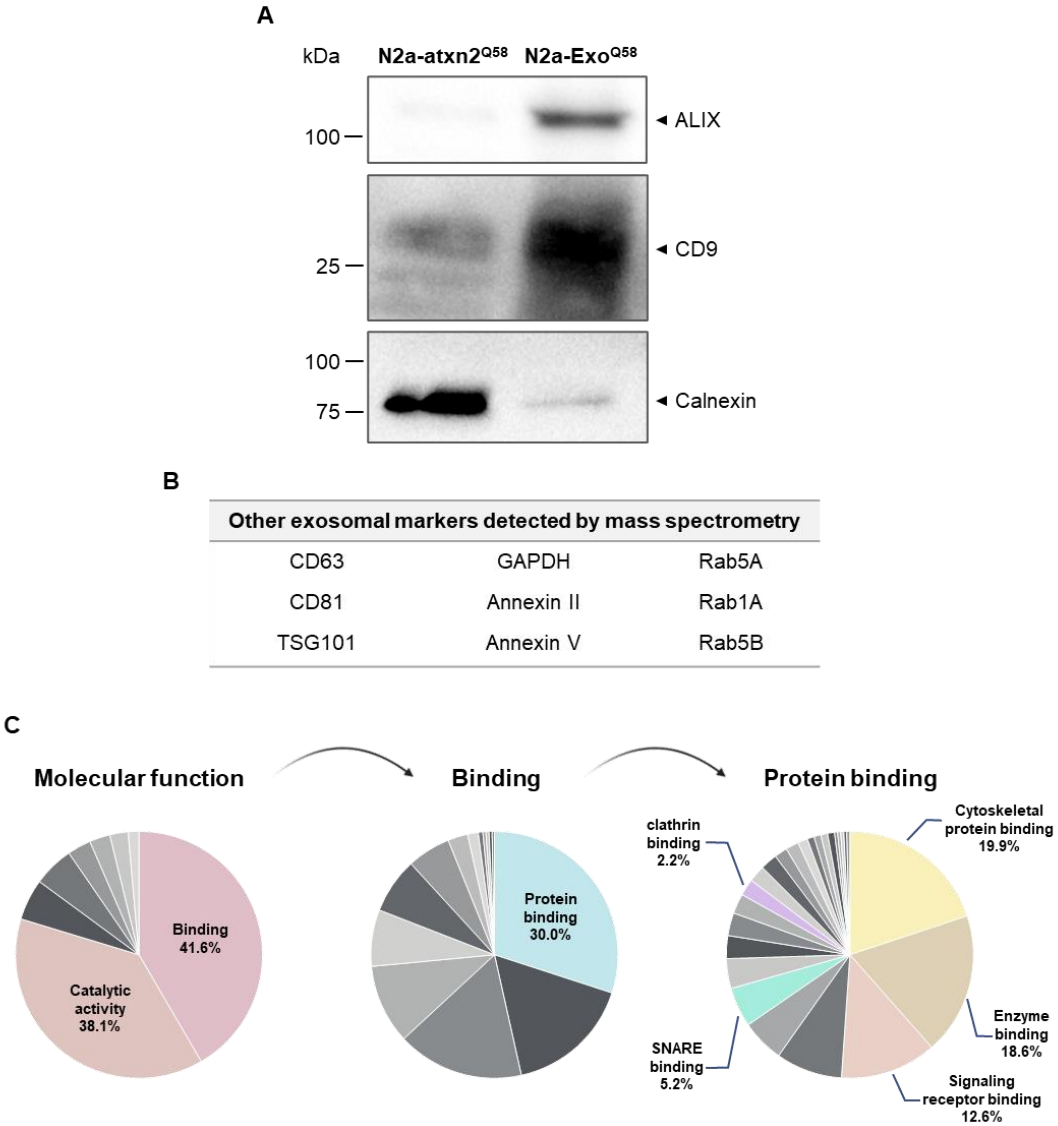

Figure 3.3 – Molecular characterization of EVs derived from N2a-atxn2Q58 cells. The population of small vesicles isolated from pEGFP-ataxin-2-(Q58)-transfected N2a cells was molecularly characterized based on their proteome. **(A)** Western blot analysis showing an enrichment of the exosomal markers ALIX and CD9 in the EV sample (N2a-Exo^{Q58}), in comparison to cell lysates obtained from the parental cells (N2a-$atxn2^{Q58}$). Results are representative of one isolation experiment. **(B** and **C)** Mass spectrometry analysis performed on the population of small vesicles revealing the presence of additional exosomal markers (B) and subsequent gene ontology enrichment analysis showing a variety of functional categories of proteins associated with the EV proteome (C). Results are representative of one isolation experiment.

Ataxin-2 mRNA is present in EVs derived from cells overexpressing human ataxin-2

In the literature, exosomes emerge as recurrent causes of the dissemination of misfolded proteins associated with several neurodegenerative diseases, including the polyQ protein huntingtin. Since we detected human ataxin-2 in non-transfected recipient cells upon culturing them in CM derived from pEGFP-ataxin-2-(Q22)- and pEGFP-ataxin-2-(Q58)-transfected cells (N2a-atxn2^{Q22} and N2a-atxn2^{Q58}, respectively), we next aimed to determine whether mutant ataxin-2 was present in exosome samples obtained from these cells.

In a preliminary approach, N2a cells were co-transfected with the pEGFP-ataxin-2-(Q58) and mCherry-CD81-10 plasmids, the latter encoding the mCherry-fused exosomal marker CD81. Then, these cells were analyzed by confocal microscopy analysis. Our results show that eGFP-atxn2^{Q58} and mCherry-CD81 co-localized in cytoplasmic foci, which resembled vesicular structures (figure 3.4A).

To address the question of whether eGFP-atxn2^{Q58} can, indeed, be found within exosomes, N2a-Exo^{Q58} and cell lysates obtained from their originating cells were submitted to SDS-PAGE and immunoblotted for the detection of ataxin-2. Immunoreactive bands with the approximate molecular weight of ataxin-2 were detected in both the N2a-atxn2^{Q58} cell lysates and N2a-Exo^{Q58}, although with a slightly higher molecular weight in the latter condition (figure 3.4B), suggesting that the presence of eGFP-atxn2^{Q58} in exosomes is inconclusive.

Most of the previous studies mainly addressed the presence of proteins associated with neurodegenerative diseases in exosomes. However, the possibility of their encoding mRNAs also being present within such vesicles should not be ruled out, as it was described that functional RNA species are as well transferred between cells by exosomes (Valadi et al., 2007). Following this rationale, we purified total exosomal RNAs from N2a-Exo^{Q58} and investigated the presence of *ATXN2*^{Q58} transcripts through RT-PCR, using primers specific for the human form of *ATXN2* (*hATXN2*^{Q58}). *hATXN2*^{Q58} mRNA was detected in N2a-Exo^{Q58} in a specific manner, since no amplification was observed in the negative control consisting of non-transfected N2a cells (figure 3.4C). In a similar manner, *hATXN2*^{Q58} mRNA was also detected in MV samples (figure S3.2). The N2a-atxn2^{Q58} condition served as a positive control for the amplification of *hATXN2*^{Q58}, while the β-actin gene (*ACTB*) was used as a control of the PCR reaction, as it is described to be present in both EVs and cell lysates.

Overall, this data suggests that *hATXN2*^{Q58} mRNA transcripts are present in N2a-derived EVs and thus could possibly be transported from one cell to another. However, the

presence of the ataxin-2 protein within exosomes is inconclusive and should be further explored.

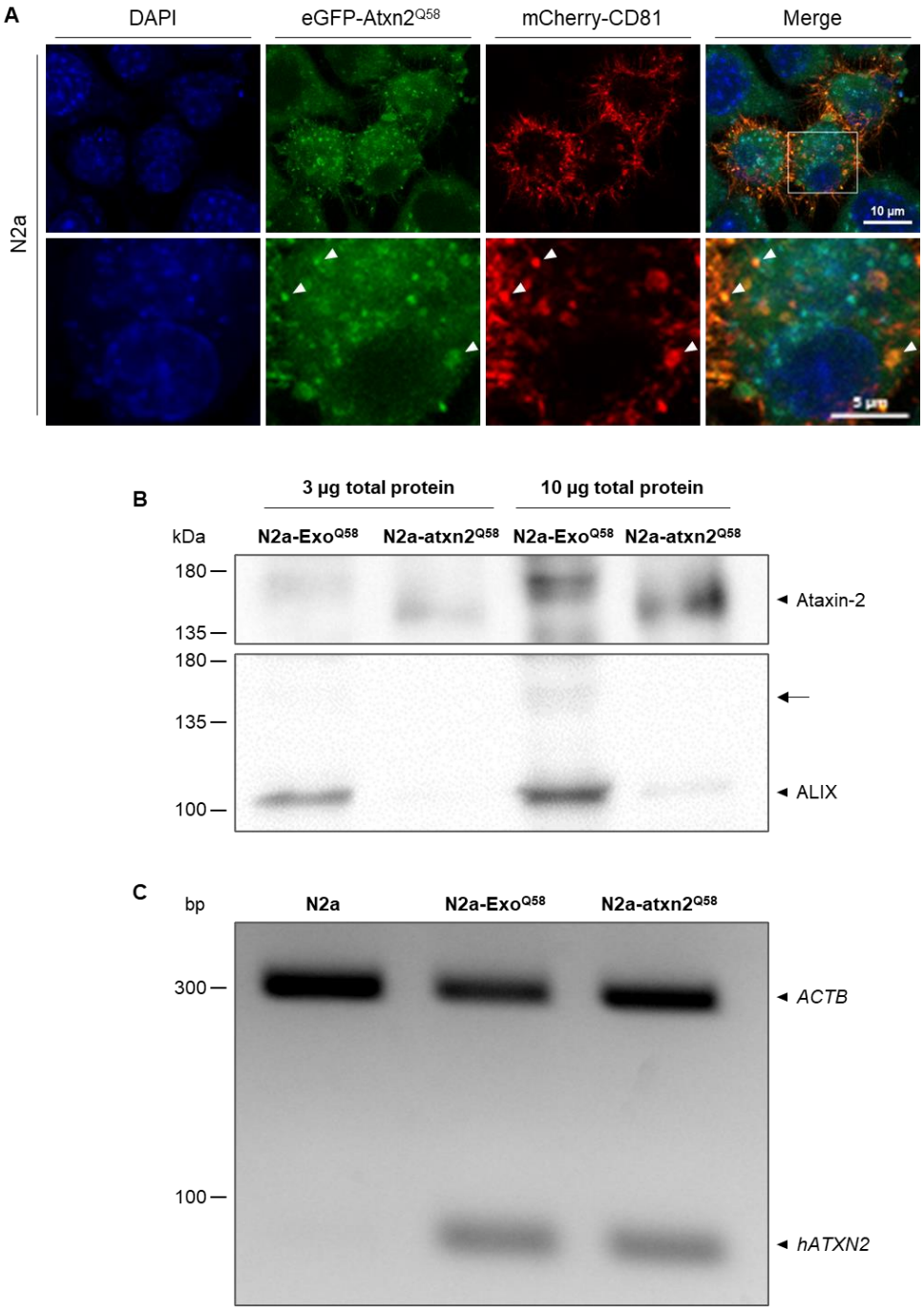

Figure 3.4 – hATXN2Q58 mRNA is present in N2a-atxn2Q58-derived exosomes. The presence or absence of the eGFP-ataxin-2 protein and mRNA within exosomes was assessed by co-localization studies with CD81, Western blot and RT-PCR analyses. **(A)** Representative images obtained by confocal microscopy of N2a cells co-transfected with the pEGFP-ataxin-2-(Q58) and mCherry-CD81-10 plasmids showing that eGFP-atxn2^{Q58} (green) co-localizes with the mCherry-fused exosomal marker CD81 (red), in vesicle-like cytosolic structures (yellow *foci*, white arrowheads). Results are representative of one independent experiment. **(B)** Western blot analysis showing the presence of immunoreactive bands with molecular weights similar to ataxin-2, and the enrichment of ALIX in exosomes. Results are representative of one isolation experiment. **(C)** Agarose gel electrophoresis of

RT-PCR analyses showing the presence of *hATXN2*^{Q58} mRNA in N2a-Exo^{Q58} obtained from N2a-atxn2^{Q58}. N2a and N2a-atxn2^{Q58} were used as negative and positive controls of the amplification of *hATXN2*^{Q58}, respectively. *ACTB* amplification was used as a positive control of the PCR reaction. Results are representative of three independent isolation experiments.

Ataxin-2-loaded EVs are internalized by N2a recipient cells

Upon observing that at least *hATXN2*^{Q58} mRNA transcripts are present in both exosomes and MVs derived from N2a-atxn2^{Q58}, we next aimed to investigate whether *hATXN2*^{Q58}-loaded EVs could be internalized by recipient cells and lead to *hATXN2*^{Q58} translation within cells. Thus, isolated exosomes and MVs from N2a-atxn2^{Q58} CM were added to non-transfected N2a cultures. Recipient cells were collected at three different time points to assess the possible evolution of internalized *hATXN2*^{Q58} expression. Confocal microscopy revealed that the human ataxin-2 protein was present within recipient cells at all time points assayed and appeared to cluster in protein aggregate-like structures, independently of being transferred by exosomes or MVs (figure 3.5A and S3.3). Interestingly, the number of ataxin-2 aggregate-like structures per cell increased with time irrespective of whether recipient cells were subjected to N2a-Exo^{Q58} or N2a-MV^{Q58}, except for the last time point for MVs, at 72 h (figure 3.5B and C). Furthermore, not only recipient cells contained an increasing number of ataxin-2 aggregate-like structures, but also the volume of those foci increased significantly with time, especially when the transfer of ataxin-2 was mediated by MVs (figure 3.5D and E).

The uptake of EVs isolated from N2a-atxn2^{Q58} CM was further confirmed by analyzing the recipient cells by flow cytometry. N2a cells incubated with N2a-Exo^{Q58} were positive for eGFP-atxn2^{Q58} at 12 h post-incubation (0.399%), with an increased uptake percentage at 24 h (0.923%) (figure 3.6A). Similarly, N2a-MV^{Q58} uptake by N2a cells was also detected at 12 h (0.332%) and 24 h post-incubation (0,472%) (figure 3.6B). Non-transfected N2a and N2a-atxn2^{Q58} were used as negative and positive controls for the detection of eGFP-atxn2^{Q58}, respectively.

Altogether, these results suggest that EVs secreted from N2a-atxn2^{Q58} cells could mediate the transfer of ataxin-2 to other cells and promote ataxin-2 aggregation in recipient N2a cells.

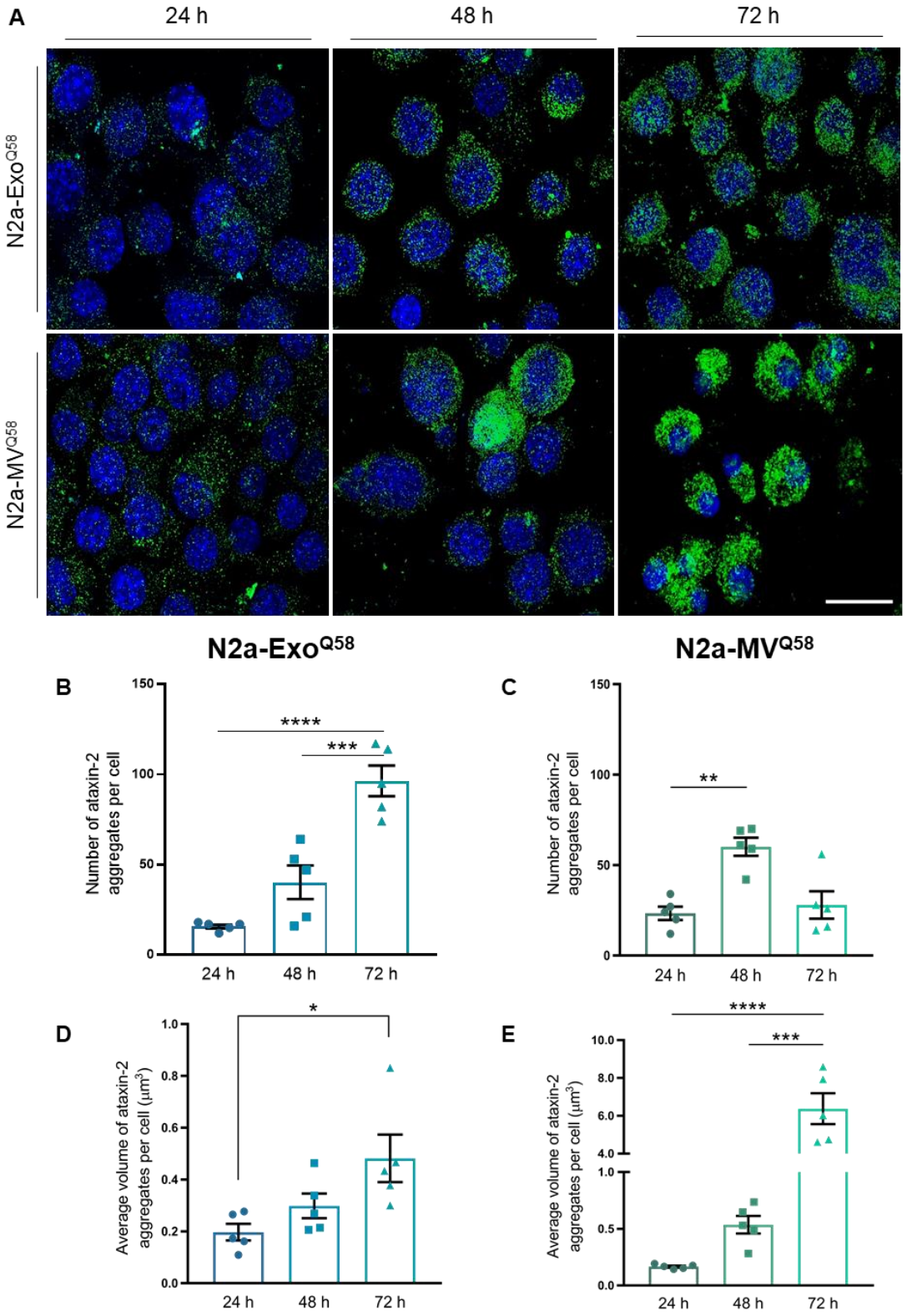

Figure 3.5 – Confocal microscopy analysis of N2a cells incubated with ataxin-2-loaded EVs. Ataxin-2-loaded exosomes and MVs obtained from N2a-atxn2^{Q58} cells (5 µg of total protein for each condition) were diluted in 750 µl of DMEM with 10% EV-depleted FBS and added to non-transfected N2a cells. Cells were harvested at three distinct time points. **(A)** Z-projections of representative images obtained by confocal microscopy showing progressive formation of eGFP-atxn2^{Q58} aggregates at 24 h, 48 h, and 72 h, consistent with the successful uptake of ataxin-2-loaded EVs. Scale bar, 20 µm. **(B** and **C)** 3D quantification of the number of eGFP-atxn2^{Q58} aggregates per cell, upon exposing the recipient cells to N2a-Exo^{Q58} (B) or N2a-MV^{Q58} (C), (n=5 cells per experimental group). **(D** and **E)** 3D quantification

of the average volume of eGFP-atxn2^{Q58} aggregates per cell, upon recipient cells' exposure to N2a-Exo^{Q58} (D) or N2a-MV^{Q58} (E), (n=5 cells per experimental group). Results are represented as the average number or volume of aggregates per cell (n=5 cells per experimental group), and as the mean ± SEM of the average number or volume of aggregates per cell and per time point. These results are representative of one independent experiment. *p<0.05, **p<0.01, ***p<0.001, ****p<0.0001, One-way analysis of variance followed by Tukey's multiple comparisons post hoc test.

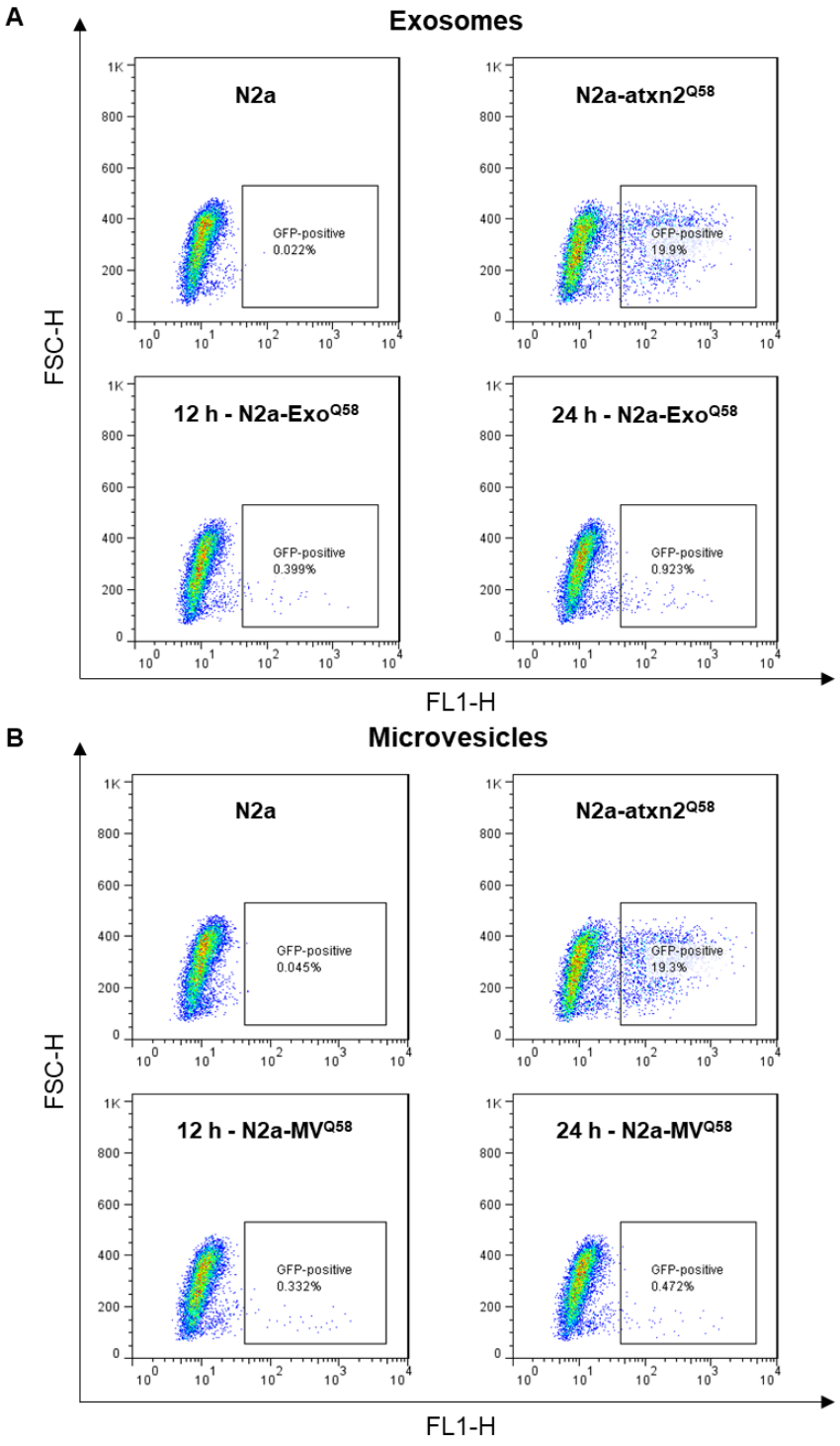

Figure 3.6 – Flow cytometry analysis of N2a cells incubated with ataxin-2-loaded EVs. Ataxin-2-loaded EVs were delivered to recipient cells, which were collected for flow cytometry analysis following 12 h or 24 h. Approximately 10.000 cells were scanned for the detection of eGFP-atxn2^{Q58}. **(A)** Detection of eGFP-positive recipient cells at 12 h (0.399%) and 24 h (0.923%), consistent with uptake of ataxin-2-loaded exosomes. **(B)** Detection of eGFP-positive recipient cells at the same time points (0.399% and

0.923%, respectively), consistent with uptake of ataxin-2-loaded MVs. N2a and N2a-atxn2^{Q58} were used as negative and positive controls for the detection of eGFP-positive cells, respectively. Results are representative of one isolation experiment.

Ataxin-2-loaded EVs spread *in vivo* and promote the formation of protein aggregate-like structures within distinct neuroanatomical regions

After observing that EVs could mediate the transfer of ataxin-2 mRNA between cells in culture and promote the formation of eGFP-atxn2^{Q58} aggregate-like structures, we aimed to investigate if EVs could spread mutant ataxin-2 *in vivo*. To accomplish this, EVs were isolated from the CM of N2a cells co-transfected with the pEGFP-ataxin-2-(Q58) and mCherry-CD81-10 plasmids (N2a-Exo$^{Q58/CD81}$ and N2a-MV$^{Q58/CD81}$), the latter serving as a tool for EV tracking *in vivo*. Subsequently, N2a-Exo$^{Q58/CD81}$ and N2a-MV$^{Q58/CD81}$ were separately injected into the right lateral ventricle of ten-week-old mice, directly into the CSF, which is known to be enriched in EVs at physiological conditions (Chiasserini et al., 2014). Twenty-four hours post-injection, mice were euthanized and their brains collected for immunostaining of eGFP-atxn2^{Q58} and mCherry-CD81 (figure 3.7A). eGFP-atxn2^{Q58}- and mCherry-CD81-positive foci were detected throughout the mice brains when subjected to either N2a-Exo$^{Q58/CD81}$ or N2a-MV$^{Q58/CD81}$ injections (figures 3.7B and 3.8B), although distinct neuroanatomical regions displayed differences in the abundance of double-positive foci (figure 3.7C and 3.8C). For instance, the pons seemed to contain more foci than the caudoputamen, in animals injected with either N2a-Exo$^{Q58/CD81}$ or N2a-MV$^{Q58/CD81}$. Moreover, the molecular and granular layers of the cerebellum were negative for the presence of eGFP-atxn2^{Q58}/mCherry-CD81 foci, whereas the Purkinje cell layer was the structure with the highest abundance of double-positive foci, also applicable for both N2a-Exo$^{Q58/CD81}$ and N2a-MV$^{Q58/CD81}$ injections (figure3.7B-C and 3.8B-C).

Although the intracerebroventricular injections of either N2a-Exo$^{Q58/CD81}$ or N2a-MV$^{Q58/CD81}$ produced similar results in terms of overall abundance of double-positive foci, slight differences were observed in particular anatomical regions, regarding the two subtypes of EVs. For instance, N2a-MV$^{Q58/CD81}$ injections led to a greater abundance of foci in the medulla and globus pallidus, but the abundance of foci in the amygdalar nuclei was slightly reduced in contrast to N2a-Exo$^{Q58/CD81}$-injected mice (figure3.7C and 3.8C). To discard the possibility of cross-reactivity between the two antibodies used for the signal amplification of eGFP-atxn2^{Q58} and mCherry-CD81, we observed several brain sections of N2a-Exo$^{Q58/CD81}$-injected mice without prior immunostaining and confirmed the co-localization of these two proteins by confocal microscopy (figure S3.4).

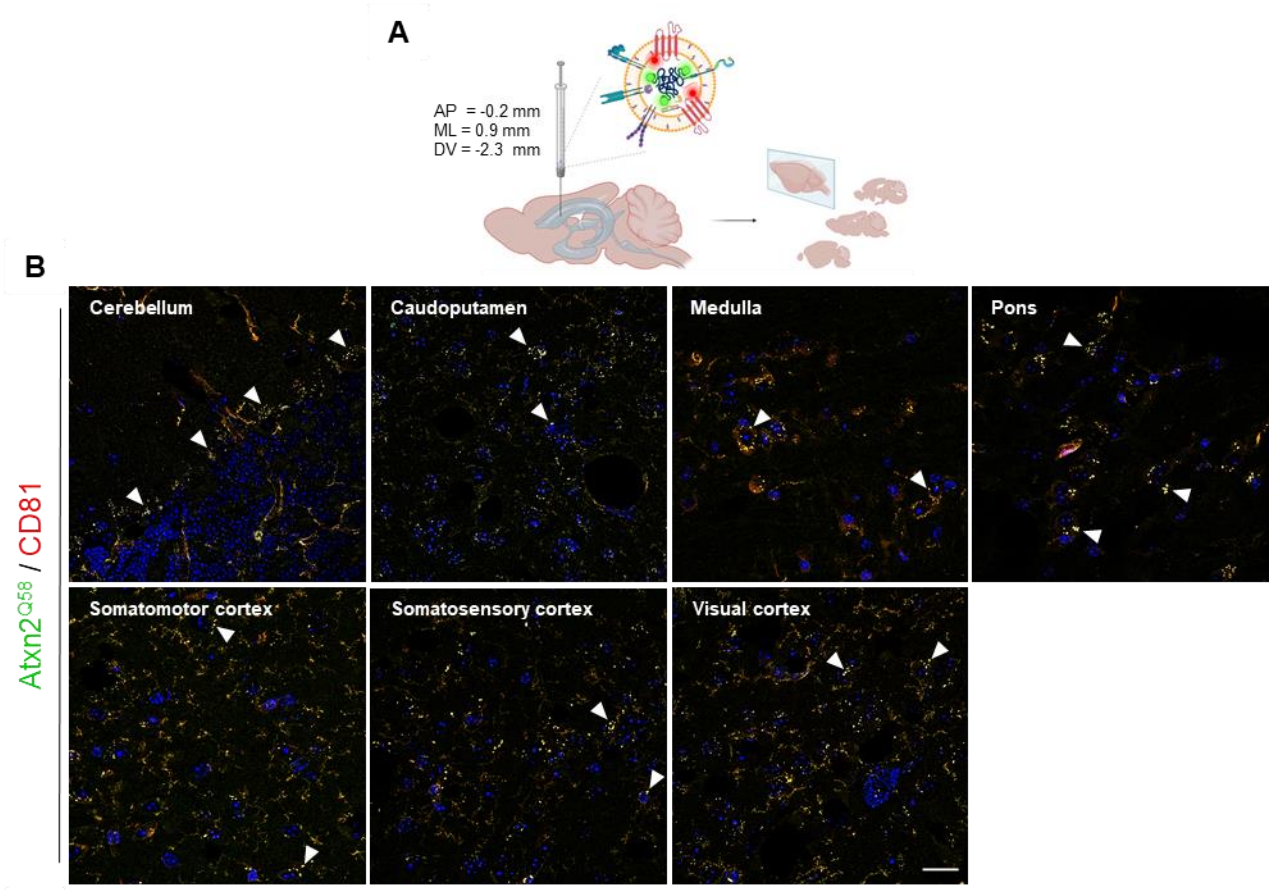

C

Brain region	CD81/Atxn2^{Q58} presence
Cerebellum	
Purkinje cell layer	++++
Molecular layer	-
Granular layer	-
Pons	+++
Medulla	++
Cerebral cortex	
Somatomotor cortex	+++
Somatosensory cortex	++
Visual cortex	+++
Caudoputamen	++
Dentate gyrus	++++
Globus pallidus	++
Thalamus	+++
Hypothalamus	+++
Amygdalar nuclei	+++
Substantia nigra	+++
Midbrain	+++

Figure 3.7 – Ataxin-2-loaded exosomes spread to distinct brain regions and allow the detection of eGFP-atxn2Q58/mCherry-CD81 foci within the neuronal tissue of mice. **(A)** Schematic representation of the intracerebroventricular injections of N2a-Exo$^{Q58/CD81}$ in the right lateral ventricle of mice (n=3). Twenty-four hours post-injection, mice were euthanized and the brains collected for sectioning and labeling with anti-GFP and anti-hCD81, for signal amplification. **(B)** Representative images obtained by confocal microscopy showing the co-localization between eGFP-atxn2^{Q58} and mCherry-CD81(yellow foci, white arrowheads) in distinct regions of the brain, consistent with the

successful uptake of N2a-Exo$^{Q58/CD81}$ in vivo. **(C)** Relative abundance of ataxin-2 aggregate-like structures in different regions of the injected mouse brain. Scale bar, 20 µm.

A

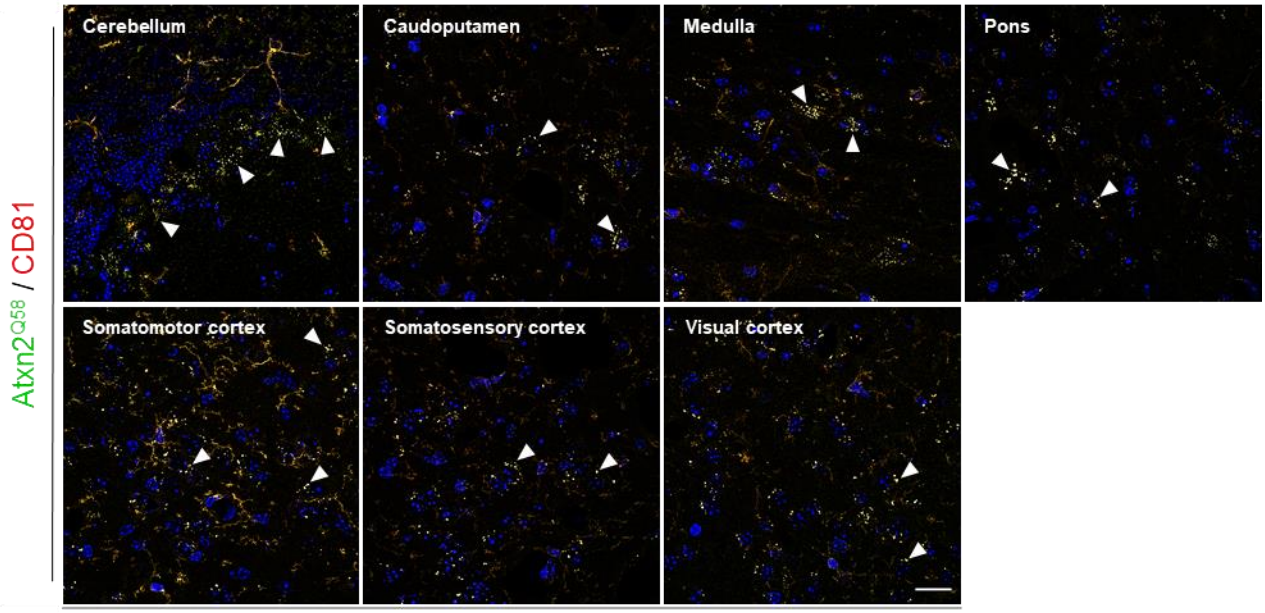

B

Brain region	CD81/Atxn2^{Q58} presence
Cerebellum	
Purkinje cell layer	++++
Molecular layer	-
Granular layer	-
Pons	+++
Medulla	++++
Cerebral cortex	
Somatomotor cortex	+++
Somatosensory cortex	++
Visual cortex	+++
Caudoputamen	++
Dentate gyrus	++++
Globus pallidus	+++
Thalamus	+++
Hypothalamus	+++
Amygdalar nuclei	++
Substantia nigra	+++
Midbrain	+++

Figure 3.8 – Ataxin-2-loaded MVs spread to distinct brain regions and allow the detection of eGFP-atxn2Q58/mCherry-CD81 foci within the neuronal tissue of mice. **(A)** Representative images obtained by confocal microscopy showing the co-localization between eGFP-atxn2^{Q58} and mCherry-CD81(yellow foci, white arrowheads) in distinct regions of the brain, consistent with the successful uptake of N2a-MV$^{Q58/CD81}$ in vivo. **(B)** Relative abundance of ataxin-2 aggregate-like structures in different regions of the injected mouse brain. Scale bar, 20 µm, n=3 animals.

Altogether, these results suggest that ataxin-2-loaded-EVs can spread to different regions of the brain and promote the formation of ataxin-2 aggregate-like structures within the nervous tissue of mice, with some degree of selectivity.

Altogether, these results suggest that ataxin-2-loaded-EVs can spread to different regions of the brain and promote the formation of ataxin-2 aggregate-like structures within the nervous tissue of mice, with some degree of selectivity.

Ataxin-2-loaded EVs can target cerebellar Purkinje cells

Purkinje cells display high expression levels of ataxin-2, which further increase with age (Ostrowski et al., 2017). Moreover, Purkinje neurons are the cells that are most affected in SCA2, being more prone to neuronal loss than cells in other regions of the brain (Estrada et al., 1999). For these reasons, it is believed that the loss of Purkinje neurons could be related to the dysfunction of ataxin-2. The results obtained so far showed that both N2a-Exo$^{Q58/CD81}$ and N2a-MV$^{Q58/CD81}$ were able to induce human ataxin-2 expression in the cerebellum and led to the detection of eGFP-atxn2^{Q58}/mCherry-CD81 foci, within the Purkinje cell layer. In order to confirm that the cerebellar region displaying eGFP-atxn2^{Q58}/mCherry-CD81 foci corresponded in fact to the Purkinje cell layer, we additionally labeled calbindin in cerebellar sections of N2a-Exo$^{Q58/CD81}$- and N2a-MV$^{Q58/CD81}$-injected mice. Calbindin is a calcium-binding protein that is present in several neuronal types throughout the CNS, but, within the cerebellum, its expression is restricted to Purkinje cells, therefore, calbindin is commonly used as a molecular marker of these neurons (Arnold and Heintz, 1997). The double-positive GFP-atxn2^{Q58}/mCherry-CD81 foci were be contained within cells that were positive for calbindin labeling. Since both the granular and molecular layers did not display any type of protein aggregates, these results suggest that ataxin-2-loaded EVs can target the Purkinje neurons in a specific manner within the cerebellum (figure 3.9). We also found that eGFP-atxn2^{Q58} aggregates in the Purkinje cells from N2a-Exo$^{Q58/CD81}$- and N2a-MV$^{Q58/CD81}$-injected mice may also co-localize with the protein degradation markers p62 and ubiquitin (figure S3.5), similar to protein aggregates of other polyQ diseases (Donaldson et al., 2003).

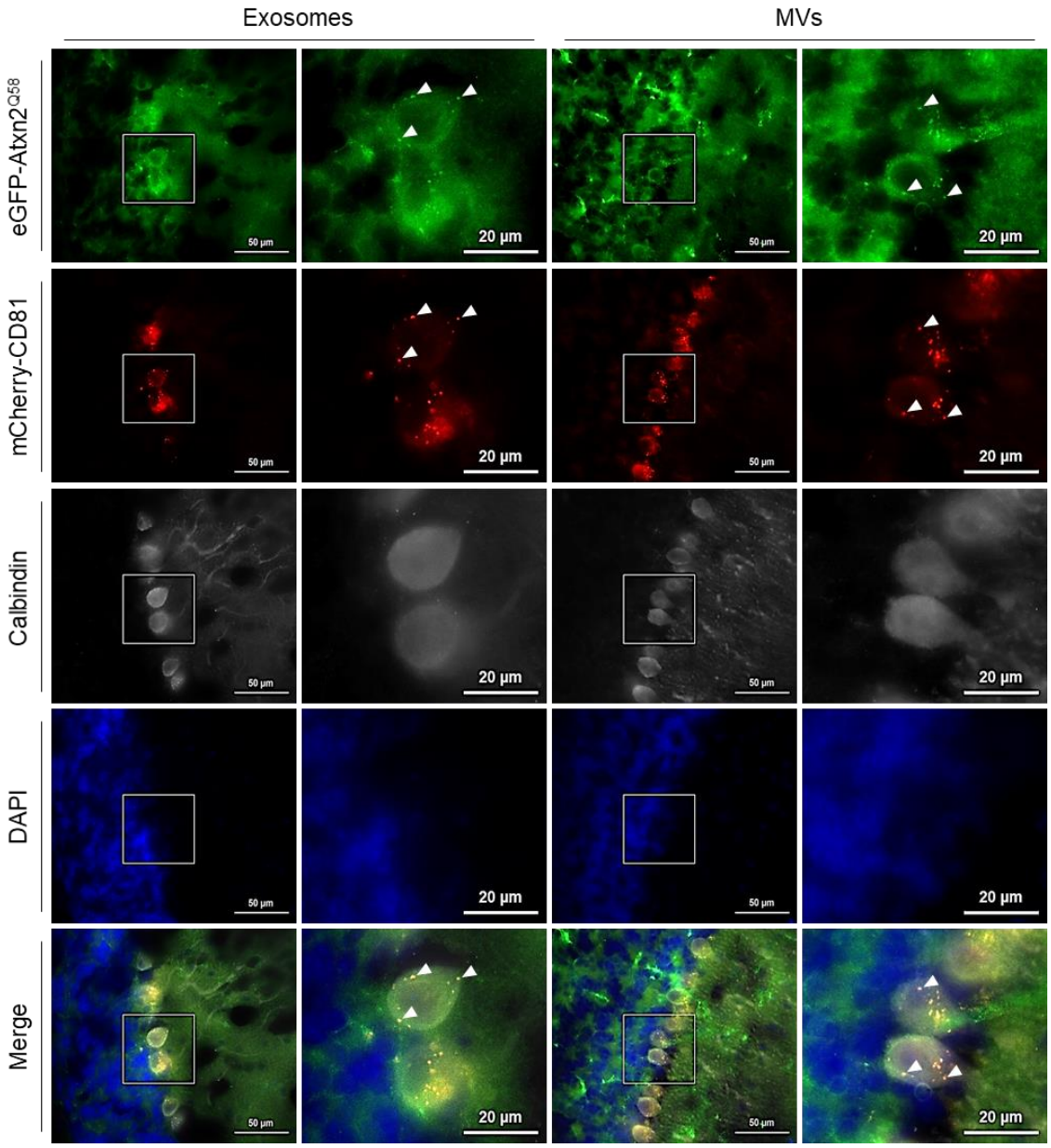

Figure 3.9 – Ataxin-2-loaded EVs may target the Purkinje cell layer. Brain sections of N2a-Exo$^{Q58/CD81}$- and N2a-MV$^{Q58/CD81}$-injected mice were immunohistochemically labelled with anti-GFP and anti-calbindin antibodies. Representative images obtained by widefield fluorescence microscopy suggest that eGFP-atxn2^{Q58}- and mCherry-CD81-positive foci (yellow, white arrowheads) are present within calbindin-positive Purkinje cells.

CHAPTER 4 – DISCUSSION

SCA2 is a hereditary autosomal dominant disease caused by an abnormal expansion of the CAG tract within the *ATXN2* gene, which encodes an expanded form of a polyQ-containing protein called ataxin-2. This expansion alters the intramolecular dynamics of ataxin-2, impairing some of its biological functions and rendering it more prone for aggregation and to establish aberrant interactions with other proteins (Liu et al., 2009). As a consequence of ataxin-2 dysfunction, neuronal death occurs in specific regions of the brain, affecting primarily the cerebellum and its Purkinje neurons, where ataxin-2 is highly expressed (Ostrowski et al., 2017). Nevertheless, as SCA2 progresses, other brain regions become affected as well, and neuronal death within those areas is the ultimate outcome (Mascalchi et al., 2014). However, the reason for this neurodegeneration spreading in SCA2 is not yet well understood.

Recently, misfolded proteins associated with other neurodegenerative diseases have been shown to adopt a prion-like behavior, spreading to other interconnected neuroanatomical regions. The spreading of these misfolded proteins has frequently been associated with EVs, which are membranous structures that can transfer many types of biomolecules between cells, including proteins, functional RNAs, and bioactive lipids. EVs come in different sizes and shapes, and they have been shown to participate both in physiological and pathogenic mechanisms (Grad et al., 2014; Raposo et al., 1996). Furthermore, EVs were shown to act as potential biomarkers of disease and suggested to constitute promising therapeutic drug carriers (Guo et al., 2019; Skog et al., 2008). Nevertheless, studying the role of subtypes of EVs may be challenging, as several of their features can overlap. However, it is of the utmost importance that researchers understand the role of EVs as disease spreading agents, because, by understanding the mechanisms of spreading, innovative treatments may arise.

The idea that dissemination of misfolded proteins in a prion-like manner seems to be common among many neurodegenerative diseases led us to hypothesize that SCA2 neuropathology may spread through a similar mechanism. Therefore, the main goal of this work was to assess whether mutant ataxin-2 can spread from one cell to another, in particular through EVs.

We have shown that CM derived from N2a cells transfected with human ataxin-2 was able to transfer human ataxin-2 into non-transfected cells. A straightforward explanation for this observation could be that ataxin-2 is directly secreted into the extracellular space and readily internalized by recipient cells. However, the existence of a secretion signal peptide within the amino acid sequence of ataxin-2 has never been described. Therefore, we hypothesized that ataxin-2 is secreted into the extracellular milieu by a protein secretion mechanism presumably in association with exosomes and/or MVs, as described for other neurodegenerative diseases (Danzer et al., 2012; Grad et al., 2014; Perez-Gonzalez et al.,

2012; Saman et al., 2012). This idea seems reasonable since ataxin-2 was shown to be part of the endocytic machinery, by interacting with endophilins and their associated partners (Nonis et al., 2008).

The hypothesis that either ataxin-2 mRNA and/or protein can be sorted into EVs is based on different evidence: i) exosomes originate from the endocytic pathway, where ataxin-2 is involved; ii) ataxin-2 is available at the intracellular submembranous region when endocytosis is occurring; and iii) many RNA species are reportedly present within EVs. Following this rationale, we isolated EVs using a differential centrifugation method and characterized them according to their physical and molecular properties. Upon running DLS analyses on EVs isolated at different steps of differential centrifugation, we confirmed the presence of two subpopulations of EVs, of different sizes. The population of larger EVs displayed an average diameter consistent with the size range described for MVs, whereas the population of smaller EVs displayed an average diameter slightly above the reported range of values for exosomes (Mathivanan et al., 2021). However, the analysis of the population of smaller EVs through TEM, SEM, and AFM revealed that these vesicles were indeed much smaller than the average size retrieved by DLS, and, in fact, more appropriately resembled exosomes. The discrepancy in the size measurement of the population of smaller EVs by DLS could be explained by the fact that larger vesicles, even when in low quantity, can strongly influence the obtained EV size profile, since they scatter more light. Consequently, the DLS method can retrieve larger EV sizes if the EV suspension is not strictly homogenous, and hence may not represent their real diameter (Szatanek et al., 2017). Considering this, EV suspensions should be very homogenous in size for an accurate DLS analysis. However, this can be difficult to achieve, and, in fact, even if EVs were all of the same size, aggregated EVs formed as a result of the differential centrifugation isolation method can be detected as single particles in DLS analysis (Linares et al., 2015). Regarding the population of larger vesicles, the average size measured by DLS was within the range to be considered as corresponding to MVs. However, once again, the average size measured by DLS may not correspond to reality, especially in this case where this population displayed a high degree of heterogeneity, something that is nonetheless typical of MVs (Anand et al., 2019).

The population of smaller EVs was further submitted to molecular characterization and displayed an enrichment of the cytosolic protein ALIX and the tetraspanin CD9, relative to their originating cells, thus confirming that these small vesicles were exosomes (Théry et al., 2018). Nevertheless, a small quantity of the negative marker calnexin was observed in N2a-Exo^{Q58} samples, suggesting a possible contamination between lanes when loading the samples into the gel, or a possible contamination with ER components during the EV isolation protocol. Mass spectrometry analysis further reinforced the presence of exosomes in the isolated

samples, by detecting proteins that are commonly associated with the exosomal biogenesis pathway, such as the tetraspanins CD63 and CD81, and the ESCRT-I component TSG101.

All things together, the physical and/or molecular characterization of isolated EVs allowed us to confirm the presence of exosomes and MVs in their respective fractions, although the latter subtype of EVs was only characterized based on size, due to the lack of knowledge on specific MV molecular markers (Anand et al., 2019). For this reason, it is essential that further research is made in order to identify specific molecular markers of MVs.

Upon successfully isolating EVs, we next aimed to assess the presence of the ataxin-2 protein within exosomes, similarly to what was reported in previous studies for other proteins associated with neurodegenerative diseases (Danzer et al., 2012; Saman et al., 2012). Confocal microscopy analysis revealed that eGFP-atxn2^{Q58} co-localized with the mCherry-fused exosomal marker CD81, in cells co-transfected with both encoding plasmids, in cytosolic structures with vesicular semblance, suggesting that ataxin-2 may be present within exosomes. However, The human fusion protein eGFP-atxn2^{Q58}, with a predicted molecular weight of 171 kDa, could not be detected in cell lysates obtained from N2a-atxn2^{Q58}, possibly because the amount of protein loaded was not sufficient for its detection. Instead, an immunoreactive band of approximately 140 kDa was detected, presumably corresponding to the endogenous ataxin-2. Even if the 171 kDa eGFP-atxn2^{Q58} would be potentially enriched in exosomes, this could not be ascertained by the results obtained with the Western blot analysis, because an unspecific band of similar molecular weight was already present due to prior labeling with the anti-ALIX antibody (figure 3.4B, black arrow). Therefore, the presence of the ataxin-2 protein within exosomes is inconclusive and it is important that, in the future, ALIX labeling is performed after ataxin-2 labeling.

An important change in the EV's research field occurred when functional RNA species were found to be transferred between cells in an exosome-mediated manner (Valadi et al., 2007). In this light, not only the transfer of misfolded proteins could contribute to spreading of neurodegenerative diseases, but also mRNAs encoding such proteins might as well be identified as important players. In line with this, we found that *hATXN*^{Q58} transcripts are present in both exosomes and MVs derived from the CM of mutant ataxin-2-transfected cells. Hence, even though there is a possibility for the eGFP-atxn2^{Q58} protein not being enriched within EVs, the fact that its mRNA transcript is present within such structures may sustain the EV-mediated disease spreading hypothesis in SCA2 pathogenesis, despite this putative mechanism differing from the classical prion-like spreading process that is hypothesized (Hafner Bratkovič, 2017).

Taking into consideration the evidence that ataxin-2 mRNA, and possibly even the protein, are present within EVs, we aimed to investigate if N2a-Exo^{Q58} and N2a-MV^{Q58} could induce ataxin-2 expression in recipient cells. We showed that eGFP-atxn2^{Q58} aggregate-like foci can be found within cells that were subjected to ataxin-2-loaded EVs. Generally, the volume of eGFP-atxn2^{Q58} foci and their number per cell increased significantly with incubation time. The number of aggregates per cell in N2a cells exposed to N2a-MV^{Q58} seemed to decrease at 72 h, however, this might be a technical artifact produced by the software used for the 3D quantification of the aggregates. In fact, at 72 h, eGFP-atxn2^{Q58} aggregate-like structures were so large in volume that the software was only able to identify few of these foci per cell, presumably due to the progressive coalescence of smaller aggregates. When comparing to exosomes, MV-mediated transfer of ataxin-2 seems to result in more and larger eGFP-atxn2^{Q58} foci within the recipient cells. This may be explained by the larger dimensions of MVs, suggesting that this subtype of EVs could transport higher amounts of cargo, relative to smaller vesicles such as exosomes. Nevertheless, flow cytometry analysis showed that a smaller percentage of recipient cells were eGFP-positive upon exposure to MVs, whereas incubation with exosomes led to a higher percentage of recipient cells expressing eGFP, at least 24 h following EV exposure. This suggests that there may be a higher percentage of exosomal uptake, possibly resulting from their molecular signature. These small vesicles may be enriched in protein ligands or proteoglycans that render them more prone to be internalized by the recipient cells.. However, it is important to note that discrepancies regarding exosome and MV-induced ataxin-2 expression may also be a result of different EV quantities added to the recipient cells. Although the same total protein amounts of EV samples were added to recipient cells, it does not necessarily mean that the same quantity of exosomes and MVs was delivered. This is because the Bradford quantification of exosomes and MVs can detect the presence of contaminating proteins within the EVs suspensions and, therefore, it can retrieve overestimated total protein amounts of EV samples. To overcome this issue, it is important to determine the actual concentration of EVs in a sample, which is usually performed by NTA. Using this method, it would be possible to use the same quantity of exosomes and MVs for cellular uptake experiments. However, NTA was not available in our laboratory, and therefore we used the Bradford method to grossly estimate the concentration of EVs in each sample.

Although we confirmed that ataxin-2-loaded EVs can lead to the formation of eGFP-atxn2^{Q58} aggregate-like structures in recipient cells, it is still elusive whether these observations are due to the EV-mediated transfer of ataxin-2 mRNA and/or protein. An interesting approach to ascertain if *hATXN2*^{Q58} mRNA is able to induce the formation of eGFP-atxn2^{Q58} aggregates would be to inhibit the translation mechanism in recipient cells prior to ataxin-2-loaded EV's exposure. Following this rationale, a decreased formation of eGFP-atxn2^{Q58} aggregates within

the recipient cells would suggest that *hATXN2*^{Q58} mRNA was responsible for ataxin-2 intercellular spreading and consequent formation of protein aggregates. This approach will be addressed in the near future.

Our *in vitro* results suggested that ataxin-2 could be transferred from one cell to another and, consequently, promote the formation of eGFP-atxn2^{Q58} aggregate-like foci. Thus, we next aimed to investigate whether the same happened *in vivo*. We found that the intracerebroventricular delivery of either ataxin-2-loaded exosomes or MVs led to the detection of eGFP-atxn2^{Q58}/mCherry-CD81 foci in distinct brain regions of injected mice. We found that different neuroanatomical regions displayed different degrees of eGFP-atxn2^{Q58}/mCherry-CD81 foci abundance. For instance, the cerebellum displayed a higher presence of these foci, whereas the caudoputamen was not so enriched. Both subtypes of EVs yielded similar distributions of eGFP-atxn2^{Q58}/mCherry-CD81 foci throughout the brain, with slightly differences in the medulla, globus pallidus, and amygdala. These differences may be a result of a variable ability for EV uptake, depending on the cell type. For example, exosomes may be more easily internalized by the cerebellar Purkinje neurons than by cells from the caudoputamen. Moreover, neurons from the medulla may display higher affinity for MVs rather than exosomes. An important limitation of these experiments is the lack of specific neuronal markers to accurately identify particular regions of the brain. Instead, we mapped the brain sections based on the structural similarities with the mouse brain atlas. Nevertheless, even without the use of neuronal markers, clear differences could be observed regarding the distribution of double-positive foci. Some studies suggest that EVs can be internalized by virtually all types of cells, although several studies have shown that cell type-specific uptake can occur (Atay et al., 2011; Fitzner et al., 2011; Morelli et al., 2004; Zech et al., 2012), sustaining the discrepancies we have observed. Another possible explanation for the differences in the distribution of foci is that EVs could eventually spread equally throughout the brain, but post-transcriptional regulation of the *hATXN2*^{Q58} mRNA inside the recipient cells could differ depending on the recipient cell type. Regarding the matter of cell type-variable ability for EV uptake, it would also be interesting to determine whether microglia cells could display enhanced EV internalization, since these cells possess an intrinsic ability to phagocyte large particles, such as apoptotic bodies, and phagocytosis is one of the routes described for EV uptake.

Our data indicate that eGFP-atxn2^{Q58}/mCherry-CD81 foci are especially enriched within cerebellar Purkinje cells, the cells that are most affected in SCA2. However, although results suggest that the aggregate-like structures are present in calbindin-positive Purkinje neurons, confocal microscopy analysis will be required to confirm colocalization between eGFP-atxn2^{Q58}/mCherry-CD81 foci and calbindin. Unfortunately, the confocal microscope available

is not properly equipped for the detection of four different channels that would be required. Nevertheless, the observation that the most affected cells in SCA2 are also the ones mostly enriched in eGFP-atxn2^{Q58} aggregate-like structures upon EV delivery would constitute an interesting finding. Some questions would, however, remain: do Purkinje cells display more aggregates and die because these are neurotoxic? Do they present more aggregates because they are subjected to higher neurotoxicity and, consequently, more aggregates are formed to protect the cells from dying? This is an unresolved question for SCA2, with parallels in many other neurodegenerative diseases (Todd and Lim, 2013).

Generally, polyQ aggregates are too large to be degraded by the UPS, therefore they tend to be cleared by autophagy (Park et al., 2013; Ravikumar et al., 2002). Briefly, in this pathway, p62/SQSTM1 recognizes ubiquitinated cargo and recruits it to the autophagosome for degradation. For this reason, polyQ aggregates, particularly in SCA3, tend to accumulate ubiquitin and p62/SQSTM1 (Yang et al., 2014). In contrast to what was reported in previous studies (Koyano et al., 1999), we found that eGFP-atxn2^{Q58} aggregates seemed to be positive for ubiquitin, in the cerebellum. It was shown that parkin was able to ubiquitinate and induce the degradation of ataxin-2, with particular relevance regarding its mutant form (Huynh et al., 2007). Moreover, eGFP-atxn2^{Q58} aggregates seemed also to be positive for p62/SQSTM1. The putative presence of ubiquitin and p62/SQSTM1 within eGFP-atxn2^{Q58} aggregates could suggest that these are being signaled for autophagy mediate-degradation, resembling what typically happens with polyQ aggregates (Jimenez-Sanchez et al., 2012). It is important to note that, once again, confocal microscopy analysis will be necessary to properly confirm the co-localization between eGFP-atxn2^{Q58}, ubiquitin, and p62/SQSTM1.

In conclusion, in this study we found that cells expressing mutant ataxin-2 secrete EVs containing ataxin-2 mRNA, and possibly also the protein. Ataxin-2 can be transferred to neighboring cells in association with EVs, and subsequently induce the formation of ataxin-2 aggregates within the recipient cells. Due to the fact that these observations were also replicated in *in vivo* experiments, we suggest that, similarly to other neurodegenerative diseases, the EV-mediated transfer of ataxin-2 may constitute an important, and previously unknown, step of SCA2 pathogenesis. Further *in vitro* and *in vivo* studies will help establish whether this EV-mediated transfer can contribute to neuronal death in the context of SCA2. One of the most puzzling aspects of polyQ diseases pathophysiology is the fact that neuronal demise is region-specific even when caused by ubiquitous proteins such as ataxin-2. A better understanding of the putative spreading mechanism hinted by the current work may constitute a basis for deciphering that puzzle, and thus contribute to the development of strategies to treat SCA2.

CHAPTER 5 – CONCLUSION AND FUTURE PERSPECTIVES

Misfolded proteins associated with several neurodegenerative diseases have been shown to spread to interconnected neuroanatomical regions of the brain in an EV-mediated fashion. This mechanism of protein spreading is thought to underly the progression of neurodegenerative diseases by resembling a prion-like propagation, where EVs act as “Trojan horses” of neurodegeneration. Similarly, SCA2 patients show region-selective neuronal death which propagates and expands to other brain regions. However, a spreading mechanism has never been reported for ataxin-2. Therefore, this work had the objective of investigating whether ataxin-2 could be transferred among neighboring cells and induce pathology.

First, we aimed to study whether ataxin-2 could be transferred between cells *in vitro*. We have shown that “naïve” cells expressed the humanized form of ataxin-2 upon contacting with the CM derived from human ataxin-2-expressing cells. Subsequently, we found that ataxin-2 mRNA was present within exosomes and MVs derived from the CM. Moreover, the ataxin-2 protein co-localized with the exosomal marker CD81 in N2a cells transfected with both plasmids, suggesting that ataxin-2 may be present within exosomes. Nevertheless, it is important that we readdress this matter. Moreover, it is important that we also address the possibility of the ataxin-2 protein being present within MVs. Despite the uncertainty of whether the ataxin-2 protein is present within EVs, we showed that cells receiving ataxin-2-loaded EVs expressed the mutant protein and that this led to progressive aggregation of ataxin-2, displayed by an increase in the number of aggregate-like structure per cell, as well as an increase in the volume of those foci. To determine whether these observations were due to the translation of the EV-carried ataxin-2 mRNA within the recipient cells, it will be important that we perform a similar experiment with the addition of mRNA translation inhibitors prior to ataxin-2-loaded EV exposure. Moreover, we did not address whether the EV-mediated transfer of ataxin-2 could induce toxicity in N2a cell cultures. Therefore, this matter should be investigated in the future to verify if the spreading of ataxin-2 could underly the molecular pathogenesis of SCA2, by promoting neuronal death. Additionally, it would also be interesting to investigate the mechanism through which ataxin-2-loaded EVs are internalized by N2a cells. Subsequently, it would be important to test whether genetic or pharmacological inhibition of such pathway would produce a beneficial outcome regarding the cellular viability in case the spreading of ataxin-2 is proven to be neurotoxic.

The second task of this work aimed to assess whether ataxin-2-loaded EVs could spread and induce mutant ataxin-2 expression *in vivo*. We have shown that the intracerebroventricular delivery of both exosomes and MVs led to the detection of ataxin-2 aggregate-like structure in distinct brain structures, with different degrees of aggregate abundance. This suggests that EVs may act as ataxin-2 carriers and spread it throughout the brain. The differences in the abundance of ataxin-2 aggregates in distinct brain regions may

be due to variable affinities between EVs and particular cell types. In this light, it would be of interest to identify which cell types are more prone to internalize EVs and what may be the molecular cause of such susceptibility, by inhibiting different EV or cell surface markers. Importantly, results suggest that greater abundance of ataxin-2 aggregate-like structures were found within Purkinje neurons, where they possibly co-localized with the autophagy marker p62/SQSTM1 and ubiquitin. However, these results need to be confirmed by confocal microscopy. It is striking that Purkinje cells are the most affected cells in SCA2, and our results suggest that they are also the ones with the highest abundance of ataxin-2 aggregate-like foci. In order to more closely assess whether EV-mediated spreading of ataxin-2 can contribute to neurodegeneration, a long-period in vivo study that evaluated the potential development of motor difficulties and neuropathological features, such as the presence of neuroinflammation and neuronal loss, should be performed.

In conclusion, we have shown that the ataxin-2 mRNA transcript is present within exosomes and MVs obtained from ataxin-2-expressing cells in vitro, and that these EVs can act as carriers for ataxin-2 spreading between cells. We further demonstrated that ataxin-2-loaded EVs promote progressive aggregation of ataxin-2 in “naïve” recipient cells. Furthermore, we show that both exosomes and MVs can disseminate ataxin-2 throughout the brains of mice, leading to the detection of ataxin-2 aggregates in distinct neuroanatomical regions, with variable degrees of abundance. Finally, results indicate that Purkinje neurons are the cells with the greatest abundance of ataxin-2 aggregate-like structure. Altogether, our results suggest that EVs may contribute to the pathogenesis of SCA2 by promoting the propagation of mutant ataxin-2 throughout the CNS. Nevertheless, it is important that further research is conducted to unravel the mechanisms of EV-mediated transfer of ataxin-2 and their potential implication in contributing to neuronal death. A better understanding of these mechanisms may contribute to the discovery of efficient and innovative therapies that may halt SCA2 progression.

REFERENCES

Abraham, K.J., Chan, J.N., Salvi, J.S., Ho, B., Hall, A., Vidya, E., Guo, R., Killackey, S.A., Liu, N., Lee, J.E.*, et al.* (2016). Intersection of calorie restriction and magnesium in the suppression of genome-destabilizing RNA-DNA hybrids. Nucleic acids research *44*, 8870-8884.

Admyre, C., Johansson, S.M., Qazi, K.R., Filén, J.J., Lahesmaa, R., Norman, M., Neve, E.P., Scheynius, A., and Gabrielsson, S. (2007). Exosomes with immune modulatory features are present in human breast milk. Journal of immunology (Baltimore, Md : 1950) *179*, 1969-1978.

Affaitati, A., de Cristofaro, T., Feliciello, A., and Varrone, S. (2001). Identification of alternative splicing of spinocerebellar ataxia type 2 gene. Gene *267*, 89-93.

Agromayor, M., Soler, N., Caballe, A., Kueck, T., Freund, S.M., Allen, M.D., Bycroft, M., Perisic, O., Ye, Y., McDonald, B.*, et al.* (2012). The UBAP1 subunit of ESCRT-I interacts with ubiquitin via a SOUBA domain. Structure *20*, 414-428.

Al-Nedawi, K., Meehan, B., Kerbel, R.S., Allison, A.C., and Rak, J. (2009). Endothelial expression of autocrine VEGF upon the uptake of tumor-derived microvesicles containing oncogenic EGFR. Proceedings of the National Academy of Sciences of the United States of America *106*, 3794-3799.

Albert, V., and Hall, M.N. (2015). mTOR signaling in cellular and organismal energetics. Current opinion in cell biology *33*, 55-66.

Alberts, B. (2015). Molecular biology of the cell, 6th edn (New York, NY: Garland Science).

Albrecht, C., McVey, J.H., Elliott, J.I., Sardini, A., Kasza, I., Mumford, A.D., Naoumova, R.P., Tuddenham, E.G., Szabo, K., and Higgins, C.F. (2005). A novel missense mutation in ABCA1 results in altered protein trafficking and reduced phosphatidylserine translocation in a patient with Scott syndrome. Blood *106*, 542-549.

Albrecht, M., Golatta, M., Wullner, U., and Lengauer, T. (2004). Structural and functional analysis of ataxin-2 and ataxin-3. European journal of biochemistry *271*, 3155-3170.

Alibhai, J., Blanco, R.A., Barria, M.A., Piccardo, P., Caughey, B., Perry, V.H., Freeman, T.C., and Manson, J.C. (2016). Distribution of Misfolded Prion Protein Seeding Activity Alone Does Not Predict Regions of Neurodegeneration. PLoS Biol *14*, e1002579-e1002579.

Almaguer-Mederos, L.E., Almaguer-Gotay, D., Aguilera-Rodriguez, R., Gonzalez-Zaldivar, Y., Cuello-Almarales, D., Laffita-Mesa, J., Vazquez-Mojena, Y., Zayas-Feria, P., Rodriguez-Labrada, R., Velazquez-Perez, L.*, et al.* (2017). Association of glutathione S-transferase omega polymorphism and spinocerebellar ataxia type 2. Journal of the neurological sciences *372*, 324-328.

Alonso, E., Martinez-Ruano, L., De Biase, I., Mader, C., Ochoa, A., Yescas, P., Gutierrez, R., White, M., Ruano, L., Fragoso-Benitez, M.*, et al.* (2007). Distinct distribution of autosomal dominant spinocerebellar ataxia in the Mexican population. Movement disorders : official journal of the Movement Disorder Society *22*, 1050-1053.

Alvarez-Erviti, L., Seow, Y., Yin, H., Betts, C., Lakhal, S., and Wood, M.J. (2011). Delivery of siRNA to the mouse brain by systemic injection of targeted exosomes. Nature biotechnology *29*, 341-345.

Anand, S., Foot, N., Ang, C.S., Gembus, K.M., Keerthikumar, S., Adda, C.G., Mathivanan, S., and Kumar, S. (2018). Arrestin-Domain Containing Protein 1 (Arrdc1) Regulates the Protein Cargo and Release of Extracellular Vesicles. Proteomics *18*, e1800266.

Anand, S., Samuel, M., Kumar, S., and Mathivanan, S. (2019). Ticket to a bubble ride: Cargo sorting into exosomes and extracellular vesicles. Biochimica et biophysica acta Proteins and proteomics *1867*, 140203.

Anderson, P., and Kedersha, N. (2006). RNA granules. The Journal of cell biology *172*, 803-808.

Anderson, R.G. (1998). The caveolae membrane system. Annu Rev Biochem *67*, 199-225.

Ando, J., Kinoshita, M., Cui, J., Yamakoshi, H., Dodo, K., Fujita, K., Murata, M., and Sodeoka, M. (2015). Sphingomyelin distribution in lipid rafts of artificial monolayer membranes visualized by Raman microscopy. Proceedings of the National Academy of Sciences of the United States of America *112*, 4558-4563.

Andres, A.M., Lao, O., Soldevila, M., Calafell, F., and Bertranpetit, J. (2003). Dynamics of CAG repeat loci revealed by the analysis of their variability. Human mutation *21*, 61-70.

Andreu, Z., and Yáñez-Mó, M. (2014). Tetraspanins in extracellular vesicle formation and function. Frontiers in immunology *5*, 442.

Antenora, A., Rinaldi, C., Roca, A., Pane, C., Lieto, M., Sacca, F., Peluso, S., De Michele, G., and Filla, A. (2017). The Multiple Faces of Spinocerebellar Ataxia type 2. Ann Clin Transl Neurol *4*, 687-695.

Arnold, D.B., and Heintz, N. (1997). A calcium responsive element that regulates expression of two calcium binding proteins in Purkinje cells. *94*, 8842-8847.

Arrasate, M., Mitra, S., Schweitzer, E.S., Segal, M.R., and Finkbeiner, S. (2004). Inclusion body formation reduces levels of mutant huntingtin and the risk of neuronal death. Nature *431*, 805-810.

Asada, A., Yamazaki, R., Kino, Y., Saito, T., Kimura, T., Miyake, M., Hasegawa, M., Nukina, N., and Hisanaga, S. (2014). Cyclin-dependent kinase 5 phosphorylates and induces the degradation of ataxin-2. Neurosci Lett *563*, 112-117.

Asai, H., Ikezu, S., Tsunoda, S., Medalla, M., Luebke, J., Haydar, T., Wolozin, B., Butovsky, O., Kügler, S., and Ikezu, T. (2015). Depletion of microglia and inhibition of exosome synthesis halt tau propagation. Nature Neuroscience *18*, 1584-1593.

Asea, A., Jean-Pierre, C., Kaur, P., Rao, P., Linhares, I.M., Skupski, D., and Witkin, S.S. (2008). Heat shock protein-containing exosomes in mid-trimester amniotic fluids. Journal of reproductive immunology *79*, 12-17.

Atay, S., Gercel-Taylor, C., and Taylor, D.D. (2011). Human trophoblast-derived exosomal fibronectin induces pro-inflammatory IL-1β production by macrophages. American journal of reproductive immunology (New York, NY : 1989) *66*, 259-269.

Avraham, E., Rott, R., Liani, E., Szargel, R., and Engelender, S. (2007). Phosphorylation of Parkin by the cyclin-dependent kinase 5 at the linker region modulates its ubiquitin-ligase activity and aggregation. The Journal of biological chemistry *282*, 12842-12850.

Babovic-Vuksanovic, D., Snow, K., Patterson, M.C., and Michels, V.V. (1998). Spinocerebellar ataxia type 2 (SCA 2) in an infant with extreme CAG repeat expansion. American journal of medical genetics *79*, 383-387.

Babst, M., Katzmann, D.J., Estepa-Sabal, E.J., Meerloo, T., and Emr, S.D. (2002a). Escrt-III: an endosome-associated heterooligomeric protein complex required for mvb sorting. Developmental cell *3*, 271-282.

Babst, M., Katzmann, D.J., Snyder, W.B., Wendland, B., and Emr, S.D. (2002b). Endosome-associated complex, ESCRT-II, recruits transport machinery for protein sorting at the multivesicular body. Developmental cell *3*, 283-289.

Bache, K.G., Brech, A., Mehlum, A., and Stenmark, H. (2003a). Hrs regulates multivesicular body formation via ESCRT recruitment to endosomes. The Journal of cell biology *162*, 435-442.

Bache, K.G., Raiborg, C., Mehlum, A., and Stenmark, H. (2003b). STAM and Hrs are subunits of a multivalent ubiquitin-binding complex on early endosomes. The Journal of biological chemistry *278*, 12513-12521.

Baietti, M.F., Zhang, Z., Mortier, E., Melchior, A., Degeest, G., Geeraerts, A., Ivarsson, Y., Depoortere, F., Coomans, C., Vermeiren, E.*, et al.* (2012). Syndecan–syntenin–ALIX regulates the biogenesis of exosomes. Nature Cell Biology *14*, 677-685.

Bakhti, M., Winter, C., and Simons, M. (2011). Inhibition of myelin membrane sheath formation by oligodendrocyte-derived exosome-like vesicles. The Journal of biological chemistry *286*, 787-796.

Baldarcara, L., Currie, S., Hadjivassiliou, M., Hoggard, N., Jack, A., Jackowski, A.P., Mascalchi, M., Parazzini, C., Reetz, K., Righini, A.*, et al.* (2015). Consensus paper: radiological biomarkers of cerebellar diseases. Cerebellum (London, England) *14*, 175-196.

Bari, R., Guo, Q., Xia, B., Zhang, Y.H., Giesert, E.E., Levy, S., Zheng, J.J., and Zhang, X.A. (2011). Tetraspanins regulate the protrusive activities of cell membrane. Biochemical and biophysical research communications *415*, 619-626.

Baron, V., and Van Obberghen, E. (1995). [Mechanism of insulin action]. Comptes rendus des seances de la Societe de biologie et de ses filiales *189*, 25-41.

Barreiro, O., Yáñez-Mó, M., Sala-Valdés, M., Gutiérrez-López, M.D., Ovalle, S., Higginbottom, A., Monk, P.N., Cabañas, C., and Sánchez-Madrid, F. (2005). Endothelial tetraspanin microdomains regulate leukocyte firm adhesion during extravasation. Blood *105*, 2852-2861.

Barrès, C., Blanc, L., Bette-Bobillo, P., André, S., Mamoun, R., Gabius, H.J., and Vidal, M. (2010). Galectin-5 is bound onto the surface of rat reticulocyte exosomes and modulates vesicle uptake by macrophages. Blood *115*, 696-705.

Barresi, M.J.F., and Gilbert, S.F. (2020). Developmental biology, 11th edn.

Basso, M., Pozzi, S., Tortarolo, M., Fiordaliso, F., Bisighini, C., Pasetto, L., Spaltro, G., Lidonnici, D., Gensano, F., Battaglia, E.*, et al.* (2013). Mutant copper-zinc superoxide dismutase (SOD1) induces protein secretion pathway alterations and exosome release in astrocytes: implications for disease spreading and motor neuron pathology in amyotrophic lateral sclerosis. The Journal of biological chemistry *288*, 15699-15711.

Bellingham, S.A., Guo, B.B., Coleman, B.M., and Hill, A.F. (2012). Exosomes: vehicles for the transfer of toxic proteins associated with neurodegenerative diseases? Frontiers in physiology *3*, 124.

Bendor, J.T., Logan, T.P., and Edwards, R.H. (2013). The function of α-synuclein. Neuron *79*, 1044-1066.

Berditchevski, F. (2001). Complexes of tetraspanins with integrins: more than meets the eye. Journal of cell science *114*, 4143-4151.

Bettencourt, C., Hensman-Moss, D., Flower, M., Wiethoff, S., Brice, A., Goizet, C., Stevanin, G., Koutsis, G., Karadima, G., Panas, M.*, et al.* (2016). DNA repair pathways underlie a common genetic mechanism modulating onset in polyglutamine diseases. Annals of neurology *79*, 983-990.

Bevers, E.M., and Williamson, P.L. (2016). Getting to the Outer Leaflet: Physiology of Phosphatidylserine Exposure at the Plasma Membrane. Physiological reviews *96*, 605-645.

Bishop, J.R., Schuksz, M., and Esko, J.D. (2007). Heparan sulphate proteoglycans fine-tune mammalian physiology. Nature *446*, 1030-1037.

Bosco, D.A., Morfini, G., Karabacak, N.M., Song, Y., Gros-Louis, F., Pasinelli, P., Goolsby, H., Fontaine, B.A., Lemay, N., McKenna-Yasek, D.*, et al.* (2010). Wild-type and mutant SOD1 share an aberrant conformation and a common pathogenic pathway in ALS. Nature neuroscience *13*, 1396-1403.

Boukouris, S., and Mathivanan, S. (2015). Exosomes in bodily fluids are a highly stable resource of disease biomarkers. Proteomics Clinical applications *9*, 358-367.

Braak, H., and Del Tredici, K. (2011). Alzheimer's pathogenesis: is there neuron-to-neuron propagation? Acta neuropathologica *121*, 589-595.

Braak, H., Del Tredici, K., Rüb, U., de Vos, R.A., Jansen Steur, E.N., and Braak, E. (2003). Staging of brain pathology related to sporadic Parkinson's disease. Neurobiology of aging *24*, 197-211.

Bravo, J., Aguilar-Henonin, L., Olmedo, G., and Guzman, P. (2005). Four distinct classes of proteins as interaction partners of the PABC domain of Arabidopsis thaliana Poly(A)-binding proteins. Molecular genetics and genomics : MGG *272*, 651-665.

Brengues, M., Teixeira, D., and Parker, R. (2005). Movement of eukaryotic mRNAs between polysomes and cytoplasmic processing bodies. Science (New York, NY) *310*, 486-489.

Brennan, K., Martin, K., FitzGerald, S.P., O'Sullivan, J., Wu, Y., Blanco, A., Richardson, C., and Mc Gee, M.M. (2020). A comparison of methods for the isolation and separation of extracellular vesicles from protein and lipid particles in human serum. Scientific Reports *10*, 1039.

Brisson, C., Azorsa, D.O., Jennings, L.K., Moog, S., Cazenave, J.P., and Lanza, F. (1997). Co-localization of CD9 and GPIIb-IIIa (alpha IIb beta 3 integrin) on activated platelet pseudopods and alpha-granule membranes. The Histochemical journal *29*, 153-165.

Brown, A.S., Meera, P., Altindag, B., Chopra, R., Perkins, E.M., Paul, S., Scoles, D.R., Tarapore, E., Magri, J., Huang, H.*, et al.* (2018). MTSS1/Src family kinase dysregulation underlies multiple inherited ataxias. Proc Natl Acad Sci U S A *115*, E12407-E12416.

Brzozowski, J.S., Bond, D.R., Jankowski, H., Goldie, B.J., Burchell, R., Naudin, C., Smith, N.D., Scarlett, C.J., Larsen, M.R., Dun, M.D.*, et al.* (2018). Extracellular vesicles with altered tetraspanin CD9 and CD151 levels confer increased prostate cell motility and invasion. Scientific Reports *8*, 8822.

Buijsen, R.A.M., Toonen, L.J.A., Gardiner, S.L., and van Roon-Mom, W.M.C. (2019). Genetics, Mechanisms, and Therapeutic Progress in Polyglutamine Spinocerebellar Ataxias. Neurotherapeutics *16*, 263-286.

Burke, M.C., Oei, M.S., Edwards, N.J., Ostrand-Rosenberg, S., and Fenselau, C. (2014). Ubiquitinated proteins in exosomes secreted by myeloid-derived suppressor cells. J Proteome Res *13*, 5965-5972.

Caby, M.P., Lankar, D., Vincendeau-Scherrer, C., Raposo, G., and Bonnerot, C. (2005). Exosomal-like vesicles are present in human blood plasma. International immunology *17*, 879-887.

Cao, M., Milosevic, I., Giovedi, S., and De Camilli, P. (2014). Upregulation of Parkin in endophilin mutant mice. The Journal of neuroscience : the official journal of the Society for Neuroscience *34*, 16544-16549.

Carmo-Silva, S., Nobrega, C., Pereira de Almeida, L., and Cavadas, C. (2017). Unraveling the Role of Ataxin-2 in Metabolism. Trends in endocrinology and metabolism: TEM *28*, 309-318.

Carnino, J.M., Ni, K., and Jin, Y. (2020). Post-translational Modification Regulates Formation and Cargo-Loading of Extracellular Vesicles. Frontiers in immunology *11*, 948-948.

Castro, B.M., Prieto, M., and Silva, L.C. (2014). Ceramide: a simple sphingolipid with unique biophysical properties. Progress in lipid research *54*, 53-67.

Chai, X., Dage, J.L., and Citron, M. (2012). Constitutive secretion of tau protein by an unconventional mechanism. Neurobiology of disease *48*, 356-366.

Chai, Y., Shao, J., Miller, V.M., Williams, A., and Paulson, H.L. (2002). Live-cell imaging reveals divergent intracellular dynamics of polyglutamine disease proteins and supports a sequestration model of pathogenesis. Proc Natl Acad Sci U S A *99*, 9310-9315.

Chairoungdua, A., Smith, D.L., Pochard, P., Hull, M., and Caplan, M.J. (2010). Exosome release of β-catenin: a novel mechanism that antagonizes Wnt signaling. The Journal of cell biology *190*, 1079-1091.

Chappie, J.S., Acharya, S., Leonard, M., Schmid, S.L., and Dyda, F. (2010). G domain dimerization controls dynamin's assembly-stimulated GTPase activity. Nature *465*, 435-440.

Charles, P., Camuzat, A., Benammar, N., Sellal, F., Destee, A., Bonnet, A.M., Lesage, S., Le Ber, I., Stevanin, G., Durr, A.*, et al.* (2007). Are interrupted SCA2 CAG repeat expansions responsible for parkinsonism? Neurology *69*, 1970-1975.

Charrin, S., Le Naour, F., Labas, V., Billard, M., Le Caer, J.-P., Emile, J.-F., Petit, M.-A., Boucheix, C., and Rubinstein, E. (2003). EWI-2 is a new component of the tetraspanin web in hepatocytes and lymphoid cells. The Biochemical journal *373*, 409-421.

Cheng, L., Sun, X., Scicluna, B.J., Coleman, B.M., and Hill, A.F. (2014). Characterization and deep sequencing analysis of exosomal and non-exosomal miRNA in human urine. Kidney international *86*, 433-444.

Chernomordik, L.V., and Kozlov, M.M. (2008). Mechanics of membrane fusion. Nature Structural & Molecular Biology *15*, 675-683.

Chernomordik, L.V., Melikyan, G.B., and Chizmadzhev, Y.A. (1987). Biomembrane fusion: a new concept derived from model studies using two interacting planar lipid bilayers. Biochimica et biophysica acta *906*, 309-352.

Chiasserini, D., van Weering, J.R., Piersma, S.R., Pham, T.V., Malekzadeh, A., Teunissen, C.E., de Wit, H., and Jiménez, C.R. (2014). Proteomic analysis of cerebrospinal fluid extracellular vesicles: a comprehensive dataset. Journal of proteomics *106*, 191-204.

Chiriacò, M.S., Bianco, M., Nigro, A., Primiceri, E., Ferrara, F., Romano, A., Quattrini, A., Furlan, R., Arima, V., and Maruccio, G. (2018). Lab-on-Chip for Exosomes and Microvesicles Detection and Characterization. *18*, 3175.

Chitnis, A.B. (1995). The role of Notch in lateral inhibition and cell fate specification. Molecular and cellular neurosciences *6*, 311-321.

Choi, D.S., Kim, D.K., Kim, Y.K., and Gho, Y.S. (2015). Proteomics of extracellular vesicles: Exosomes and ectosomes. Mass spectrometry reviews *34*, 474-490.

Chuo, S.T.-Y., Chien, J.C.-Y., and Lai, C.P.-K. (2018). Imaging extracellular vesicles: current and emerging methods. Journal of Biomedical Science *25*, 91.

Clayton, A., Turkes, A., Dewitt, S., Steadman, R., Mason, M.D., and Hallett, M.B. (2004). Adhesion and signaling by B cell-derived exosomes: the role of integrins. FASEB journal : official publication of the Federation of American Societies for Experimental Biology *18*, 977-979.

Coleman, B.M., Hanssen, E., Lawson, V.A., and Hill, A.F. (2012). Prion-infected cells regulate the release of exosomes with distinct ultrastructural features. FASEB journal : official publication of the Federation of American Societies for Experimental Biology *26*, 4160-4173.

Collinge, J. (2001). Prion diseases of humans and animals: their causes and molecular basis. Annual review of neuroscience *24*, 519-550.

Collino, F., Pomatto, M., Bruno, S., Lindoso, R.S., Tapparo, M., Sicheng, W., Quesenberry, P., and Camussi, G. (2017). Exosome and Microvesicle-Enriched Fractions Isolated from Mesenchymal Stem Cells by Gradient Separation Showed Different Molecular Signatures and Functions on Renal Tubular Epithelial Cells. Stem Cell Rev Rep *13*, 226-243.

Colombo, M., Moita, C., van Niel, G., Kowal, J., Vigneron, J., Benaroch, P., Manel, N., Moita, L.F., Théry, C., and Raposo, G. (2013). Analysis of ESCRT functions in exosome biogenesis, composition and secretion highlights the heterogeneity of extracellular vesicles. Journal of cell science *126*, 5553-5565.

Cooper, J.K., Schilling, G., Peters, M.F., Herring, W.J., Sharp, A.H., Kaminsky, Z., Masone, J., Khan, F.A., Delanoy, M., Borchelt, D.R.*, et al.* (1998). Truncated N-terminal fragments of huntingtin with expanded glutamine repeats form nuclear and cytoplasmic aggregates in cell culture. Human molecular genetics *7*, 783-790.

Cornelius, N., Wardman, J.H., Hargreaves, I.P., Neergheen, V., Bie, A.S., Tumer, Z., Nielsen, J.E., and Nielsen, T.T. (2017). Evidence of oxidative stress and mitochondrial dysfunction in spinocerebellar ataxia type 2 (SCA2) patient fibroblasts: Effect of coenzyme Q10 supplementation on these parameters. Mitochondrion *34*, 103-114.

Cortes, C.J., and La Spada, A.R. (2015). Autophagy in polyglutamine disease: Imposing order on disorder or contributing to the chaos? Mol Cell Neurosci *66*, 53-61.

Cougot, N., Babajko, S., and Seraphin, B. (2004). Cytoplasmic foci are sites of mRNA decay in human cells. The Journal of cell biology *165*, 31-40.

Cvjetkovic, A., Lötvall, J., and Lässer, C. (2014). The influence of rotor type and centrifugation time on the yield and purity of extracellular vesicles. J Extracell Vesicles *3*.

Dansithong, W., Paul, S., Figueroa, K.P., Rinehart, M.D., Wiest, S., Pflieger, L.T., Scoles, D.R., and Pulst, S.M. (2015). Ataxin-2 regulates RGS8 translation in a new BAC-SCA2 transgenic mouse model. PLoS genetics *11*, e1005182.

Danzer, K.M., Kranich, L.R., Ruf, W.P., Cagsal-Getkin, O., Winslow, A.R., Zhu, L., Vanderburg, C.R., and McLean, P.J. (2012). Exosomal cell-to-cell transmission of alpha synuclein oligomers. Molecular neurodegeneration *7*, 42.

Deas, E., Plun-Favreau, H., and Wood, N.W. (2009). PINK1 function in health and disease. EMBO Mol Med *1*, 152-165.

Dehay, B., Bourdenx, M., Gorry, P., Przedborski, S., Vila, M., Hunot, S., Singleton, A., Olanow, C.W., Merchant, K.M., Bezard, E.*, et al.* (2015). Targeting α-synuclein for treatment of Parkinson's disease: mechanistic and therapeutic considerations. The Lancet Neurology *14*, 855-866.

Denzer, K., van Eijk, M., Kleijmeer, M.J., Jakobson, E., de Groot, C., and Geuze, H.J. (2000). Follicular dendritic cells carry MHC class II-expressing microvesicles at their surface. Journal of immunology (Baltimore, Md : 1950) *165*, 1259-1265.

Deville, S., Berckmans, P., Van Hoof, R., Lambrichts, I., Salvati, A., and Nelissen, I. (2021). Comparison of extracellular vesicle isolation and storage methods using high-sensitivity flow cytometry. PloS one *16*, e0245835.

Dewey, C.M., Cenik, B., Sephton, C.F., Johnson, B.A., Herz, J., and Yu, G. (2012). TDP-43 aggregation in neurodegeneration: are stress granules the key? Brain Res *1462*, 16-25.

Di Fabio, R., Santorelli, F., Bertini, E., Balestri, M., Cursi, L., Tessa, A., Pierelli, F., and Casali, C. (2012). Infantile childhood onset of spinocerebellar ataxia type 2. Cerebellum (London, England) *11*, 526-530.

Dinkins, M.B., Dasgupta, S., Wang, G., Zhu, G., and Bieberich, E. (2014). Exosome reduction in vivo is associated with lower amyloid plaque load in the 5XFAD mouse model of Alzheimer's disease. Neurobiology of aging *35*, 1792-1800.

Doherty, G.J., and McMahon, H.T. (2009). Mechanisms of endocytosis. Annu Rev Biochem *78*, 857-902.

Dohlinger, S., Hauser, T.K., Borkert, J., Luft, A.R., and Schulz, J.B. (2008). Magnetic resonance imaging in spinocerebellar ataxias. Cerebellum (London, England) *7*, 204-214.

Donaldson, K.M., Li, W., Ching, K.A., Batalov, S., Tsai, C.-C., and Joazeiro, C.A.P. (2003). Ubiquitin-mediated sequestration of normal cellular proteins into polyglutamine aggregates. *100*, 8892-8897.

Dragovic, R.A., Gardiner, C., Brooks, A.S., Tannetta, D.S., Ferguson, D.J.P., Hole, P., Carr, B., Redman, C.W.G., Harris, A.L., Dobson, P.J.*, et al.* (2011). Sizing and phenotyping of cellular vesicles using Nanoparticle Tracking Analysis. Nanomedicine: Nanotechnology, Biology and Medicine *7*, 780-788.

Dunning, C.J., Reyes, J.F., Steiner, J.A., and Brundin, P. (2012). Can Parkinson's disease pathology be propagated from one neuron to another? Prog Neurobiol *97*, 205-219.

Dustin, M.L., and Choudhuri, K. (2016). Signaling and Polarized Communication Across the T Cell Immunological Synapse. Annual review of cell and developmental biology *32*, 303-325.

Egorova, P.A., and Bezprozvanny, I.B. (2019). Molecular Mechanisms and Therapeutics for Spinocerebellar Ataxia Type 2. Neurotherapeutics *16*, 1050-1073.

Elden, A.C., Kim, H.J., Hart, M.P., Chen-Plotkin, A.S., Johnson, B.S., Fang, X., Armakola, M., Geser, F., Greene, R., Lu, M.M.*, et al.* (2010). Ataxin-2 intermediate-length polyglutamine expansions are associated with increased risk for ALS. Nature *466*, 1069-1075.

Ellerby, L.M. (2019). Repeat Expansion Disorders: Mechanisms and Therapeutics. Neurotherapeutics *16*, 924-927.

Emmanouilidou, E., Melachroinou, K., Roumeliotis, T., Garbis, S.D., Ntzouni, M., Margaritis, L.H., Stefanis, L., and Vekrellis, K. (2010). Cell-produced alpha-synuclein is secreted in a calcium-dependent manner by exosomes and impacts neuronal survival. J Neurosci *30*, 6838-6851.

Escrevente, C., Keller, S., Altevogt, P., and Costa, J. (2011). Interaction and uptake of exosomes by ovarian cancer cells. BMC Cancer *11*, 108.

Escudier, B., Dorval, T., Chaput, N., André, F., Caby, M.P., Novault, S., Flament, C., Leboulaire, C., Borg, C., Amigorena, S.*, et al.* (2005). Vaccination of metastatic melanoma patients with autologous dendritic cell (DC) derived-exosomes: results of thefirst phase I clinical trial. Journal of translational medicine *3*, 10.

Estrada, R., Galarraga, J., Orozco, G., Nodarse, A., and Auburger, G. (1999). Spinocerebellar ataxia 2 (SCA2): morphometric analyses in 11 autopsies. Acta neuropathologica *97*, 306-310.

Fabbri, M., Paone, A., Calore, F., Galli, R., Gaudio, E., Santhanam, R., Lovat, F., Fadda, P., Mao, C., Nuovo, G.J.*, et al.* (2012). MicroRNAs bind to Toll-like receptors to induce prometastatic inflammatory response. Proceedings of the National Academy of Sciences of the United States of America *109*, E2110-2116.

Falker, C., Hartmann, A., Guett, I., Dohler, F., Altmeppen, H., Betzel, C., Schubert, R., Thurm, D., Wegwitz, F., Joshi, P.*, et al.* (2016). Exosomal cellular prion protein drives fibrillization of amyloid beta and counteracts amyloid beta-mediated neurotoxicity. Journal of neurochemistry *137*, 88-100.

Fallon, L., Belanger, C.M., Corera, A.T., Kontogiannea, M., Regan-Klapisz, E., Moreau, F., Voortman, J., Haber, M., Rouleau, G., Thorarinsdottir, T.*, et al.* (2006). A regulated

interaction with the UIM protein Eps15 implicates parkin in EGF receptor trafficking and PI(3)K-Akt signalling. Nat Cell Biol *8*, 834-842.

Farg, M.A., Soo, K.Y., Warraich, S.T., Sundaramoorthy, V., Blair, I.P., and Atkin, J.D. (2013). Ataxin-2 interacts with FUS and intermediate-length polyglutamine expansions enhance FUS-related pathology in amyotrophic lateral sclerosis. Human molecular genetics *22*, 717-728.

Feng, D., Zhao, W.L., Ye, Y.Y., Bai, X.C., Liu, R.Q., Chang, L.F., Zhou, Q., and Sui, S.F. (2010). Cellular internalization of exosomes occurs through phagocytosis. Traffic (Copenhagen, Denmark) *11*, 675-687.

Fernagut, P.O., and Tison, F. (2012). Animal models of multiple system atrophy. Neuroscience *211*, 77-82.

Fevrier, B., Vilette, D., Archer, F., Loew, D., Faigle, W., Vidal, M., Laude, H., and Raposo, G. (2004). Cells release prions in association with exosomes. Proceedings of the National Academy of Sciences of the United States of America *101*, 9683-9688.

Fitzner, D., Schnaars, M., van Rossum, D., Krishnamoorthy, G., Dibaj, P., Bakhti, M., Regen, T., Hanisch, U.K., and Simons, M. (2011). Selective transfer of exosomes from oligodendrocytes to microglia by macropinocytosis. Journal of cell science *124*, 447-458.

Flanagan, M.D., and Lin, S. (1980). Cytochalasins block actin filament elongation by binding to high affinity sites associated with F-actin. The Journal of biological chemistry *255*, 835-838.

François-Martin, C., and Pincet, F. (2017). Actual fusion efficiency in the lipid mixing assay - Comparison between nanodiscs and liposomes. Scientific Reports *7*, 43860.

Frühbeis, C., Fröhlich, D., Kuo, W.P., Amphornrat, J., Thilemann, S., Saab, A.S., Kirchhoff, F., Möbius, W., Goebbels, S., Nave, K.-A.*, et al.* (2013). Neurotransmitter-Triggered Transfer of Exosomes Mediates Oligodendrocyte–Neuron Communication. PLoS Biol *11*, e1001604.

Furtado, S., Farrer, M., Tsuboi, Y., Klimek, M.L., de la Fuente-Fernandez, R., Hussey, J., Lockhart, P., Calne, D.B., Suchowersky, O., Stoessl, A.J.*, et al.* (2002). SCA-2 presenting as parkinsonism in an Alberta family: clinical, genetic, and PET findings. Neurology *59*, 1625-1627.

Gandelman, M., Dansithong, W., Figueroa, K.P., Paul, S., Scoles, D.R., and Pulst, S.M. (2020). Staufen 1 amplifies proapoptotic activation of the unfolded protein response. Cell Death Differ *27*, 2942-2951.

Gardiner, C., Di Vizio, D., Sahoo, S., Théry, C., Witwer, K.W., Wauben, M., and Hill, A.F. (2016). Techniques used for the isolation and characterization of extracellular vesicles: results of a worldwide survey. J Extracell Vesicles *5*, 32945.

Gardiner, C., Ferreira, Y.J., Dragovic, R.A., Redman, C.W., and Sargent, I.L. (2013). Extracellular vesicle sizing and enumeration by nanoparticle tracking analysis. J Extracell Vesicles *2*.

Gatchel, J.R., and Zoghbi, H.Y. (2005). Diseases of unstable repeat expansion: mechanisms and common principles. Nat Rev Genet *6*, 743-755.

Geschwind, D.H., Perlman, S., Figueroa, C.P., Treiman, L.J., and Pulst, S.M. (1997). The prevalence and wide clinical spectrum of the spinocerebellar ataxia type 2 trinucleotide repeat in patients with autosomal dominant cerebellar ataxia. American journal of human genetics *60*, 842-850.

Gierga, K., Burk, K., Bauer, M., Orozco Diaz, G., Auburger, G., Schultz, C., Vuksic, M., Schols, L., de Vos, R.A., Braak, H.*, et al.* (2005). Involvement of the cranial nerves and their nuclei in spinocerebellar ataxia type 2 (SCA2). Acta neuropathologica *109*, 617-631.

Gispert, S., Twells, R., Orozco, G., Brice, A., Weber, J., Heredero, L., Scheufler, K., Riley, B., Allotey, R., Nothers, C.*, et al.* (1993). Chromosomal assignment of the second locus for autosomal dominant cerebellar ataxia (SCA2) to chromosome 12q23-24.1. Nature genetics *4*, 295-299.

Goedert, M., Clavaguera, F., and Tolnay, M. (2010). The propagation of prion-like protein inclusions in neurodegenerative diseases. Trends in neurosciences *33*, 317-325.

Goustin, A.S., Betsholtz, C., Pfeifer-Ohlsson, S., Persson, H., Rydnert, J., Bywater, M., Holmgren, G., Heldin, C.H., Westermark, B., and Ohlsson, R. (1985). Coexpression of the sis and myc proto-oncogenes in developing human placenta suggests autocrine control of trophoblast growth. Cell *41*, 301-312.

Grad, L.I., Yerbury, J.J., Turner, B.J., Guest, W.C., Pokrishevsky, E., O'Neill, M.A., Yanai, A., Silverman, J.M., Zeineddine, R., Corcoran, L.*, et al.* (2014). Intercellular propagated misfolding of wild-type Cu/Zn superoxide dismutase occurs via exosome-dependent and -independent mechanisms. Proceedings of the National Academy of Sciences of the United States of America *111*, 3620-3625.

Graner, M.W., Alzate, O., Dechkovskaia, A.M., Keene, J.D., Sampson, J.H., Mitchell, D.A., and Bigner, D.D. (2009). Proteomic and immunologic analyses of brain tumor exosomes. FASEB journal : official publication of the Federation of American Societies for Experimental Biology *23*, 1541-1557.

Grey, M., Dunning, C.J., Gaspar, R., Grey, C., Brundin, P., Sparr, E., and Linse, S. (2015). Acceleration of α-synuclein aggregation by exosomes. The Journal of biological chemistry *290*, 2969-2982.

Grimmer, S., van Deurs, B., and Sandvig, K. (2002). Membrane ruffling and macropinocytosis in A431 cells require cholesterol. Journal of cell science *115*, 2953-2962.

Grootjans, J.J., Zimmermann, P., Reekmans, G., Smets, A., Degeest, G., Dürr, J., and David, G. (1997). Syntenin, a PDZ protein that binds syndecan cytoplasmic domains. *94*, 13683-13688.

Gruenberg, J. (2001). The endocytic pathway: a mosaic of domains. Nature Reviews Molecular Cell Biology *2*, 721-730.

Guix, F.X., Sannerud, R., Berditchevski, F., Arranz, A.M., Horré, K., Snellinx, A., Thathiah, A., Saido, T., Saito, T., Rajesh, S.*, et al.* (2017). Tetraspanin 6: a pivotal protein of the multiple vesicular body determining exosome release and lysosomal degradation of amyloid precursor protein fragments. Molecular neurodegeneration *12*, 25.

Guo, B.B., Bellingham, S.A., and Hill, A.F. (2016). Stimulating the Release of Exosomes Increases the Intercellular Transfer of Prions. The Journal of biological chemistry *291*, 5128-5137.

Guo, M., Wu, F., Hu, G., Chen, L., Xu, J., Xu, P., Wang, X., Li, Y., Liu, S., Zhang, S.*, et al.* (2019). Autologous tumor cell-derived microparticle-based targeted chemotherapy in lung cancer patients with malignant pleural effusion. Science translational medicine *11*.

Gutekunst, C.A., Li, S.H., Yi, H., Mulroy, J.S., Kuemmerle, S., Jones, R., Rye, D., Ferrante, R.J., Hersch, S.M., and Li, X.J. (1999). Nuclear and neuropil aggregates in Huntington's disease: relationship to neuropathology. The Journal of neuroscience : the official journal of the Society for Neuroscience *19*, 2522-2534.

Gwinn-Hardy, K., Chen, J.Y., Liu, H.C., Liu, T.Y., Boss, M., Seltzer, W., Adam, A., Singleton, A., Koroshetz, W., Waters, C.*, et al.* (2000). Spinocerebellar ataxia type 2 with parkinsonism in ethnic Chinese. Neurology *55*, 800-805.

Hafner Bratkovič, I. (2017). Prions, prionoid complexes and amyloids: the bad, the good and something in between. Swiss medical weekly *147*, w14424.

Hankins, H.M., Baldridge, R.D., Xu, P., and Graham, T.R. (2015). Role of flippases, scramblases and transfer proteins in phosphatidylserine subcellular distribution. Traffic (Copenhagen, Denmark) *16*, 35-47.

Hannafon, B.N., and Ding, W.Q. (2013). Intercellular communication by exosome-derived microRNAs in cancer. Int J Mol Sci *14*, 14240-14269.

Hannun, Y.A., and Obeid, L.M. (2008). Principles of bioactive lipid signalling: lessons from sphingolipids. Nature reviews Molecular cell biology *9*, 139-150.

Haraszti, R.A., Didiot, M.C., Sapp, E., Leszyk, J., Shaffer, S.A., Rockwell, H.E., Gao, F., Narain, N.R., DiFiglia, M., Kiebish, M.A.*, et al.* (2016). High-resolution proteomic and lipidomic analysis of exosomes and microvesicles from different cell sources. J Extracell Vesicles *5*, 32570.

Harding, C., Heuser, J., and Stahl, P. (1983). Receptor-mediated endocytosis of transferrin and recycling of the transferrin receptor in rat reticulocytes. The Journal of cell biology *97*, 329-339.

Hayes, S., Turecki, G., Brisebois, K., Lopes-Cendes, I., Gaspar, C., Riess, O., Ranum, L.P., Pulst, S.M., and Rouleau, G.A. (2000). CAG repeat length in RAI1 is associated with age at onset variability in spinocerebellar ataxia type 2 (SCA2). Human molecular genetics *9*, 1753-1758.

Hemler, M.E. (2005). Tetraspanin functions and associated microdomains. Nature Reviews Molecular Cell Biology *6*, 801-811.

Hernandez-Castillo, C.R., Galvez, V., Mercadillo, R., Diaz, R., Campos-Romo, A., and Fernandez-Ruiz, J. (2015). Extensive White Matter Alterations and Its Correlations with Ataxia Severity in SCA 2 Patients. PLoS One *10*, e0135449.

Hernández, A., Magariño, C., Gispert, S., Santos, N., Lunkes, A., Orozco, G., Beckmann, J., Auburger, G., and Heredero, L. (1995). Genetic mapping of the spinocerebellar ataxia 2 (SCA2) locus on chromosome 12q23–q24.1. Genomics *25*, 433-435.

Herskovits, J.S., Burgess, C.C., Obar, R.A., and Vallee, R.B. (1993). Effects of mutant rat dynamin on endocytosis. The Journal of cell biology *122*, 565-578.

Hessvik, N.P., and Llorente, A. (2018). Current knowledge on exosome biogenesis and release. Cell Mol Life Sci *75*, 193-208.

Houali, K., Wang, X., Shimizu, Y., Djennaoui, D., Nicholls, J., Fiorini, S., Bouguermouh, A., and Ooka, T. (2007). A new diagnostic marker for secreted Epstein-Barr virus encoded LMP1 and BARF1 oncoproteins in the serum and saliva of patients with nasopharyngeal carcinoma. Clinical cancer research : an official journal of the American Association for Cancer Research *13*, 4993-5000.

Hsu, C., Morohashi, Y., Yoshimura, S.-I., Manrique-Hoyos, N., Jung, S., Lauterbach, M.A., Bakhti, M., Grønborg, M., Möbius, W., Rhee, J.*, et al.* (2010). Regulation of exosome secretion by Rab35 and its GTPase-activating proteins TBC1D10A-C. The Journal of cell biology *189*, 223-232.

Huynh, D.P., Del Bigio, M.R., Ho, D.H., and Pulst, S.M. (1999). Expression of ataxin-2 in brains from normal individuals and patients with Alzheimer's disease and spinocerebellar ataxia 2. Annals of neurology *45*, 232-241.

Huynh, D.P., Figueroa, K., Hoang, N., and Pulst, S.M. (2000). Nuclear localization or inclusion body formation of ataxin-2 are not necessary for SCA2 pathogenesis in mouse or human. Nature genetics *26*, 44-50.

Huynh, D.P., Nguyen, D.T., Pulst-Korenberg, J.B., Brice, A., and Pulst, S.M. (2007). Parkin is an E3 ubiquitin-ligase for normal and mutant ataxin-2 and prevents ataxin-2-induced cell death. Exp Neurol *203*, 531-541.

Huynh, D.P., Yang, H.T., Vakharia, H., Nguyen, D., and Pulst, S.M. (2003). Expansion of the polyQ repeat in ataxin-2 alters its Golgi localization, disrupts the Golgi complex and causes cell death. Human molecular genetics *12*, 1485-1496.

Im, H., Shao, H., Park, Y.I., Peterson, V.M., Castro, C.M., Weissleder, R., and Lee, H. (2014). Label-free detection and molecular profiling of exosomes with a nano-plasmonic sensor. Nature biotechnology *32*, 490-495.

Imbert, G., Saudou, F., Yvert, G., Devys, D., Trottier, Y., Garnier, J.M., Weber, C., Mandel, J.L., Cancel, G., Abbas, N.*, et al.* (1996). Cloning of the gene for spinocerebellar ataxia 2 reveals a locus with high sensitivity to expanded CAG/glutamine repeats. Nature genetics *14*, 285-291.

Inagaki, A., Iida, A., Matsubara, M., and Inagaki, H. (2005). Positron emission tomography and magnetic resonance imaging in spinocerebellar ataxia type 2: a study of symptomatic and asymptomatic individuals. European journal of neurology *12*, 725-728.

Infante, J., Berciano, J., Volpini, V., Corral, J., Polo, J.M., Pascual, J., and Combarros, O. (2004). Spinocerebellar ataxia type 2 with Levodopa-responsive parkinsonism culminating in motor neuron disease. Movement disorders : official journal of the Movement Disorder Society *19*, 848-852.

Israels, S.J., and McMillan-Ward, E.M. (2007). Platelet tetraspanin complexes and their association with lipid rafts. Thrombosis and haemostasis *98*, 1081-1087.

Jacobi, H., Bauer, P., Giunti, P., Labrum, R., Sweeney, M.G., Charles, P., Durr, A., Marelli, C., Globas, C., Linnemann, C.*, et al.* (2011). The natural history of spinocerebellar ataxia type 1, 2, 3, and 6: a 2-year follow-up study. Neurology *77*, 1035-1041.

Jahn, R., Lang, T., and Südhof, T.C. (2003). Membrane fusion. Cell *112*, 519-533.

Jahn, R., and Scheller, R.H. (2006). SNAREs--engines for membrane fusion. Nature reviews Molecular cell biology *7*, 631-643.

Jahn, R., and Südhof, T.C. (1999). Membrane fusion and exocytosis. Annu Rev Biochem *68*, 863-911.

Jankovičová, J., Sečová, P., Michalková, K., and Antalíková, J. (2020). Tetraspanins, More than Markers of Extracellular Vesicles in Reproduction. Int J Mol Sci *21*, 7568.

Janmey, P.A., and Kinnunen, P.K.J. (2006). Biophysical properties of lipids and dynamic membranes. Trends in Cell Biology *16*, 538-546.

Jeon, I., Cicchetti, F., Cisbani, G., Lee, S., Li, E., Bae, J., Lee, N., Li, L., Im, W., Kim, M.*, et al.* (2016). Human-to-mouse prion-like propagation of mutant huntingtin protein. Acta neuropathologica *132*, 577-592.

Jeyaram, A., and Jay, S.M. (2017). Preservation and Storage Stability of Extracellular Vesicles for Therapeutic Applications. The AAPS journal *20*, 1.

Jiang, H., Mankodi, A., Swanson, M.S., Moxley, R.T., and Thornton, C.A. (2004). Myotonic dystrophy type 1 is associated with nuclear foci of mutant RNA, sequestration of muscleblind proteins and deregulated alternative splicing in neurons. Human molecular genetics *13*, 3079-3088.

Jimenez-Sanchez, M., Thomson, F., Zavodszky, E., and Rubinsztein, D.C. (2012). Autophagy and polyglutamine diseases. Prog Neurobiol *97*, 67-82.

Johnstone, R.M., Adam, M., Hammond, J.R., Orr, L., and Turbide, C. (1987). Vesicle formation during reticulocyte maturation. Association of plasma membrane activities with released vesicles (exosomes). The Journal of biological chemistry *262*, 9412-9420.

Joshi, P., Turola, E., Ruiz, A., Bergami, A., Libera, D.D., Benussi, L., Giussani, P., Magnani, G., Comi, G., Legname, G.*, et al.* (2014). Microglia convert aggregated amyloid-β into neurotoxic forms through the shedding of microvesicles. Cell death and differentiation *21*, 582-593.

Jucker, M., and Walker, L.C. (2011). Pathogenic protein seeding in Alzheimer disease and other neurodegenerative disorders. Annals of neurology *70*, 532-540.

Jucker, M., and Walker, L.C. (2013). Self-propagation of pathogenic protein aggregates in neurodegenerative diseases. Nature *501*, 45-51.

Jung, B.C., Choi, S.I., Du, A.X., Cuzzocreo, J.L., Ying, H.S., Landman, B.A., Perlman, S.L., Baloh, R.W., Zee, D.S., Toga, A.W.*, et al.* (2012). MRI shows a region-specific pattern of atrophy in spinocerebellar ataxia type 2. Cerebellum (London, England) *11*, 272-279.

Kalra, H., Drummen, G.P., and Mathivanan, S. (2016). Focus on Extracellular Vesicles: Introducing the Next Small Big Thing. Int J Mol Sci *17*, 170.

Kanai, K., and Kuwabara, S. (2009). Motor nerve hyperexcitability and muscle cramps in Machado-Joseph disease. Archives of neurology *66*, 139; author reply 139-140.

Katoh, K., Shibata, H., Suzuki, H., Nara, A., Ishidoh, K., Kominami, E., Yoshimori, T., and Maki, M. (2003). The ALG-2-interacting protein Alix associates with CHMP4b, a human homologue of yeast Snf7 that is involved in multivesicular body sorting. The Journal of biological chemistry *278*, 39104-39113.

Keerthikumar, S., Gangoda, L., Liem, M., Fonseka, P., Atukorala, I., Ozcitti, C., Mechler, A., Adda, C.G., Ang, C.S., and Mathivanan, S. (2015). Proteogenomic analysis reveals exosomes are more oncogenic than ectosomes. Oncotarget *6*, 15375-15396.

Kiebler, M.A., Hemraj, I., Verkade, P., Kohrmann, M., Fortes, P., Marion, R.M., Ortin, J., and Dotti, C.G. (1999). The mammalian staufen protein localizes to the somatodendritic domain of cultured hippocampal neurons: implications for its involvement in mRNA transport. The Journal of neuroscience : the official journal of the Society for Neuroscience *19*, 288-297.

Kim, J.M., Hong, S., Kim, G.P., Choi, Y.J., Kim, Y.K., Park, S.S., Kim, S.E., and Jeon, B.S. (2007a). Importance of low-range CAG expansion and CAA interruption in SCA2 Parkinsonism. Archives of neurology *64*, 1510-1518.

Kim, Y.K., Furic, L., Desgroseillers, L., and Maquat, L.E. (2005). Mammalian Staufen1 recruits Upf1 to specific mRNA 3'UTRs so as to elicit mRNA decay. Cell *120*, 195-208.

Kim, Y.K., Furic, L., Parisien, M., Major, F., DesGroseillers, L., and Maquat, L.E. (2007b). Staufen1 regulates diverse classes of mammalian transcripts. The EMBO journal *26*, 2670-2681.

Kirchhausen, T. (2000). Clathrin. Annu Rev Biochem *69*, 699-727.

Koivusalo, M., Welch, C., Hayashi, H., Scott, C.C., Kim, M., Alexander, T., Touret, N., Hahn, K.M., and Grinstein, S. (2010). Amiloride inhibits macropinocytosis by lowering submembranous pH and preventing Rac1 and Cdc42 signaling. The Journal of cell biology *188*, 547-563.

Kowal, J., Arras, G., Colombo, M., Jouve, M., Morath, J.P., Primdal-Bengtson, B., Dingli, F., Loew, D., Tkach, M., and Théry, C. (2016). Proteomic comparison defines novel markers to characterize heterogeneous populations of extracellular vesicle subtypes. *113*, E968-E977.

Kowal, J., Tkach, M., and Théry, C. (2014). Biogenesis and secretion of exosomes. Current opinion in cell biology *29*, 116-125.

Koyano, S., Uchihara, T., Fujigasaki, H., Nakamura, A., Yagishita, S., and Iwabuchi, K. (1999). Neuronal intranuclear inclusions in spinocerebellar ataxia type 2: triple-labeling immunofluorescent study. Neurosci Lett *273*, 117-120.

Krämer-Albers, E.M., Bretz, N., Tenzer, S., Winterstein, C., Möbius, W., Berger, H., Nave, K.A., Schild, H., and Trotter, J. (2007). Oligodendrocytes secrete exosomes containing major myelin and stress-protective proteins: Trophic support for axons? Proteomics Clinical applications *1*, 1446-1461.

Kreimer, S., Belov, A.M., Ghiran, I., Murthy, S.K., Frank, D.A., and Ivanov, A.R. (2015). Mass-spectrometry-based molecular characterization of extracellular vesicles: lipidomics and proteomics. J Proteome Res *14*, 2367-2384.

Kuemmerle, S., Gutekunst, C.A., Klein, A.M., Li, X.J., Li, S.H., Beal, M.F., Hersch, S.M., and Ferrante, R.J. (1999). Huntington aggregates may not predict neuronal death in Huntington's disease. Annals of neurology *46*, 842-849.

Kuo, L., and Freed, E.O. (2012). ARRDC1 as a mediator of microvesicle budding. *109*, 4025-4026.

Kurzchalia, T.V., and Parton, R.G. (1999). Membrane microdomains and caveolae. Current opinion in cell biology *11*, 424-431.

Kutateladze, T.G. (2006). Phosphatidylinositol 3-phosphate recognition and membrane docking by the FYVE domain. Biochimica et biophysica acta *1761*, 868-877.

La Spada, A.R., and Taylor, J.P. (2010). Repeat expansion disease: progress and puzzles in disease pathogenesis. Nat Rev Genet *11*, 247-258.

Laffita-Mesa, J.M., Almaguer-Mederos, L.E., Kouri, V., Bauer, P.O., Vazquez-Mojena, Y., Cruz Marino, T., and Velazquez-Perez, L. (2014). Large normal alleles and SCA2 prevalence: lessons from a nationwide study and analysis of the literature. Clinical genetics *86*, 96-98.

Laffita-Mesa, J.M., Velazquez-Perez, L.C., Santos Falcon, N., Cruz-Marino, T., Gonzalez Zaldivar, Y., Vazquez Mojena, Y., Almaguer-Gotay, D., Almaguer Mederos, L.E., and Rodriguez Labrada, R. (2012). Unexpanded and intermediate CAG polymorphisms at the SCA2 locus (ATXN2) in the Cuban population: evidence about the origin of expanded SCA2 alleles. European journal of human genetics : EJHG *20*, 41-49.

Lamaze, C., Fujimoto, L.M., Yin, H.L., and Schmid, S.L. (1997). The actin cytoskeleton is required for receptor-mediated endocytosis in mammalian cells. The Journal of biological chemistry *272*, 20332-20335.

Lamichhane, T.N., Jeyaram, A., Patel, D.B., Parajuli, B., Livingston, N.K., Arumugasaamy, N., Schardt, J.S., and Jay, S.M. (2016). Oncogene Knockdown via Active Loading of Small RNAs into Extracellular Vesicles by Sonication. Cellular and molecular bioengineering *9*, 315-324.

Lastres-Becker, I., Nonis, D., Eich, F., Klinkenberg, M., Gorospe, M., Kotter, P., Klein, F.A., Kedersha, N., and Auburger, G. (2016). Mammalian ataxin-2 modulates translation control at the pre-initiation complex via PI3K/mTOR and is induced by starvation. Biochimica et biophysica acta *1862*, 1558-1569.

Lastres-Becker, I., Nonis, D., Nowock, J., and Auburger, G. (2019). New alternative splicing variants of the ATXN2 transcript. Neurol Res Pract *1*, 22.

Laulagnier, K., Motta, C., Hamdi, S., Roy, S., Fauvelle, F., Pageaux, J.F., Kobayashi, T., Salles, J.P., Perret, B., Bonnerot, C.*, et al.* (2004). Mast cell- and dendritic cell-derived exosomes display a specific lipid composition and an unusual membrane organization. The Biochemical journal *380*, 161-171.

Lawrie, A.S., Albanyan, A., Cardigan, R.A., Mackie, I.J., and Harrison, P. (2009). Microparticle sizing by dynamic light scattering in fresh-frozen plasma. Vox sanguinis *96*, 206-212.

Lee, J.A., Tang, Z.Z., and Black, D.L. (2009). An inducible change in Fox-1/A2BP1 splicing modulates the alternative splicing of downstream neuronal target exons. Genes Dev *23*, 2284-2293.

Lee, S., Kim, W., Li, Z., and Hall, G.F. (2012). Accumulation of vesicle-associated human tau in distal dendrites drives degeneration and tau secretion in an in situ cellular tauopathy model. International journal of Alzheimer's disease *2012*, 172837.

Lee, S.J., Desplats, P., Sigurdson, C., Tsigelny, I., and Masliah, E. (2010). Cell-to-cell transmission of non-prion protein aggregates. Nature reviews Neurology *6*, 702-706.

Li, P.P., Sun, X., Xia, G., Arbez, N., Paul, S., Zhu, S., Peng, H.B., Ross, C.A., Koeppen, A.H., Margolis, R.L.*, et al.* (2016). ATXN2-AS, a gene antisense to ATXN2, is associated with spinocerebellar ataxia type 2 and amyotrophic lateral sclerosis. Annals of neurology *80*, 600-615.

Liangsupree, T., Multia, E., and Riekkola, M.-L. (2021). Modern isolation and separation techniques for extracellular vesicles. Journal of Chromatography A *1636*, 461773.

Lim, J., Hao, T., Shaw, C., Patel, A.J., Szabo, G., Rual, J.F., Fisk, C.J., Li, N., Smolyar, A., Hill, D.E.*, et al.* (2006). A protein-protein interaction network for human inherited ataxias and disorders of Purkinje cell degeneration. Cell *125*, 801-814.

Lima, M., Mayer, F., Coutinho, P., and Abade, A. (1997). Prevalence, geographic distribution, and genealogical investigation of Machado-Joseph disease in the Azores (Portugal). Human biology *69*, 383-391.

Lin, M.T., and Beal, M.F. (2006). Mitochondrial dysfunction and oxidative stress in neurodegenerative diseases. Nature *443*, 787-795.

Linares, R., Tan, S., Gounou, C., Arraud, N., and Brisson, A.R. (2015). High-speed centrifugation induces aggregation of extracellular vesicles. J Extracell Vesicles *4*, 29509-29509.

Liu, H., Wang, H., Peterson, M., Zhang, W., Hou, G., and Zhang, Z.W. (2019). N-terminal alternative splicing of GluN1 regulates the maturation of excitatory synapses and seizure susceptibility. Proc Natl Acad Sci U S A *116*, 21207-21212.

Liu, J., Tang, T.S., Tu, H., Nelson, O., Herndon, E., Huynh, D.P., Pulst, S.M., and Bezprozvanny, I. (2009). Deranged calcium signaling and neurodegeneration in spinocerebellar ataxia type 2. The Journal of neuroscience : the official journal of the Society for Neuroscience *29*, 9148-9162.

Liu, L., Drouet, V., Wu, J.W., Witter, M.P., Small, S.A., Clelland, C., and Duff, K. (2012). Trans-synaptic spread of tau pathology in vivo. PloS one *7*, e31302.

Logan, T., Bendor, J., Toupin, C., Thorn, K., and Edwards, R.H. (2017). α-Synuclein promotes dilation of the exocytotic fusion pore. Nat Neurosci *20*, 681-689.

Lőrincz, Á.M., Timár, C.I., Marosvári, K.A., Veres, D.S., Otrokocsi, L., Kittel, Á., and Ligeti, E. (2014). Effect of storage on physical and functional properties of extracellular vesicles derived from neutrophilic granulocytes. J Extracell Vesicles *3*, 25465.

Maas, S.L.N., Breakefield, X.O., and Weaver, A.M. (2017). Extracellular Vesicles: Unique Intercellular Delivery Vehicles. Trends in Cell Biology *27*, 172-188.

Madison, M.N., Welch, J.L., and Okeoma, C.M. (2017). Isolation of Exosomes from Semen for in vitro Uptake and HIV-1 Infection Assays. Bio Protoc *7*, e2216.

Magana, J.J., Velazquez-Perez, L., and Cisneros, B. (2013). Spinocerebellar ataxia type 2: clinical presentation, molecular mechanisms, and therapeutic perspectives. Molecular neurobiology *47*, 90-104.

Malenica, M., Vukomanović, M., Kurtjak, M., Masciotti, V., Dal Zilio, S., Greco, S., Lazzarino, M., Krušić, V., Perčić, M., Jelovica Badovinac, I.*, et al.* (2021). Perspectives of Microscopy Methods for Morphology Characterisation of Extracellular Vesicles from Human Biofluids. Biomedicines *9*, 603.

Malkin, E.Z., and Bratman, S.V. (2020). Bioactive DNA from extracellular vesicles and particles. Cell Death & Disease *11*, 584.

Mao, R., Aylsworth, A.S., Potter, N., Wilson, W.G., Breningstall, G., Wick, M.J., Babovic-Vuksanovic, D., Nance, M., Patterson, M.C., Gomez, C.M.*, et al.* (2002). Childhood-onset ataxia: testing for large CAG-repeats in SCA2 and SCA7. American journal of medical genetics *110*, 338-345.

Marcelo, A., Koppenol, R., de Almeida, L.P., Matos, C.A., and Nobrega, C. (2021). Stress granules, RNA-binding proteins and polyglutamine diseases: too much aggregation? Cell death & disease *12*, 592.

Marks, B., Stowell, M.H.B., Vallis, Y., Mills, I.G., Gibson, A., Hopkins, C.R., and McMahon, H.T. (2001). GTPase activity of dynamin and resulting conformation change are essential for endocytosis. Nature *410*, 231-235.

Martin, J.B. (1999). Molecular basis of the neurodegenerative disorders. The New England journal of medicine *340*, 1970-1980.

Martindale, D., Hackam, A., Wieczorek, A., Ellerby, L., Wellington, C., McCutcheon, K., Singaraja, R., Kazemi-Esfarjani, P., Devon, R., Kim, S.U.*, et al.* (1998). Length of huntingtin and its polyglutamine tract influences localization and frequency of intracellular aggregates. Nature genetics *18*, 150-154.

Mascalchi, M., Diciotti, S., Giannelli, M., Ginestroni, A., Soricelli, A., Nicolai, E., Aiello, M., Tessa, C., Galli, L., Dotti, M.T.*, et al.* (2014). Progression of brain atrophy in spinocerebellar ataxia type 2: a longitudinal tensor-based morphometry study. PLoS One *9*, e89410.

Mathivanan, S., Fonseka, P., Nedeva, C., and Atukorala, I. (2021). New frontiers : extracellular vesicles, Vol 97 (Springer Nature Switzerland AG).

Matos, C.A., Almeida, L.P., and Nobrega, C. (2017). Proteolytic Cleavage of Polyglutamine Disease-Causing Proteins: Revisiting the Toxic Fragment Hypothesis. Current pharmaceutical design *23*, 753-775.

Matsuda, S., Kitagishi, Y., and Kobayashi, M. (2013). Function and characteristics of PINK1 in mitochondria. Oxid Med Cell Longev *2013*, 601587.

Mazurov, D., Barbashova, L., and Filatov, A. (2013). Tetraspanin protein CD9 interacts with metalloprotease CD10 and enhances its release via exosomes. The FEBS journal *280*, 1200-1213.

McCullough, J., Colf, L.A., and Sundquist, W.I. (2013). Membrane fission reactions of the mammalian ESCRT pathway. Annu Rev Biochem *82*, 663-692.

McCullough, J., Fisher, R.D., Whitby, F.G., Sundquist, W.I., and Hill, C.P. (2008). ALIX-CHMP4 interactions in the human ESCRT pathway. Proceedings of the National Academy of Sciences of the United States of America *105*, 7687-7691.

Menck, K., Bleckmann, A., Schulz, M., Ries, L., and Binder, C. (2017a). Isolation and Characterization of Microvesicles from Peripheral Blood. J Vis Exp, 55057.

Menck, K., Klemm, F., Gross, J.C., Pukrop, T., Wenzel, D., and Binder, C. (2013). Induction and transport of Wnt 5a during macrophage-induced malignant invasion is mediated by two types of extracellular vesicles. Oncotarget *4*, 2057-2066.

Menck, K., Sönmezer, C., Worst, T.S., Schulz, M., Dihazi, G.H., Streit, F., Erdmann, G., Kling, S., Boutros, M., Binder, C.*, et al.* (2017b). Neutral sphingomyelinases control extracellular vesicles budding from the plasma membrane. J Extracell Vesicles *6*, 1378056-1378056.

Mettlen, M., Pucadyil, T., Ramachandran, R., and Schmid, S.L. (2009). Dissecting dynamin's role in clathrin-mediated endocytosis. Biochem Soc Trans *37*, 1022-1026.

Michael, A., Bajracharya, S.D., Yuen, P.S., Zhou, H., Star, R.A., Illei, G.G., and Alevizos, I. (2010). Exosomes from human saliva as a source of microRNA biomarkers. Oral diseases *16*, 34-38.

Mohammadi, M.R., Riazifar, M., Pone, E.J., Yeri, A., Van Keuren-Jensen, K., Lässer, C., Lotvall, J., and Zhao, W. (2020). Isolation and characterization of microvesicles from mesenchymal stem cells. Methods (San Diego, Calif) *177*, 50-57.

Mol, E.A., Goumans, M.J., Doevendans, P.A., Sluijter, J.P.G., and Vader, P. (2017). Higher functionality of extracellular vesicles isolated using size-exclusion chromatography compared to ultracentrifugation. Nanomedicine : nanotechnology, biology, and medicine *13*, 2061-2065.

Moller, A., and Lobb, R.J. (2020). The evolving translational potential of small extracellular vesicles in cancer. Nat Rev Cancer *20*, 697-709.

Montecalvo, A., Larregina, A.T., Shufesky, W.J., Stolz, D.B., Sullivan, M.L.G., Karlsson, J.M., Baty, C.J., Gibson, G.A., Erdos, G., Wang, Z.*, et al.* (2012). Mechanism of transfer of functional microRNAs between mouse dendritic cells via exosomes. Blood *119*, 756-766.

Morelli, A.E., Larregina, A.T., Shufesky, W.J., Sullivan, M.L., Stolz, D.B., Papworth, G.D., Zahorchak, A.F., Logar, A.J., Wang, Z., Watkins, S.C.*, et al.* (2004). Endocytosis, intracellular sorting, and processing of exosomes by dendritic cells. Blood *104*, 3257-3266.

Moretti, P., Blazo, M., Garcia, L., Armstrong, D., Lewis, R.A., Roa, B., and Scaglia, F. (2004). Spinocerebellar ataxia type 2 (SCA2) presenting with ophthalmoplegia and developmental delay in infancy. American journal of medical genetics Part A *124A*, 392-396.

Morse, M.A., Garst, J., Osada, T., Khan, S., Hobeika, A., Clay, T.M., Valente, N., Shreeniwas, R., Sutton, M.A., Delcayre, A.*, et al.* (2005). A phase I study of dexosome immunotherapy in patients with advanced non-small cell lung cancer. Journal of translational medicine *3*, 9.

Mulcahy, L.A., Pink, R.C., and Carter, D.R. (2014). Routes and mechanisms of extracellular vesicle uptake. J Extracell Vesicles *3*.

Müller, P., and Schier, A.F. (2011). Extracellular movement of signaling molecules. Developmental cell *21*, 145-158.

Muralidharan-Chari, V., Clancy, J., Plou, C., Romao, M., Chavrier, P., Raposo, G., and D'Souza-Schorey, C. (2009). ARF6-regulated shedding of tumor cell-derived plasma membrane microvesicles. Curr Biol *19*, 1875-1885.

Nabhan, J.F., Hu, R., Oh, R.S., Cohen, S.N., and Lu, Q. (2012). Formation and release of arrestin domain-containing protein 1-mediated microvesicles (ARMMs) at plasma membrane by recruitment of TSG101 protein. *109*, 4146-4151.

Nabi, I.R., and Le, P.U. (2003). Caveolae/raft-dependent endocytosis. The Journal of cell biology *161*, 673-677.

Nanbo, A., Kawanishi, E., Yoshida, R., and Yoshiyama, H. (2013). Exosomes derived from Epstein-Barr virus-infected cells are internalized via caveola-dependent endocytosis and promote phenotypic modulation in target cells. Journal of virology *87*, 10334-10347.

Nanetti, L., Fancellu, R., Tomasello, C., Gellera, C., Pareyson, D., and Mariotti, C. (2009). Rare association of motor neuron disease and spinocerebellar ataxia type 2 (SCA2): a new case and review of the literature. Journal of neurology *256*, 1926-1928.

Nechiporuk, T., Huynh, D.P., Figueroa, K., Sahba, S., Nechiporuk, A., and Pulst, S.M. (1998). The mouse SCA2 gene: cDNA sequence, alternative splicing and protein expression. Human molecular genetics *7*, 1301-1309.

Neuwald, A.F., and Koonin, E.V. (1998). Ataxin-2, global regulators of bacterial gene expression, and spliceosomal snRNP proteins share a conserved domain. Journal of molecular medicine (Berlin, Germany) *76*, 3-5.

Newton, A.J., Kirchhausen, T., and Murthy, V.N. (2006). Inhibition of dynamin completely blocks compensatory synaptic vesicle endocytosis. *103*, 17955-17960.

Nihei, Y., Ito, D., and Suzuki, N. (2012). Roles of ataxin-2 in pathological cascades mediated by TAR DNA-binding protein 43 (TDP-43) and Fused in Sarcoma (FUS). The Journal of biological chemistry *287*, 41310-41323.

Nobrega, C., Carmo-Silva, S., Albuquerque, D., Vasconcelos-Ferreira, A., Vijayakumar, U.G., Mendonca, L., Hirai, H., and de Almeida, L.P. (2015). Re-establishing ataxin-2 downregulates translation of mutant ataxin-3 and alleviates Machado-Joseph disease. Brain : a journal of neurology *138*, 3537-3554.

Nobrega, C., Nascimento-Ferreira, I., Onofre, I., Albuquerque, D., Conceicao, M., Deglon, N., and de Almeida, L.P. (2013). Overexpression of mutant ataxin-3 in mouse cerebellum induces ataxia and cerebellar neuropathology. Cerebellum (London, England) *12*, 441-455.

Nóbrega, C., and Pereira de Almeida, L. (2018). *Polyglutamine Disorders*, 1 edn (Springer International Publishing).

Nonhoff, U., Ralser, M., Welzel, F., Piccini, I., Balzereit, D., Yaspo, M.L., Lehrach, H., and Krobitsch, S. (2007). Ataxin-2 interacts with the DEAD/H-box RNA helicase DDX6 and interferes with P-bodies and stress granules. Mol Biol Cell *18*, 1385-1396.

Nonis, D., Schmidt, M.H.H., van de Loo, S., Eich, F., Dikic, I., Nowock, J., and Auburger, G. (2008). Ataxin-2 associates with the endocytosis complex and affects EGF receptor trafficking. Cellular signalling *20*, 1725-1739.

Nordin, J.Z., Lee, Y., Vader, P., Mäger, I., Johansson, H.J., Heusermann, W., Wiklander, O.P.B., Hällbrink, M., Seow, Y., Bultema, J.J.*, et al.* (2015). Ultrafiltration with size-exclusion liquid chromatography for high yield isolation of extracellular vesicles preserving intact biophysical and functional properties. Nanomedicine: Nanotechnology, Biology and Medicine *11*, 879-883.

Nucifora, F.C., Jr., Sasaki, M., Peters, M.F., Huang, H., Cooper, J.K., Yamada, M., Takahashi, H., Tsuji, S., Troncoso, J., Dawson, V.L.*, et al.* (2001). Interference by huntingtin and

atrophin-1 with cbp-mediated transcription leading to cellular toxicity. Science (New York, NY) *291*, 2423-2428.

Ogorevc, E., Kralj-Iglic, V., and Veranic, P. (2013). The role of extracellular vesicles in phenotypic cancer transformation. Radiol Oncol *47*, 197-205.

Ohlendieck, K. (2010). Centrifugation. In Principles and Techniques of Biochemistry and Molecular Biology, J. Walker, and K. Wilson, eds. (Cambridge: Cambridge University Press), pp. 73-99.

Okajima, F. (2002). Plasma lipoproteins behave as carriers of extracellular sphingosine 1-phosphate: is this an atherogenic mediator or an anti-atherogenic mediator? Biochimica et Biophysica Acta (BBA) - Molecular and Cell Biology of Lipids *1582*, 132-137.

Olanow, C.W., and Prusiner, S.B. (2009). Is Parkinson's disease a prion disorder? *106*, 12571-12572.

Oram, J.F., and Vaughan, A.M. (2000). ABCA1-mediated transport of cellular cholesterol and phospholipids to HDL apolipoproteins. Current opinion in lipidology *11*, 253-260.

Ordway, J.M., Tallaksen-Greene, S., Gutekunst, C.A., Bernstein, E.M., Cearley, J.A., Wiener, H.W., Dure, L.S.t., Lindsey, R., Hersch, S.M., Jope, R.S.*, et al.* (1997). Ectopically expressed CAG repeats cause intranuclear inclusions and a progressive late onset neurological phenotype in the mouse. Cell *91*, 753-763.

Ostrowski, L.A., Hall, A.C., and Mekhail, K. (2017). Ataxin-2: From RNA Control to Human Health and Disease. Genes (Basel) *8*, 157.

Ostrowski, M., Carmo, N.B., Krumeich, S., Fanget, I., Raposo, G., Savina, A., Moita, C.F., Schauer, K., Hume, A.N., Freitas, R.P.*, et al.* (2010). Rab27a and Rab27b control different steps of the exosome secretion pathway. Nat Cell Biol *12*, 19-30; sup pp 11-13.

Paciorkowski, A.R., Shafrir, Y., Hrivnak, J., Patterson, M.C., Tennison, M.B., Clark, H.B., and Gomez, C.M. (2011). Massive expansion of SCA2 with autonomic dysfunction, retinitis pigmentosa, and infantile spasms. Neurology *77*, 1055-1060.

Pan, B.T., Teng, K., Wu, C., Adam, M., and Johnstone, R.M. (1985). Electron microscopic evidence for externalization of the transferrin receptor in vesicular form in sheep reticulocytes. The Journal of cell biology *101*, 942-948.

Park, S.H., Kukushkin, Y., Gupta, R., Chen, T., Konagai, A., Hipp, M.S., Hayer-Hartl, M., and Hartl, F.U. (2013). PolyQ proteins interfere with nuclear degradation of cytosolic proteins by sequestering the Sis1p chaperone. Cell *154*, 134-145.

Park, S.J., Jeon, H., Yoo, S.-M., and Lee, M.-S. (2018). The effect of storage temperature on the biological activity of extracellular vesicles for the complement system. In Vitro Cellular & Developmental Biology - Animal *54*, 423-429.

Parolini, I., Federici, C., Raggi, C., Lugini, L., Palleschi, S., De Milito, A., Coscia, C., Iessi, E., Logozzi, M., Molinari, A.*, et al.* (2009). Microenvironmental pH is a key factor for exosome traffic in tumor cells. The Journal of biological chemistry *284*, 34211-34222.

Parton, R.G., and Simons, K. (2007). The multiple faces of caveolae. Nature Reviews Molecular Cell Biology *8*, 185-194.

Pathan, M., Fonseka, P., Chitti, S.V., Kang, T., Sanwlani, R., Van Deun, J., Hendrix, A., and Mathivanan, S. (2019). Vesiclepedia 2019: a compendium of RNA, proteins, lipids and metabolites in extracellular vesicles. Nucleic acids research *47*, D516-d519.

Paul, S., Dansithong, W., Figueroa, K.P., Scoles, D.R., and Pulst, S.M. (2018). Staufen1 links RNA stress granules and autophagy in a model of neurodegeneration. Nat Commun *9*, 3648.

Paul, S., Dansithong, W., and Pulst, S. (2014). ATAXIN-2 (ATXN2) Regulates RGS8 Expression Via RNA Interaction (P1.045). *82*, P1.045.

Paulson, H. (2018). Repeat expansion diseases. Handb Clin Neurol *147*, 105-123.

Paxinos, G., and Keith B. J. Franklin, M. (2007). The Mouse Brain in Stereotaxic Coordinates (Elsevier Science).

Perez-Gonzalez, R., Gauthier, S.A., Kumar, A., and Levy, E. (2012). The exosome secretory pathway transports amyloid precursor protein carboxyl-terminal fragments from the cell into the brain extracellular space. The Journal of biological chemistry *287*, 43108-43115.

Perez-Hernandez, D., Gutiérrez-Vázquez, C., Jorge, I., López-Martín, S., Ursa, A., Sánchez-Madrid, F., Vázquez, J., and Yáñez-Mó, M. (2013). The intracellular interactome of tetraspanin-enriched microdomains reveals their function as sorting machineries toward exosomes. The Journal of biological chemistry *288*, 11649-11661.

Petersen, S.H., Odintsova, E., Haigh, T.A., Rickinson, A.B., Taylor, G.S., and Berditchevski, F. (2011). The role of tetraspanin CD63 in antigen presentation via MHC class II. European journal of immunology *41*, 2556-2561.

Pisitkun, T., Shen, R.F., and Knepper, M.A. (2004). Identification and proteomic profiling of exosomes in human urine. Proceedings of the National Academy of Sciences of the United States of America *101*, 13368-13373.

Pocsfalvi, G., Stanly, C., Vilasi, A., Fiume, I., Capasso, G., Turiák, L., Buzas, E.I., and Vékey, K. (2016). Mass spectrometry of extracellular vesicles. Mass spectrometry reviews *35*, 3-21.

Poliakov, A., Spilman, M., Dokland, T., Amling, C.L., and Mobley, J.A. (2009). Structural heterogeneity and protein composition of exosome-like vesicles (prostasomes) in human semen. The Prostate *69*, 159-167.

Pollet, H., Conrard, L., Cloos, A.S., and Tyteca, D. (2018). Plasma Membrane Lipid Domains as Platforms for Vesicle Biogenesis and Shedding? Biomolecules *8*.

Pornillos , O., Higginson , D.S., Stray , K.M., Fisher , R.D., Garrus , J.E., Payne , M., He , G.-P., Wang , H.E., Morham , S.G., and Sundquist , W.I. (2003). HIV Gag mimics the Tsg101-recruiting activity of the human Hrs protein. Journal of Cell Biology *162*, 425-434.

Potolicchio, I., Carven, G.J., Xu, X., Stipp, C., Riese, R.J., Stern, L.J., and Santambrogio, L. (2005). Proteomic analysis of microglia-derived exosomes: metabolic role of the aminopeptidase CD13 in neuropeptide catabolism. Journal of immunology (Baltimore, Md : 1950) *175*, 2237-2243.

Prusiner, S.B. (1982). Novel proteinaceous infectious particles cause scrapie. Science (New York, NY) *216*, 136-144.

Pulst, S.M., Nechiporuk, A., Nechiporuk, T., Gispert, S., Chen, X.N., Lopes-Cendes, I., Pearlman, S., Starkman, S., Orozco-Diaz, G., Lunkes, A.*, et al.* (1996). Moderate expansion of a normally biallelic trinucleotide repeat in spinocerebellar ataxia type 2. Nature genetics *14*, 269-276.

Pulst, S.M., Santos, N., Wang, D., Yang, H., Huynh, D., Velazquez, L., and Figueroa, K.P. (2005). Spinocerebellar ataxia type 2: polyQ repeat variation in the CACNA1A calcium channel modifies age of onset. Brain : a journal of neurology *128*, 2297-2303.

Raimondo, F., Morosi, L., Chinello, C., Magni, F., and Pitto, M. (2011). Advances in membranous vesicle and exosome proteomics improving biological understanding and biomarker discovery. Proteomics *11*, 709-720.

Rajendran, L., Honsho, M., Zahn, T.R., Keller, P., Geiger, K.D., Verkade, P., and Simons, K. (2006). Alzheimer's disease beta-amyloid peptides are released in association with exosomes. Proceedings of the National Academy of Sciences of the United States of America *103*, 11172-11177.

Ralser, M., Nonhoff, U., Albrecht, M., Lengauer, T., Wanker, E.E., Lehrach, H., and Krobitsch, S. (2005). Ataxin-2 and huntingtin interact with endophilin-A complexes to function in plastin-associated pathways. Human molecular genetics *14*, 2893-2909.

Raposo, G., Nijman, H.W., Stoorvogel, W., Liejendekker, R., Harding, C.V., Melief, C.J., and Geuze, H.J. (1996). B lymphocytes secrete antigen-presenting vesicles. The Journal of experimental medicine *183*, 1161-1172.

Rapraeger, A.C., Krufka, A., and Olwin, B.B. (1991). Requirement of heparan sulfate for bFGF-mediated fibroblast growth and myoblast differentiation. Science (New York, NY) *252*, 1705-1708.

Rauch, S., and Martin-Serrano, J. (2011). Multiple interactions between the ESCRT machinery and arrestin-related proteins: implications for PPXY-dependent budding. Journal of virology *85*, 3546-3556.

Ravikumar, B., Duden, R., and Rubinsztein, D.C. (2002). Aggregate-prone proteins with polyglutamine and polyalanine expansions are degraded by autophagy. Human molecular genetics *11*, 1107-1117.

Rego, A.C., and de Almeida, L.P. (2005). Molecular targets and therapeutic strategies in Huntington's disease. Current drug targets CNS and neurological disorders *4*, 361-381.

Richardson, M.M., Jennings, L.K., and Zhang, X.A. (2011). Tetraspanins and tumor progression. Clinical & experimental metastasis *28*, 261-270.

Ridley, A.J. (2006). Rho GTPases and actin dynamics in membrane protrusions and vesicle trafficking. Trends Cell Biol *16*, 522-529.

Rigby, M., Heavens, R.P., Smith, D., O'Donnell, R., Hill, R.G., and Sirinathsinghji, D.I.S. (2002). Distribution of NMDA receptors in brain and spinal cord. In NMDA Antagonists as Potential Analgesic Drugs, D.J.S. Sirinathsinghji, and R.G. Hill, eds. (Basel: Birkhäuser Basel), pp. 45-65.

Robbins, P.D., and Morelli, A.E. (2014). Regulation of immune responses by extracellular vesicles. Nature Reviews Immunology *14*, 195-208.

Rodriguez-Boulan, E., Kreitzer, G., and Müsch, A. (2005). Organization of vesicular trafficking in epithelia. Nature reviews Molecular cell biology *6*, 233-247.

Ronquist, G., and Brody, I. (1985). The prostasome: its secretion and function in man. Biochimica et biophysica acta *822*, 203-218.

Ross, C.A., and Poirier, M.A. (2004). Protein aggregation and neurodegenerative disease. Nature medicine *10 Suppl*, S10-17.

Ross, O.A., Rutherford, N.J., Baker, M., Soto-Ortolaza, A.I., Carrasquillo, M.M., DeJesus-Hernandez, M., Adamson, J., Li, M., Volkening, K., Finger, E.*, et al.* (2011). Ataxin-2 repeat-length variation and neurodegeneration. Human molecular genetics *20*, 3207-3212.

Rub, U., Del Tredici, K., Schultz, C., Thal, D.R., Braak, E., and Braak, H. (2000). The evolution of Alzheimer's disease-related cytoskeletal pathology in the human raphe nuclei. Neuropathology and applied neurobiology *26*, 553-567.

Rub, U., Schols, L., Paulson, H., Auburger, G., Kermer, P., Jen, J.C., Seidel, K., Korf, H.W., and Deller, T. (2013). Clinical features, neurogenetics and neuropathology of the polyglutamine spinocerebellar ataxias type 1, 2, 3, 6 and 7. Prog Neurobiol *104*, 38-66.

Rub, U., Seidel, K., Ozerden, I., Gierga, K., Brunt, E.R., Schols, L., de Vos, R.A., den Dunnen, W., Schultz, C., Auburger, G.*, et al.* (2007). Consistent affection of the central somatosensory system in spinocerebellar ataxia type 2 and type 3 and its significance for clinical symptoms and rehabilitative therapy. Brain research reviews *53*, 235-249.

Rubinstein, E., Le Naour, F., Lagaudrière-Gesbert, C., Billard, M., Conjeaud, H., and Boucheix, C. (1996). CD9, CD63, CD81, and CD82 are components of a surface tetraspan network connected to HLA-DR and VLA integrins. European journal of immunology *26*, 2657-2665.

Rudnicki, D.D., Holmes, S.E., Lin, M.W., Thornton, C.A., Ross, C.A., and Margolis, R.L. (2007). Huntington's disease--like 2 is associated with CUG repeat-containing RNA foci. Annals of neurology *61*, 272-282.

Rufa, A., Dotti, M.T., Galli, L., Orrico, A., Sicurelli, F., and Federico, A. (2002). Spinocerebellar ataxia type 2 (SCA2) associated with retinal pigmentary degeneration. Eur Neurol *47*, 128-129.

Sagini, K., Costanzi, E., Emiliani, C., Buratta, S., and Urbanelli, L. (2018). Extracellular Vesicles as Conveyors of Membrane-Derived Bioactive Lipids in Immune System. Int J Mol Sci *19*, 1227.

Saitoh, O., Masuho, I., Itoh, M., Abe, H., Komori, K., and Odagiri, M. (2003). Distribution of regulator of G protein signaling 8 (RGS8) protein in the cerebellum. Cerebellum (London, England) *2*, 154-160.

Saleem, Q., Choudhry, S., Mukerji, M., Bashyam, L., Padma, M.V., Chakravarthy, A., Maheshwari, M.C., Jain, S., and Brahmachari, S.K. (2000). Molecular analysis of autosomal dominant hereditary ataxias in the Indian population: high frequency of SCA2 and evidence for a common founder mutation. Human genetics *106*, 179-187.

Salvi, J.S., Chan, J.N., Szafranski, K., Liu, T.T., Wu, J.D., Olsen, J.B., Khanam, N., Poon, B.P., Emili, A., and Mekhail, K. (2014). Roles for Pbp1 and caloric restriction in genome and

lifespan maintenance via suppression of RNA-DNA hybrids. Developmental cell *30*, 177-191.

Saman, S., Kim, W., Raya, M., Visnick, Y., Miro, S., Saman, S., Jackson, B., McKee, A.C., Alvarez, V.E., Lee, N.C.*, et al.* (2012). Exosome-associated tau is secreted in tauopathy models and is selectively phosphorylated in cerebrospinal fluid in early Alzheimer disease. The Journal of biological chemistry *287*, 3842-3849.

Sanpei, K., Takano, H., Igarashi, S., Sato, T., Oyake, M., Sasaki, H., Wakisaka, A., Tashiro, K., Ishida, Y., Ikeuchi, T.*, et al.* (1996). Identification of the spinocerebellar ataxia type 2 gene using a direct identification of repeat expansion and cloning technique, DIRECT. Nature genetics *14*, 277-284.

Satterfield, T.F., Jackson, S.M., and Pallanck, L.J. (2002). A Drosophila homolog of the polyglutamine disease gene SCA2 is a dosage-sensitive regulator of actin filament formation. Genetics *162*, 1687-1702.

Savina, A., Fader, C.M., Damiani, M.T., and Colombo, M.I. (2005). Rab11 promotes docking and fusion of multivesicular bodies in a calcium-dependent manner. Traffic (Copenhagen, Denmark) *6*, 131-143.

Savina, A., Vidal, M., and Colombo, M.I. (2002). The exosome pathway in K562 cells is regulated by Rab11. Journal of cell science *115*, 2505-2515.

Schafferer, S., Khurana, R., Refolo, V., Venezia, S., Sturm, E., Piatti, P., Hechenberger, C., Hackl, H., Kessler, R., Willi, M.*, et al.* (2016). Changes in the miRNA-mRNA Regulatory Network Precede Motor Symptoms in a Mouse Model of Multiple System Atrophy: Clinical Implications. PloS one *11*, e0150705.

Schlessinger, J., Plotnikov, A.N., Ibrahimi, O.A., Eliseenkova, A.V., Yeh, B.K., Yayon, A., Linhardt, R.J., and Mohammadi, M. (2000). Crystal structure of a ternary FGF-FGFR-heparin complex reveals a dual role for heparin in FGFR binding and dimerization. Molecular cell *6*, 743-750.

Schmidt, O., and Teis, D. (2012). The ESCRT machinery. Curr Biol *22*, R116-R120.

Schols, L., Bauer, P., Schmidt, T., Schulte, T., and Riess, O. (2004). Autosomal dominant cerebellar ataxias: clinical features, genetics, and pathogenesis. The Lancet Neurology *3*, 291-304.

Scoles, D.R., Pflieger, L.T., Thai, K.K., Hansen, S.T., Dansithong, W., and Pulst, S.M. (2012). ETS1 regulates the expression of ATXN2. Human molecular genetics *21*, 5048-5065.

Scoles, D.R., and Pulst, S.M. (2018). Spinocerebellar Ataxia Type 2. Advances in experimental medicine and biology *1049*, 175-195.

Seidel, K., Siswanto, S., Brunt, E.R., den Dunnen, W., Korf, H.W., and Rub, U. (2012). Brain pathology of spinocerebellar ataxias. Acta neuropathologica *124*, 1-21.

Seidel, K., Siswanto, S., Fredrich, M., Bouzrou, M., den Dunnen, W.F.A., Ozerden, I., Korf, H.W., Melegh, B., de Vries, J.J., Brunt, E.R.*, et al.* (2017). On the distribution of intranuclear and cytoplasmic aggregates in the brainstem of patients with spinocerebellar ataxia type 2 and 3. Brain pathology (Zurich, Switzerland) *27*, 345-355.

Sen, N.E., Drost, J., Gispert, S., Torres-Odio, S., Damrath, E., Klinkenberg, M., Hamzeiy, H., Akdal, G., Gulluoglu, H., Basak, A.N.*, et al.* (2016). Search for SCA2 blood RNA

biomarkers highlights Ataxin-2 as strong modifier of the mitochondrial factor PINK1 levels. Neurobiology of disease *96*, 115-126.

Sequeiros, J., Seneca, S., and Martindale, J. (2010). Consensus and controversies in best practices for molecular genetic testing of spinocerebellar ataxias. European journal of human genetics : EJHG *18*, 1188-1195.

Shao, H., Im, H., Castro, C.M., Breakefield, X., Weissleder, R., and Lee, H. (2018). New Technologies for Analysis of Extracellular Vesicles. Chemical reviews *118*, 1917-1950.

Sharma, S., Rasool, H.I., Palanisamy, V., Mathisen, C., Schmidt, M., Wong, D.T., and Gimzewski, J.K. (2010). Structural-mechanical characterization of nanoparticle exosomes in human saliva, using correlative AFM, FESEM, and force spectroscopy. ACS Nano *4*, 1921-1926.

Sharples, R.A., Vella, L.J., Nisbet, R.M., Naylor, R., Perez, K., Barnham, K.J., Masters, C.L., and Hill, A.F. (2008). Inhibition of gamma-secretase causes increased secretion of amyloid precursor protein C-terminal fragments in association with exosomes. FASEB journal : official publication of the Federation of American Societies for Experimental Biology *22*, 1469-1478.

Shelke, G.V., Lässer, C., Gho, Y.S., and Lötvall, J. (2014). Importance of exosome depletion protocols to eliminate functional and RNA-containing extracellular vesicles from fetal bovine serum. J Extracell Vesicles *3*, 10.3402/jev.v3403.24783.

Sherer, N.M., and Mothes, W. (2008). Cytonemes and tunneling nanotubules in cell–cell communication and viral pathogenesis. Trends in Cell Biology *18*, 414-420.

Shibata, H., Huynh, D.P., and Pulst, S.M. (2000). A novel protein with RNA-binding motifs interacts with ataxin-2. Human molecular genetics *9*, 1303-1313.

Simón, D., García-García, E., Royo, F., Falcón-Pérez, J.M., and Avila, J. (2012). Proteostasis of tau. Tau overexpression results in its secretion via membrane vesicles. FEBS letters *586*, 47-54.

Simon, D.K., Zheng, K., Velazquez, L., Santos, N., Almaguer, L., Figueroa, K.P., and Pulst, S.M. (2007). Mitochondrial complex I gene variant associated with early age at onset in spinocerebellar ataxia type 2. Archives of neurology *64*, 1042-1044.

Simons, M., and Raposo, G. (2009). Exosomes--vesicular carriers for intercellular communication. Current opinion in cell biology *21*, 575-581.

Simpson, R.J., Jensen, S.S., and Lim, J.W. (2008). Proteomic profiling of exosomes: current perspectives. Proteomics *8*, 4083-4099.

Skog, J., Würdinger, T., van Rijn, S., Meijer, D.H., Gainche, L., Curry, W.T., Carter, B.S., Krichevsky, A.M., and Breakefield, X.O. (2008). Glioblastoma microvesicles transport RNA and proteins that promote tumour growth and provide diagnostic biomarkers. Nature Cell Biology *10*, 1470-1476.

Skotland, T., Sandvig, K., and Llorente, A. (2017). Lipids in exosomes: Current knowledge and the way forward. Progress in lipid research *66*, 30-41.

Sokolova, V., Ludwig, A.-K., Hornung, S., Rotan, O., Horn, P.A., Epple, M., and Giebel, B. (2011). Characterisation of exosomes derived from human cells by nanoparticle tracking

analysis and scanning electron microscopy. Colloids and Surfaces B: Biointerfaces *87*, 146-150.

Soria, F.N., Pampliega, O., Bourdenx, M., Meissner, W.G., Bezard, E., and Dehay, B. (2017). Exosomes, an Unmasked Culprit in Neurodegenerative Diseases. Frontiers in neuroscience *11*, 26.

Soto, C. (2003). Unfolding the role of protein misfolding in neurodegenerative diseases. Nature Reviews Neuroscience *4*, 49-60.

Spillantini, M.G., Schmidt, M.L., Lee, V.M.Y., Trojanowski, J.Q., Jakes, R., and Goedert, M. (1997). α-Synuclein in Lewy bodies. Nature *388*, 839-840.

Stenmark, H. (2009). Rab GTPases as coordinators of vesicle traffic. Nature Reviews Molecular Cell Biology *10*, 513-525.

Stephens, L., Ellson, C., and Hawkins, P. (2002). Roles of PI3Ks in leukocyte chemotaxis and phagocytosis. Current opinion in cell biology *14*, 203-213.

Stipp, C.S., Kolesnikova, T.V., and Hemler, M.E. (2001). EWI-2 is a major CD9 and CD81 partner and member of a novel Ig protein subfamily. The Journal of biological chemistry *276*, 40545-40554.

Stipp, C.S., Kolesnikova, T.V., and Hemler, M.E. (2003). Functional domains in tetraspanin proteins. Trends in biochemical sciences *28*, 106-112.

Stoorvogel, W., Strous, G.J., Geuze, H.J., Oorschot, V., and Schwartz, A.L. (1991). Late endosomes derive from early endosomes by maturation. Cell *65*, 417-427.

Strack, B., Calistri, A., Craig, S., Popova, E., and Göttlinger, H.G. (2003). AIP1/ALIX is a binding partner for HIV-1 p6 and EIAV p9 functioning in virus budding. Cell *114*, 689-699.

Stubenvoll, M.D., Medley, J.C., Irwin, M., and Song, M.H. (2016). ATX-2, the C. elegans Ortholog of Human Ataxin-2, Regulates Centrosome Size and Microtubule Dynamics. PLoS genetics *12*, e1006370.

Stuendl, A., Kunadt, M., Kruse, N., Bartels, C., Moebius, W., Danzer, K.M., Mollenhauer, B., and Schneider, A. (2016). Induction of α-synuclein aggregate formation by CSF exosomes from patients with Parkinson's disease and dementia with Lewy bodies. Brain : a journal of neurology *139*, 481-494.

Stuffers, S., Sem Wegner, C., Stenmark, H., and Brech, A. (2009). Multivesicular endosome biogenesis in the absence of ESCRTs. Traffic (Copenhagen, Denmark) *10*, 925-937.

Subra, C., Laulagnier, K., Perret, B., and Record, M. (2007). Exosome lipidomics unravels lipid sorting at the level of multivesicular bodies. Biochimie *89*, 205-212.

Svensson, K.J., Christianson, H.C., Wittrup, A., Bourseau-Guilmain, E., Lindqvist, E., Svensson, L.M., Mörgelin, M., and Belting, M. (2013). Exosome uptake depends on ERK1/2-heat shock protein 27 signaling and lipid Raft-mediated endocytosis negatively regulated by caveolin-1. The Journal of biological chemistry *288*, 17713-17724.

Swanson, J.A. (2008). Shaping cups into phagosomes and macropinosomes. Nature Reviews Molecular Cell Biology *9*, 639-649.

Szatanek, R., Baj-Krzyworzeka, M., Zimoch, J., Lekka, M., Siedlar, M., and Baran, J. (2017). The Methods of Choice for Extracellular Vesicles (EVs) Characterization. Int J Mol Sci *18*, 1153.

Takahara, T., and Maeda, T. (2012). Transient sequestration of TORC1 into stress granules during heat stress. Molecular cell *47*, 242-252.

Takahashi, H., Mayers, J.R., Wang, L., Edwardson, J.M., and Audhya, A. (2015). Hrs and STAM function synergistically to bind ubiquitin-modified cargoes in vitro. Biophys J *108*, 76-84.

Takahashi, T., Kikuchi, S., Katada, S., Nagai, Y., Nishizawa, M., and Onodera, O. (2008). Soluble polyglutamine oligomers formed prior to inclusion body formation are cytotoxic. Human molecular genetics *17*, 345-356.

Takeuchi, T., and Nagai, Y. (2017). Protein Misfolding and Aggregation as a Therapeutic Target for Polyglutamine Diseases. Brain sciences *7*.

Tang, S.J., Meulemans, D., Vazquez, L., Colaco, N., and Schuman, E. (2001). A role for a rat homolog of staufen in the transport of RNA to neuronal dendrites. Neuron *32*, 463-475.

Tauro, B.J., Greening, D.W., Mathias, R.A., Mathivanan, S., Ji, H., and Simpson, R.J. (2013). Two distinct populations of exosomes are released from LIM1863 colon carcinoma cell-derived organoids. Molecular & cellular proteomics : MCP *12*, 587-598.

Taylor, D.D., and Gercel-Taylor, C. (2008). MicroRNA signatures of tumor-derived exosomes as diagnostic biomarkers of ovarian cancer. Gynecologic oncology *110*, 13-21.

Taylor, J., Azimi, I., Monteith, G., and Bebawy, M. (2020). Ca(2+) mediates extracellular vesicle biogenesis through alternate pathways in malignancy. J Extracell Vesicles *9*, 1734326-1734326.

Teo, H., Gill, D.J., Sun, J., Perisic, O., Veprintsev, D.B., Vallis, Y., Emr, S.D., and Williams, R.L. (2006). ESCRT-I core and ESCRT-II GLUE domain structures reveal role for GLUE in linking to ESCRT-I and membranes. Cell *125*, 99-111.

Tharun, S. (2009). Roles of eukaryotic Lsm proteins in the regulation of mRNA function. International review of cell and molecular biology *272*, 149-189.

Thery, C., Amigorena, S., Raposo, G., and Clayton, A. (2006). Isolation and characterization of exosomes from cell culture supernatants and biological fluids. Current protocols in cell biology *Chapter 3*, Unit 3 22.

Théry, C., Amigorena, S., Raposo, G., and Clayton, A. (2006). Isolation and characterization of exosomes from cell culture supernatants and biological fluids. Current protocols in cell biology *Chapter 3*, Unit 3.22.

Théry, C., Regnault, A., Garin, J., Wolfers, J., Zitvogel, L., Ricciardi-Castagnoli, P., Raposo, G., and Amigorena, S. (1999). Molecular characterization of dendritic cell-derived exosomes. Selective accumulation of the heat shock protein hsc73. The Journal of cell biology *147*, 599-610.

Théry, C., Witwer, K.W., Aikawa, E., Alcaraz, M.J., Anderson, J.D., Andriantsitohaina, R., Antoniou, A., Arab, T., Archer, F., Atkin-Smith, G.K.*, et al.* (2018). Minimal information for studies of extracellular vesicles 2018 (MISEV2018): a position statement of the

International Society for Extracellular Vesicles and update of the MISEV2014 guidelines. J Extracell Vesicles *7*, 1535750.

Thomas, M.G., Martinez Tosar, L.J., Desbats, M.A., Leishman, C.C., and Boccaccio, G.L. (2009). Mammalian Staufen 1 is recruited to stress granules and impairs their assembly. Journal of cell science *122*, 563-573.

Tian, F., Zhang, S., Liu, C., Han, Z., Liu, Y., Deng, J., Li, Y., Wu, X., Cai, L., Qin, L.*, et al.* (2021). Protein analysis of extracellular vesicles to monitor and predict therapeutic response in metastatic breast cancer. Nature Communications *12*, 2536.

Ting-Beall, H.P. (1980). Interactions of uranyl ions with lipid bilayer membranes. Journal of microscopy *118*, 221-227.

Todd, T.W., and Lim, J. (2013). Aggregation formation in the polyglutamine diseases: protection at a cost? Mol Cells *36*, 185-194.

Trajkovic, K., Hsu, C., Chiantia, S., Rajendran, L., Wenzel, D., Wieland, F., Schwille, P., Brügger, B., and Simons, M. (2008). Ceramide triggers budding of exosome vesicles into multivesicular endosomes. Science (New York, NY) *319*, 1244-1247.

Tricarico, C., Clancy, J., and D'Souza-Schorey, C. (2017). Biology and biogenesis of shed microvesicles. Small GTPases *8*, 220-232.

Trott, A., Jardim, L.B., Ludwig, H.T., Saute, J.A., Artigalas, O., Kieling, C., Wanderley, H.Y., Rieder, C.R., Monte, T.L., Socal, M.*, et al.* (2006). Spinocerebellar ataxias in 114 Brazilian families: clinical and molecular findings. Clinical genetics *70*, 173-176.

Ubhi, K., Rockenstein, E., Kragh, C., Inglis, C., Spencer, B., Michael, S., Mante, M., Adame, A., Galasko, D., and Masliah, E. (2014). Widespread microRNA dysregulation in multiple system atrophy - disease-related alteration in miR-96. The European journal of neuroscience *39*, 1026-1041.

Uchihara, T., Fujigasaki, H., Koyano, S., Nakamura, A., Yagishita, S., and Iwabuchi, K. (2001). Non-expanded polyglutamine proteins in intranuclear inclusions of hereditary ataxias--triple-labeling immunofluorescence study. Acta neuropathologica *102*, 149-152.

Valadi, H., Ekström, K., Bossios, A., Sjöstrand, M., Lee, J.J., and Lötvall, J.O. (2007). Exosome-mediated transfer of mRNAs and microRNAs is a novel mechanism of genetic exchange between cells. Nature Cell Biology *9*, 654-659.

Vallee, R.B., Herskovits, J.S., Aghajanian, J.G., Burgess, C.C., and Shpetner, H.S. (1993). Dynamin, a GTPase involved in the initial stages of endocytosis. Ciba Foundation symposium *176*, 185-193; discussion 193-187.

Van Damme, P., Veldink, J.H., van Blitterswijk, M., Corveleyn, A., van Vught, P.W., Thijs, V., Dubois, B., Matthijs, G., van den Berg, L.H., and Robberecht, W. (2011). Expanded ATXN2 CAG repeat size in ALS identifies genetic overlap between ALS and SCA2. Neurology *76*, 2066-2072.

van de Loo, S., Eich, F., Nonis, D., Auburger, G., and Nowock, J. (2009). Ataxin-2 associates with rough endoplasmic reticulum. Exp Neurol *215*, 110-118.

van Dijk, E., Cougot, N., Meyer, S., Babajko, S., Wahle, E., and Seraphin, B. (2002). Human Dcp2: a catalytically active mRNA decapping enzyme located in specific cytoplasmic structures. The EMBO journal *21*, 6915-6924.

van Niel, G., Charrin, S., Simoes, S., Romao, M., Rochin, L., Saftig, P., Marks, M.S., Rubinstein, E., and Raposo, G. (2011). The tetraspanin CD63 regulates ESCRT-independent and -dependent endosomal sorting during melanogenesis. Developmental cell *21*, 708-721.

van Niel, G., D'Angelo, G., and Raposo, G. (2018). Shedding light on the cell biology of extracellular vesicles. Nature Reviews Molecular Cell Biology *19*, 213-228.

Veerman, R.E., Teeuwen, L., Czarnewski, P., Güclüler Akpinar, G., Sandberg, A., Cao, X., Pernemalm, M., Orre, L.M., Gabrielsson, S., and Eldh, M. (2021). Molecular evaluation of five different isolation methods for extracellular vesicles reveals different clinical applicability and subcellular origin. *10*, e12128.

Velazquez-Perez, L., Rodriguez-Labrada, R., Cruz-Rivas, E.M., Fernandez-Ruiz, J., Vaca-Palomares, I., Lilia-Campins, J., Cisneros, B., Pena-Acosta, A., Vazquez-Mojena, Y., Diaz, R.*, et al.* (2014). Comprehensive study of early features in spinocerebellar ataxia 2: delineating the prodromal stage of the disease. Cerebellum (London, England) *13*, 568-579.

Velazquez-Perez, L., Rodriguez-Labrada, R., Garcia-Rodriguez, J.C., Almaguer-Mederos, L.E., Cruz-Marino, T., and Laffita-Mesa, J.M. (2011). A comprehensive review of spinocerebellar ataxia type 2 in Cuba. Cerebellum (London, England) *10*, 184-198.

Velazquez-Perez, L.C., Rodriguez-Labrada, R., and Fernandez-Ruiz, J. (2017). Spinocerebellar Ataxia Type 2: Clinicogenetic Aspects, Mechanistic Insights, and Management Approaches. Front Neurol *8*, 472.

Velazquez Perez, L., Cruz, G.S., Santos Falcon, N., Enrique Almaguer Mederos, L., Escalona Batallan, K., Rodriguez Labrada, R., Paneque Herrera, M., Laffita Mesa, J.M., Rodriguez Diaz, J.C., Rodriguez, R.A.*, et al.* (2009). Molecular epidemiology of spinocerebellar ataxias in Cuba: insights into SCA2 founder effect in Holguin. Neurosci Lett *454*, 157-160.

Vella, L.J., Greenwood, D.L., Cappai, R., Scheerlinck, J.P., and Hill, A.F. (2008). Enrichment of prion protein in exosomes derived from ovine cerebral spinal fluid. Veterinary immunology and immunopathology *124*, 385-393.

Vella, L.J., Sharples, R.A., Lawson, V.A., Masters, C.L., Cappai, R., and Hill, A.F. (2007). Packaging of prions into exosomes is associated with a novel pathway of PrP processing. The Journal of pathology *211*, 582-590.

Venkatraman, P., Wetzel, R., Tanaka, M., Nukina, N., and Goldberg, A.L. (2004). Eukaryotic proteasomes cannot digest polyglutamine sequences and release them during degradation of polyglutamine-containing proteins. Molecular cell *14*, 95-104.

Verbeek, D.S., Goedhart, J., Bruinsma, L., Sinke, R.J., and Reits, E.A. (2008). PKC gamma mutations in spinocerebellar ataxia type 14 affect C1 domain accessibility and kinase activity leading to aberrant MAPK signaling. Journal of cell science *121*, 2339-2349.

Veziroglu, E.M., and Mias, G.I. (2020). Characterizing Extracellular Vesicles and Their Diverse RNA Contents. *11*.

Wadia, N.H., and Swami, R.K. (1971). A new form of heredo-familial spinocerebellar degeneration with slow eye movements (nine families). Brain : a journal of neurology *94*, 359-374.

Walsh, D.M., and Selkoe, D.J. (2016). A critical appraisal of the pathogenic protein spread hypothesis of neurodegeneration. Nature reviews Neuroscience *17*, 251-260.

Wang, L.H., Rothberg, K.G., and Anderson, R.G. (1993). Mis-assembly of clathrin lattices on endosomes reveals a regulatory switch for coated pit formation. The Journal of cell biology *123*, 1107-1117.

Wanowska, E., Kubiak, M.R., Rosikiewicz, W., Makalowska, I., and Szczesniak, M.W. (2018). Natural antisense transcripts in diseases: From modes of action to targeted therapies. Wiley Interdiscip Rev RNA *9*, e1461.

Wei, Y., Wang, D., Jin, F., Bian, Z., Li, L., Liang, H., Li, M., Shi, L., Pan, C., Zhu, D.*, et al.* (2017). Pyruvate kinase type M2 promotes tumour cell exosome release via phosphorylating synaptosome-associated protein 23. Nature Communications *8*, 14041.

Wei, Z., Batagov, A.O., Carter, D.R.F., and Krichevsky, A.M. (2016). Fetal Bovine Serum RNA Interferes with the Cell Culture derived Extracellular RNA. Scientific Reports *6*, 31175.

Williams, A.J., and Paulson, H.L. (2008). Polyglutamine neurodegeneration: protein misfolding revisited. Trends in neurosciences *31*, 521-528.

Willms, E., Johansson, H.J., Mäger, I., Lee, Y., Blomberg, K.E.M., Sadik, M., Alaarg, A., Smith, C.I.E., Lehtiö, J., El Andaloussi, S.*, et al.* (2016). Cells release subpopulations of exosomes with distinct molecular and biological properties. Scientific Reports *6*, 22519.

Witwer, K.W., Buzás, E.I., Bemis, L.T., Bora, A., Lässer, C., Lötvall, J., Nolte-'t Hoen, E.N., Piper, M.G., Sivaraman, S., Skog, J.*, et al.* (2013). Standardization of sample collection, isolation and analysis methods in extracellular vesicle research. J Extracell Vesicles *2*, 20360.

Wollert, T., and Hurley, J.H. (2010). Molecular mechanism of multivesicular body biogenesis by ESCRT complexes. Nature *464*, 864-869.

Xiao, Z., Blonder, J., Zhou, M., and Veenstra, T.D. (2009). Proteomic analysis of extracellular matrix and vesicles. Journal of proteomics *72*, 34-45.

Yáñez-Mó, M., Barreiro, O., Gordon-Alonso, M., Sala-Valdés, M., and Sánchez-Madrid, F. (2009). Tetraspanin-enriched microdomains: a functional unit in cell plasma membranes. Trends Cell Biol *19*, 434-446.

Yang, D., and Hurley, J.H. (2010). Structural role of the Vps4-Vta1 interface in ESCRT-III recycling. Structure *18*, 976-984.

Yang, H., Li, J.J., Liu, S., Zhao, J., Jiang, Y.J., Song, A.X., and Hu, H.Y. (2014). Aggregation of polyglutamine-expanded ataxin-3 sequesters its specific interacting partners into inclusions: implication in a loss-of-function pathology. Sci Rep *4*, 6410.

Yang, L., Peng, X., Li, Y., Zhang, X., Ma, Y., Wu, C., Fan, Q., Wei, S., Li, H., and Liu, J. (2019). Long non-coding RNA HOTAIR promotes exosome secretion by regulating RAB35 and SNAP23 in hepatocellular carcinoma. Molecular Cancer *18*, 78.

Yang, Y., Chen, J., Guo, Z., Deng, S., Du, X., Zhu, S., Ye, C., Shi, Y.S., and Liu, J.J. (2018). Endophilin A1 Promotes Actin Polymerization in Dendritic Spines Required for Synaptic Potentiation. Front Mol Neurosci *11*, 177.

Yim, Y.-I., Park, B.-C., Yadavalli, R., Zhao, X., Eisenberg, E., and Greene, L.E. (2015). The multivesicular body is the major internal site of prion conversion. Journal of cell science *128*, 1434-1443.

Yokoshi, M., Li, Q., Yamamoto, M., Okada, H., Suzuki, Y., and Kawahara, Y. (2014). Direct binding of Ataxin-2 to distinct elements in 3' UTRs promotes mRNA stability and protein expression. Molecular cell *55*, 186-198.

Yu, Z., Zhu, Y., Chen-Plotkin, A.S., Clay-Falcone, D., McCluskey, L., Elman, L., Kalb, R.G., Trojanowski, J.Q., Lee, V.M., Van Deerlin, V.M.*, et al.* (2011). PolyQ repeat expansions in ATXN2 associated with ALS are CAA interrupted repeats. PLoS One *6*, e17951.

Yuana, Y., Böing, A.N., Grootemaat, A.E., van der Pol, E., Hau, C.M., Cizmar, P., Buhr, E., Sturk, A., and Nieuwland, R. (2015). Handling and storage of human body fluids for analysis of extracellular vesicles. J Extracell Vesicles *4*, 29260.

Yuana, Y., Oosterkamp, T.H., Bahatyrova, S., Ashcroft, B., Garcia Rodriguez, P., Bertina, R.M., and Osanto, S. (2010). Atomic force microscopy: a novel approach to the detection of nanosized blood microparticles. Journal of thrombosis and haemostasis : JTH *8*, 315-323.

Yuyama, K., Sun, H., Mitsutake, S., and Igarashi, Y. (2012). Sphingolipid-modulated exosome secretion promotes clearance of amyloid-β by microglia. The Journal of biological chemistry *287*, 10977-10989.

Zabeo, D., Cvjetkovic, A., Lässer, C., Schorb, M., Lötvall, J., and Höög, J.L. (2017). Exosomes purified from a single cell type have diverse morphology. J Extracell Vesicles *6*, 1329476.

Zech, D., Rana, S., Büchler, M.W., and Zöller, M. (2012). Tumor-exosomes and leukocyte activation: an ambivalent crosstalk. Cell communication and signaling : CCS *10*, 37.

Zhang, F., Michaelson, J.E., Moshiach, S., Sachs, N., Zhao, W., Sun, Y., Sonnenberg, A., Lahti, J.M., Huang, H., and Zhang, X.A. (2011a). Tetraspanin CD151 maintains vascular stability by balancing the forces of cell adhesion and cytoskeletal tension. Blood *118*, 4274-4284.

Zhang, Y.-w., Thompson, R., Zhang, H., and Xu, H. (2011b). APP processing in Alzheimer's disease. Molecular Brain *4*, 3.

Zhu, Q., Yamakuchi, M., and Lowenstein, C.J. (2015). SNAP23 Regulates Endothelial Exocytosis of von Willebrand Factor. PloS one *10*, e0118737.

Zitvogel, L., Regnault, A., Lozier, A., Wolfers, J., Flament, C., Tenza, D., Ricciardi-Castagnoli, P., Raposo, G., and Amigorena, S. (1998). Eradication of established murine tumors using a novel cell-free vaccine: dendritic cell-derived exosomes. Nature medicine *4*, 594-600.

APPENDIX

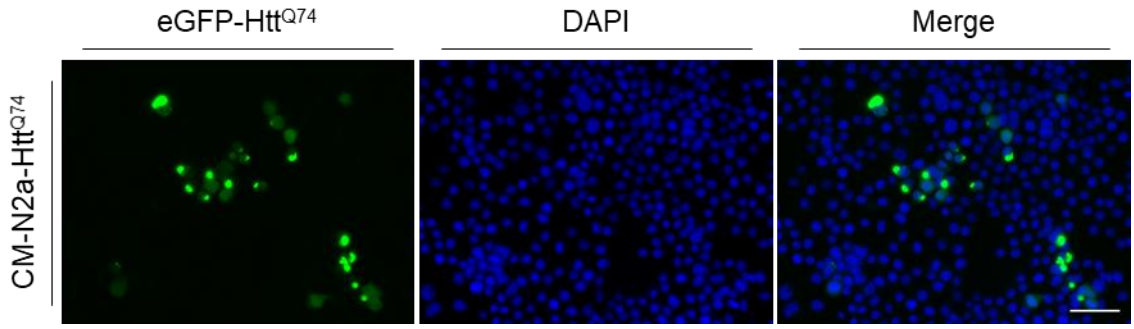

FigureS3.1 – Mutant eGFP-HttQ74 is detected in non-transfected N2a recipient cells upon the transfer of CM derived from pEGFP-HttQ74-transfected cells. N2a cells were transfected with the pEGFP-Htt^{Q74} plasmid using PEI. Cells were then cultured for 24 h in EV-free medium for EV harvesting. Non-transfected N2a recipient cells were cultured in N2a-Htt^{Q74}-derived CM (mixed with fresh EV-free medium for nutritional support) for 24 h and then fixed and stained with DAPI for observation. eGFP-Htt^{Q74}-positive cells were detected in non-transfected recipient cells (green) and were used as a positive control for the experiment setup. DAPI-stained nuclei can be observed in blue. Scale bar, 50 µm. Results are representative of four independent experiments.

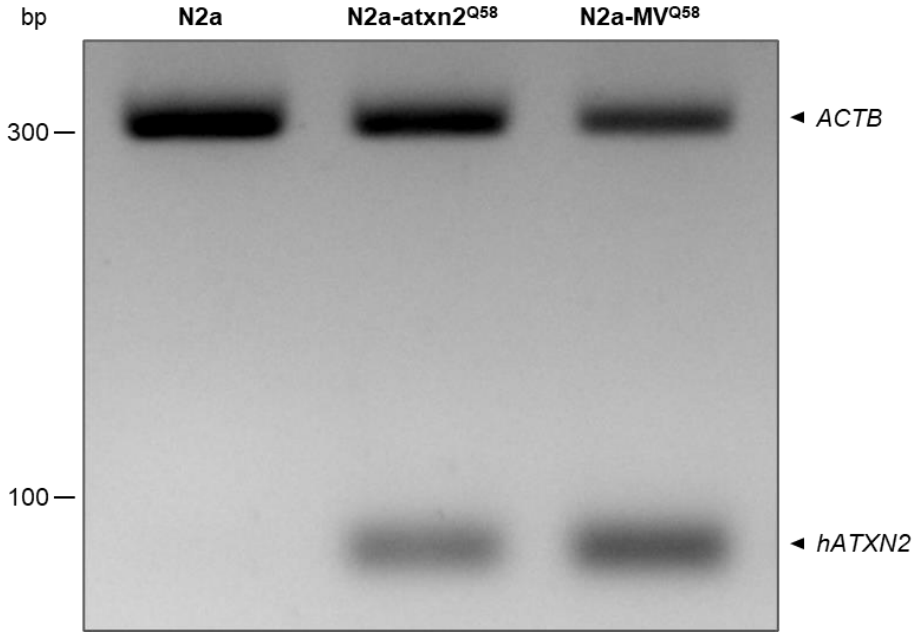

Figure S3.2 – hATXN2Q58 mRNA is present in N2a-atxn2Q58-derived microvesicles. MVs isolated from N2a-atxn2^{Q58} cells were submitted to RT-PCR analyses for the detection of the human ataxin-2 mRNA. Agarose gel electrophoresis of RT-PCR analyses showing the presence of hATXN2^{Q58} mRNA in N2a-MV^{Q58} obtained from N2a-atxn2^{Q58}. N2a and N2a-atxn2^{Q58} were used as negative and positive controls of the amplification of hATXN2^{Q58}, respectively. ACTB amplification was used as a positive control of the PCR reaction. Results are representative of two independent isolation experiments.

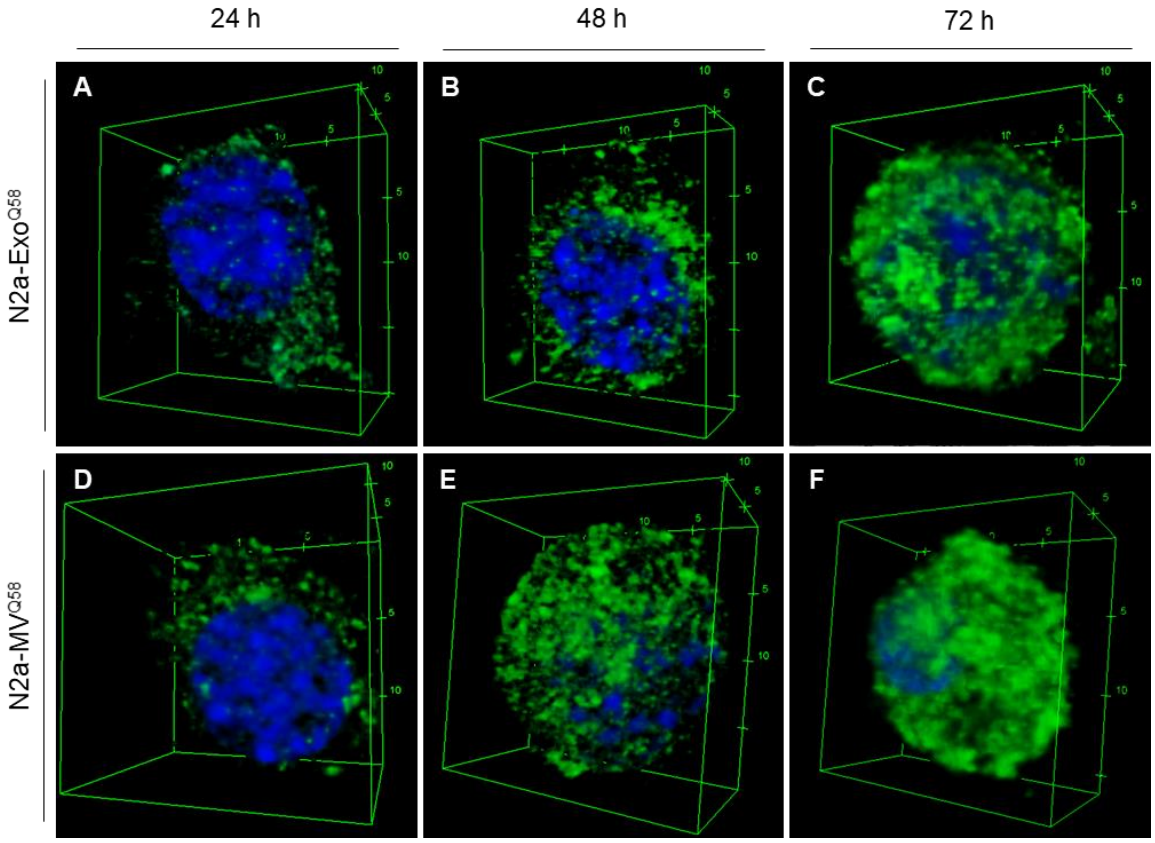

Figure S3.3 – 3D representations of eGFP-atxn2Q58 aggregates upon the delivery of ataxin-2-loaded EVs. Z-stacks were obtained by confocal microscopy for each experimental condition and assembled into 3D models. The 3D models show a progressive accumulation of eGFP-atxn2^{Q58} aggregates, which increase in number and volume at each time point, upon the delivery of either N2a-Exo^{Q58} **(A-C)** or N2a-MV^{Q58} **(D-F)** to N2a recipient cells.

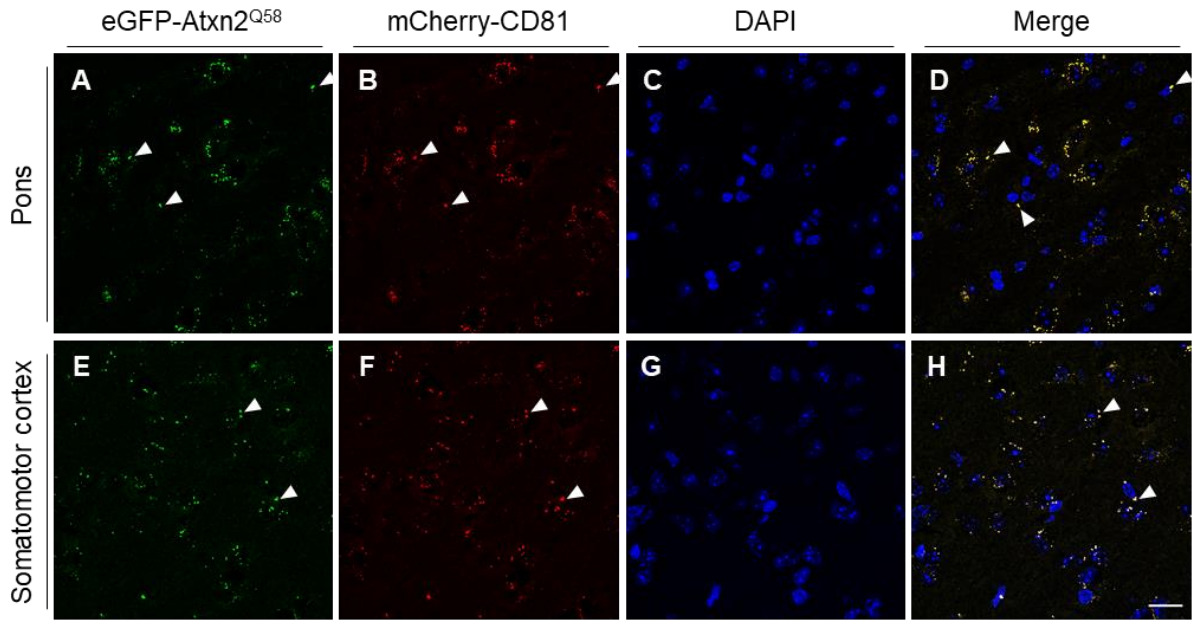

Figure S32.4 – Co-localization between eGFP-atxn2Q58 and mCherry-CD81 is detected within the nervous tissue of mice by direct fluorescence. Brain sections of N2a-Exo$^{Q58/CD81}$-injected mice were directly observed under a confocal microscope without prior labeling with antibodies. The fusion proteins eGFP-atxn2^{Q58} (green) and mCherry-CD81 (red) co-localize within the nervous tissue of N2a-Exo$^{Q58/CD81}$-injected mice (yellow, white arrowheads). Scale bar, 20 µm.

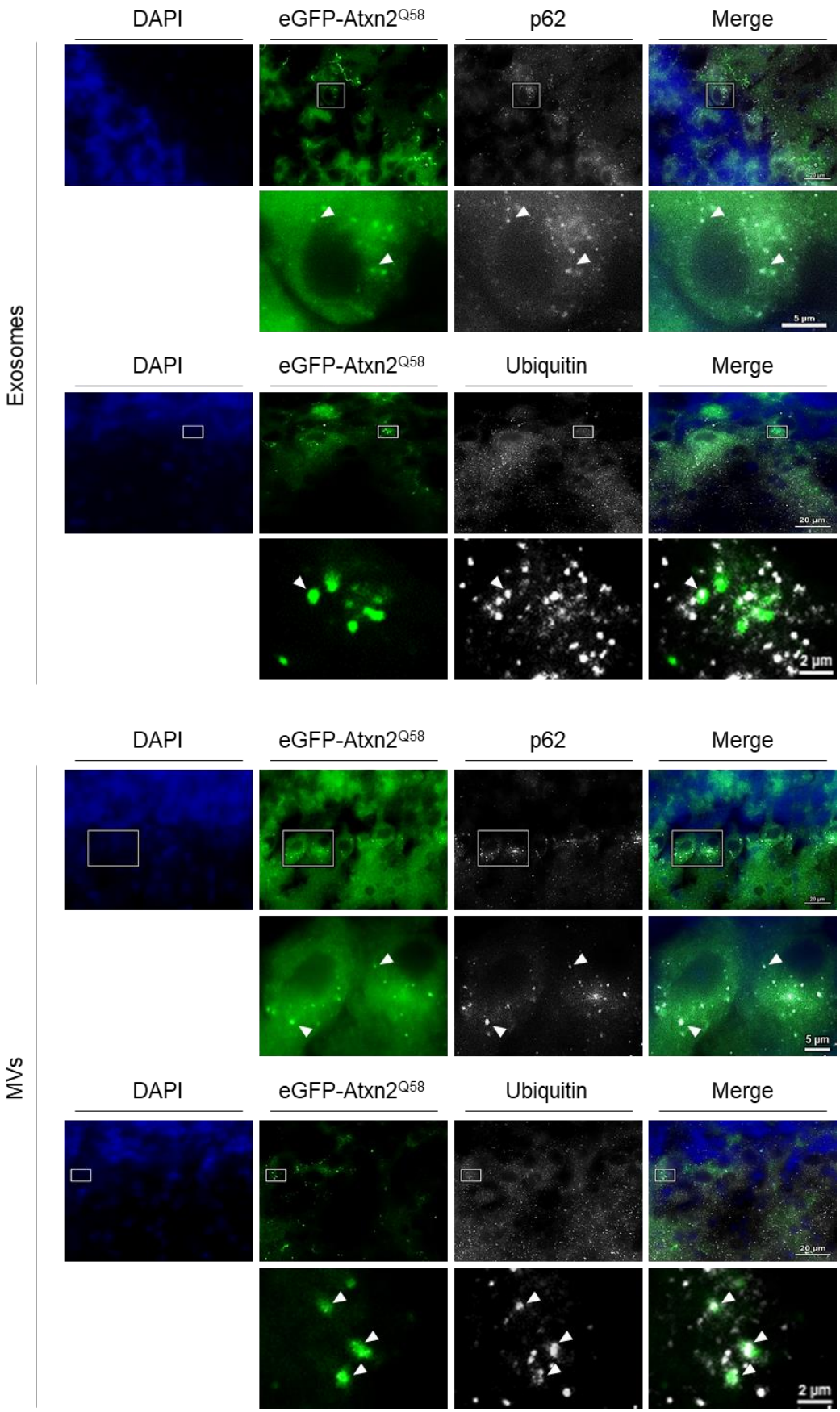

Figure S3.5 – Widefield fluorescence microscopy analysis of eGFP-atxn2Q58, p62 and ubiquitin foci. Brain sections of N2a-Exo$^{Q58/CD81}$- and N2a-MV$^{Q58/CD81}$-injected mice were immunohistochemically labelled with anti-GFP and either anti-p62 or anti-ubiquitin antibodies. Representative images obtained

by widefield fluorescence microscopy suggest that both p62 and ubiquitin are present in eGFP-atxn2^{Q58} aggregates.